Position Paper on Systematics for CC analysis

J.Thomas, P. Vahle
University College London

December 29, 2005

Executive Summary

Topic

We take an alternative approach to the oscillation measurement by attempting to predict the non-oscillated spectrum at the Far detector using ratios of the F/N energy (both reconstructed and true) and also using a more complicated full matrix transport method.

Relevance to CC Measurement

This approach can be used to study the effects of known systematic errors on the parameter measurement. The fit procedure is very fast, using the MINUIT package, and many pseudo runs can be used to study the effects that the statistical errors may produce together with systematic errors. This overall systematic error can be quantified.

Method

In the case of no oscillations, the predicted Far Detector spectrum is given by taking each bin of the measured Near Detector reconstructed energy spectrum and multiplying by the ratio of Far/Near event rate in that bin as given from the Monte Carlo. This is extended to use the true Far/Near ratio and then finally to use a full matrix method which takes into account the off-diagonal parts which the ratio methods ignore.

Conclusion

Many systematic effects have been studied. The most important one is the calibration error which must be kept within 5%. Beam uncertainties well outside our level of understanding can be absorbed by this method as can large uncertainties in the generator parameters.

1 Introduction

In this note, we investigate what effect different systematic errors will have on the measurement of Δm^2 and $\sin^2 2\theta$ compared to the statistical errors resulting from the 1×10^{20} protons on target data set. Using fake data sets generated from modified MC samples, hundreds of pseudo experiments are performed, and the errors on the fit parameters can be evaluated for many different random runs where the number of Far Detector events is statistically varied around the prediction. In this analysis, we have studied the effect of a number of different sources of systematic errors:

- variations in cross section parameters
- intranuke
- calibration errors
- different beam models
- proton on target normalization errors
- systematic increases in Near Detector event rates for some energies without a corresponding increase in the Far Detector event rate.
- errors on neutral current background

This study will tell us how well the ND data and MC have to agree before a reliable measurement of the parameters can be performed and the box can be opened. The method described here is very robust against large changes associated with the generator (anything that affects the ND and FD in the same way) and against systematic differences between beam models. Uncertainties in normalization which might stem from pot counting uncertainty or fiducial volume modeling are accounted for in the fit and do not pose a problem. The calibration is the critical systematic which must be kept within 5% to not render the parameter measurement impossible.

2 The Method

For this study, we have used the Far/Near ratio approach instead of Dave Petyt's approach. The Petyt method is too CPU intensive to perform the thousands of pseudo experiments required to assess the effects of each of the systematics studied.

2.1 Data Selection Criteria

For this note, the Monte Carlo was generated with the avocado Monte Carlo release, using LE flux version 17, and reconstructed with R1.16. To select a sample of CC-like events, we apply a set of cuts to select well-reconstructed events with a CC-like topology. The selection criteria are applied to both the data and Monte Carlo and are as follows:

- Require the event vertex is in the fiducial volume.

  - ND: 0.6 m < z < 3.56 m,0.3 m < u < 1.8 m, $r < 0.5$ m
  - FD: 0.5 m < z < 14.5 m, 16.5 m < z < 29.4 m, $r < 2.5$ m
- reconstruction variable $trk.fit.pass == 1$, which ensures a well fit track.
- track fit $\frac{\chi^2}{NDF} < 10$
- One and only one reconstructed track
- no other event within 50 ns of the selected event
- $\left| \frac{\Delta\left(\frac{q}{p}\right)}{\frac{q}{p}} \right| < 0.2$
- 90% of reconstructed shower energy is deposited in the fully instrumented region (ND only)
- muon charge < 0
- track vertex z position > 0.6 m

When applied to the data, this set of cuts will be supplemented with a set of cuts designed to ensure beam and detector quality.

2.2 Predicting the Far Detector Spectrum via Far/Near Ratio

In the case of no oscillations, the predicted Far Detector spectrum is given by taking each bin of the measured Near Detector reconstructed energy spectrum and multiplying by the ratio of Far/Near in that bin as given from the Monte Carlo. In symbols, we predict the number of neutrinos with reconstructed energy in the i(th) energy bin to be:

$$F_i^{predicted} = N_i^{data} \times \frac{f_i^{MC}}{n_i^{MC}} \tag{1}$$

where N_i^{data} is the number of neutrinos measured in the Near Detector with reconstructed energy in the i(th) energy bin, n_i^{MC} is the number of neutrinos in the i(th) reconstructed energy bin in the Near Detector Monte Carlo, and f_i^{MC} is the number of neutrinos in the i(th) reconstructed energy bin in the Far Detector Monte Carlo. Figure 1 shows the performance of the Far/Near ratio, in which the LE Monte Carlo was used to form the Far/Near ratio, and the LE10 Monte Carlo was used as the "data". While the Far/Near ratio does not exactly predict the LE10 Far Detector spectrum, the predicted spectrum more closely resembles the LE10 spectrum than the original LE spectrum does.

In the case of oscillations, one has to apply the oscillation probability to the true neutrino energy before one can predict the Far Detector spectrum. This is done by using a 2-d histogram of reconstructed vs. true neutrino energy for all events that pass the selection cuts in the Far Detector. This 2-d histogram is made for both the standard Far Detector Monte Carlo and for the Monte Carlo in which all ν_μ's have been oscillated into ν_τ's. Then, for each bin of true neutrino energy, the ν_μ disappearance probability, P_{ν_μ} is computed. It is assumed that $\nu_\mu \to \nu_\tau$ only, so the ν_τ appearance probability is taken as $1 - P_{\nu_\mu}$. Using the reconstructed vs. true neutrino energy histogram, a projection of reconstructed energy is

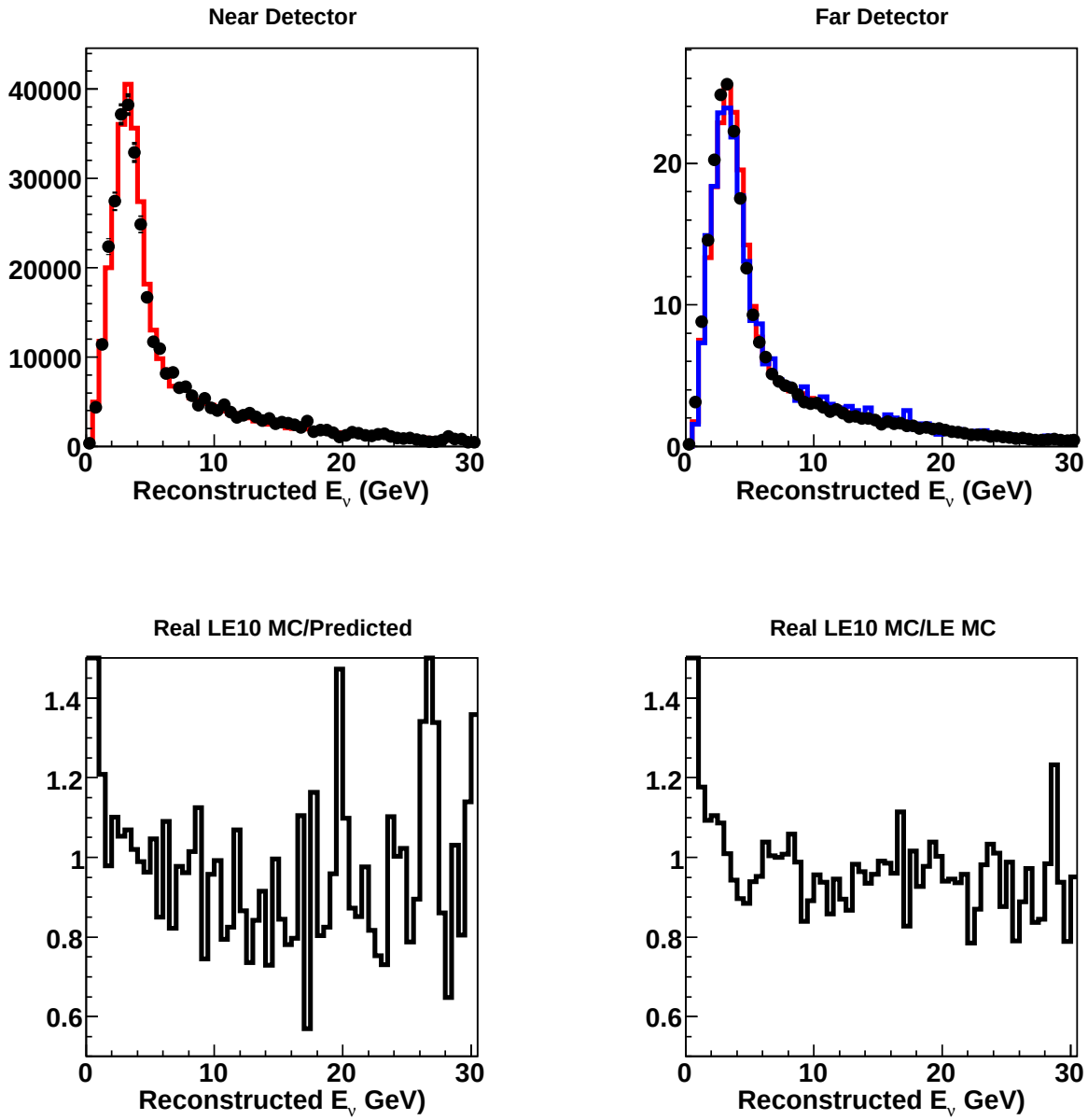


Figure 1: Comparison between the LE10 Monte Carlo reconstructed neutrino energy distribution and the predicted spectra arising from the ratio of Far/Near from the LE Monte Carlo. Top left plot shows the Near Detector spectra. The red histogram comes from LE Monte Carlo, while the black points come from the LE10 Monte Carlo. Top right plot shows Far Detector spectra; red shows the LE spectrum, blue shows the predicted spectrum arising from the Far/Near ratio; black shows the LE10 spectrum. Bottom left shows the ratio of the LE10 Far Detector spectrum divided by the predicted spectrum. Bottom right shows the ratio of the LE10 Far Detector spectrum divided by the LE Far Detector spectrum

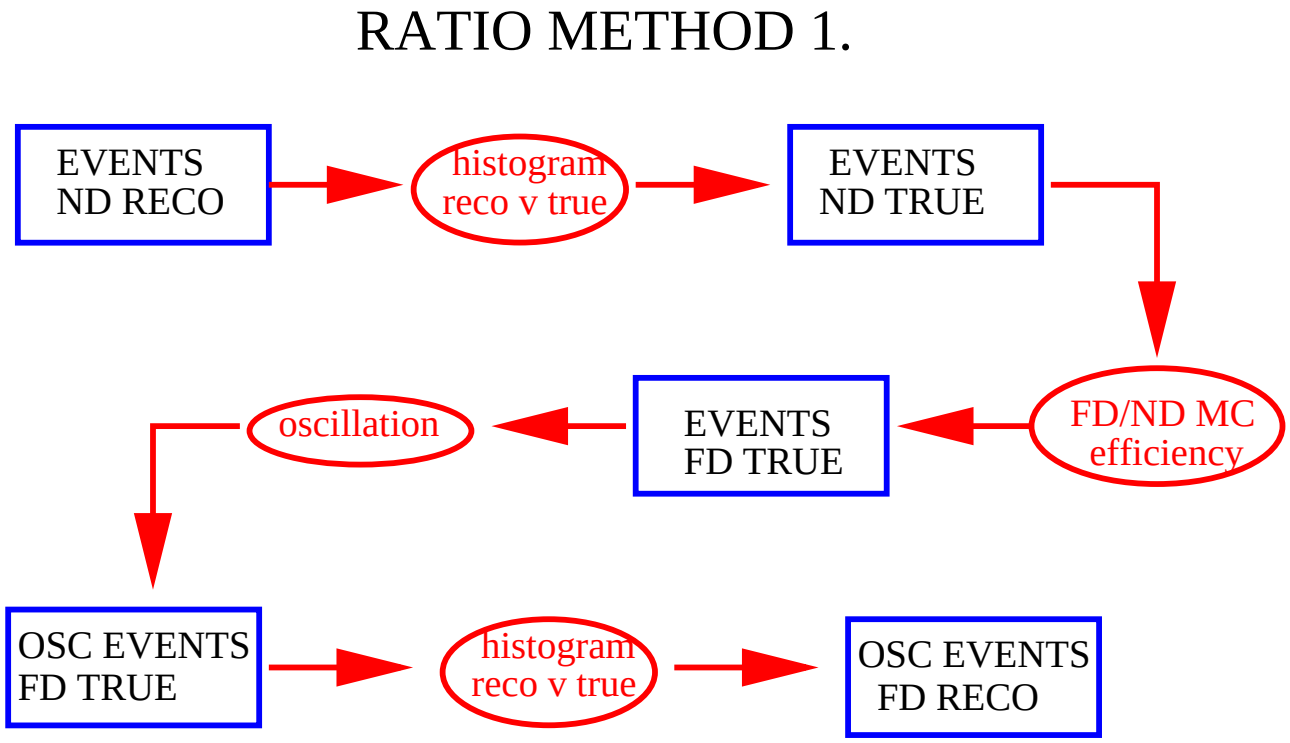


Figure 2: A schematic diagram of the steps involved in predicting the Far Detector Spectrum using the F/N ratio method.

made for one bin of true neutrino energy and is multiplied by P_{ν_μ}. The same projection is made for the ν_τ histogram and multiplied by $1 - P_{\nu_\mu}$. These oscillation scaled projections are added together. This process is done for each true neutrino energy bin, and the resulting histograms are summed. The summed histogram is modulated by the measured distribution in the Near Detector by multiplying by the ratio N_i/n_i to give the Far Detector predicted spectrum.

Originally, the F/N ratio was taken from the reconstructed histograms; however, for the work shown in this paper, the method has been modified to take the ratio histogram constructed from the true neutrino energy. When using the true energy F/N ratio, the Near Detector reconstructed neutrino energy spectrum from the data must first be converted to a true energy spectrum. This is done by using a 2-d histogram of reconstructed energy vs. true energy in the Near Detector. Figure 2 shows a schematic diagram of the steps involved in predicting the Far Detector reconstructed neutrino energy spectrum.

2.3 Generating Fake Data

A set of "fake" data is generated from samples of modified Monte Carlo runs. The modifications are designed to introduce a source of systematic error, and each modification is described in the result sections below. The Near Detector spectrum from the modified MC is taken as the "data", and a

	Δm^2	$\sin^2 2\theta$
Ratio	0.0021±0.0003	0.97±0.07
Petyt	0.0022	0.925
Truth	0.0021	0.881

Table 1: Mock Data Challenge Results

predicted Far Detector spectrum is produced, where the histograms involved in the F/N ratio are taken from the standard Monte Carlo sample. A Far Detector data spectrum is generated using the modified Monte Carlo in the Far Detector. This Far Detector data spectrum is oscillated using a input set of oscillation parameters, then each bin is fluctuated by drawing a random number from a Gaussian with a width of the error of the number of events in that bin. Many hundreds of pseudo-experiments are generated with different fluctuations in the number of events of each bin.

2.4 The Fitting

Using Minuit, the log likelihood between the oscillated predicted spectrum and the data spectrum is maximized to derive the oscillation parameters and their errors. A χ^2 fit has also been used, and the results are consistent with the log likelihood fit. Three parameters are included in the fit, Δm^2 , $\sin^2 2\theta$, and an overall normalization. The fits are studied in two ways: the sensitivity contour is derived by increasing -2*loglikelihood by 3.53 (67% contour) and 6.25 (90% contour) for the data set where the number of events in each bin is given by the oscillation parameters and the p.o.t for the FD, and the statistical errors are given by sqrt(entries) in each bin.

3 Results from the Ratio Method

3.1 Mock Data Challenge Results

To confirm the efficacy of the Far/Near ratio method, we applied our method to the Mock Data Challenge. Figure 3 shows the spectra in each of the detectors from the Monte Carlo and the mock data. The left plot shows the Near Detector Monte Carlo and mock data spectra, while the right plot shows the Far Detector Monte Carlo, predicted, and mock data spectra. The mock data sample corresponds to 7.4×10^{20} protons on target. Figure 4 shows the results of fitting the mock data. The top left plot shows the predicted Far Detector spectrum in the case of no oscillations and the mock data. The top right plot shows the contributions of each different class of events to the spectrum. The bottom left plot shows the spectrum produced by the best fit values of Δm^2 and $\sin^2 2\theta$. The bottom right plot shows the 90% confidence region and quotes the best fit values. Table 3.1 summarizes the results. Our results are in agreement with both the generated values and Dave Petyt's values.

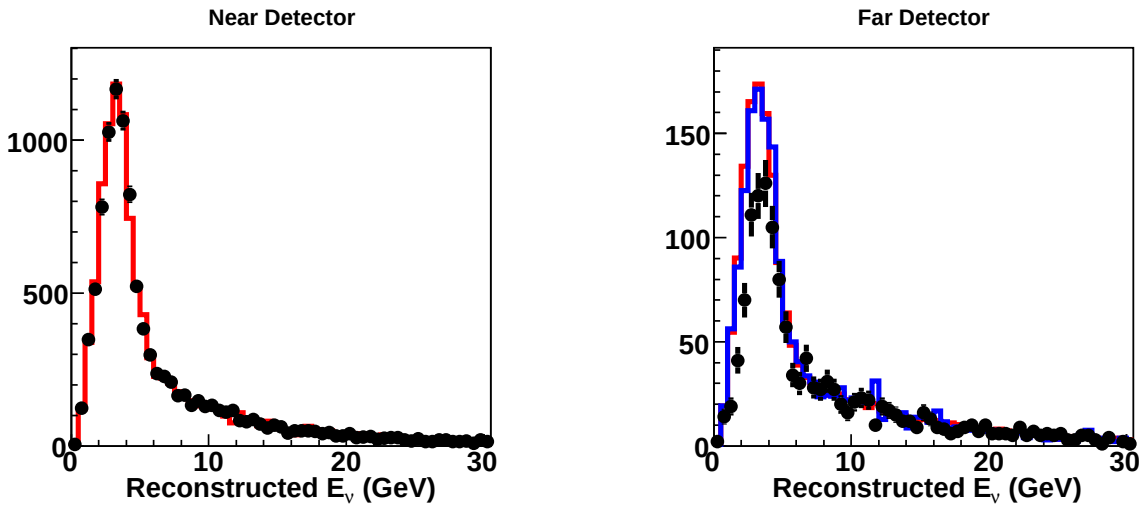


Figure 3: Mock data challenge spectra. To the left, the Near Detector neutrino energy spectrum. Red shows Monte Carlo, black shows mock data. To the right, the Far Detector neutrino energy spectrum. Red shows Monte Carlo, blue shows the predicted Far Detector spectrum in the case of no oscillations, black shows the mock data.

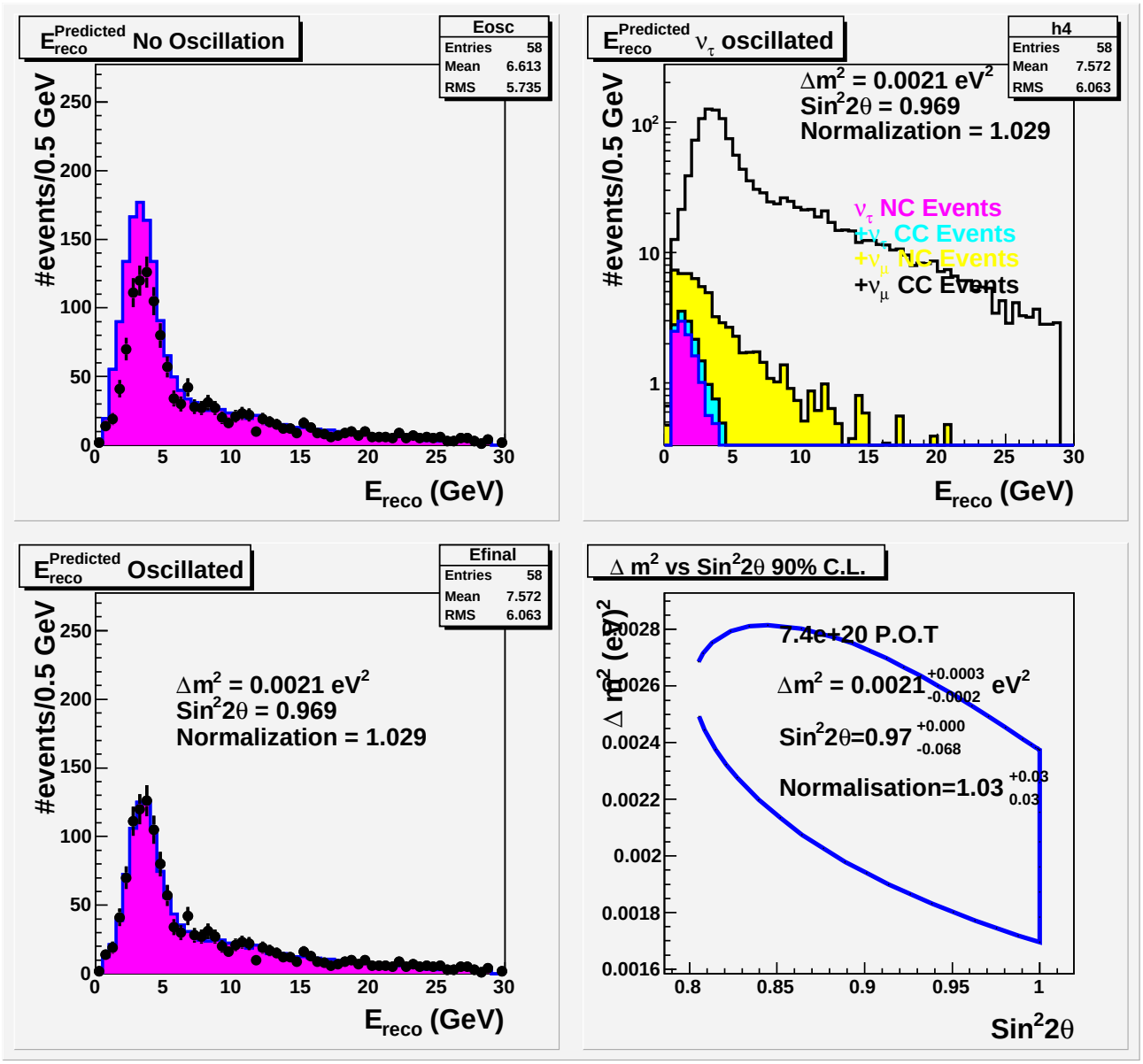


Figure 4: Results from the Mock Data Challenge. Top left shows the predicted far spectrum with no oscillations in blue, and the mock data spectrum in black. Top right shows the different components of the spectrum. Bottom left shows the mock data spectrum with the predicted spectrum from the best fit superimposed. Bottom right shows the 90% confidence region and quotes the best fit parameters with their errors.

3.2 No Systematic Included

Figure 5 shows the results of fitting the Far Detector spectrum with no systematic effects included. The fake data come from the same underlying distribution as the Monte Carlo, but with oscillation parameters of $\Delta m^2 = 0.0022$ eV^2 and $\sin^2 2\theta = 0.9$. The spectrum shown corresponds to a "smoothed" experiment. The spectrum comes from a Monte Carlo sample with 2.6×10^{22} protons on target, and is scaled to 1×10^{20} protons on target; no statistical fluctuations are introduced. The top left plot shows the Far Detector predicted spectrum in the case of no oscillations in blue, and the fake data in black. The top right plot shows the components of the predicted spectrum. The bottom left plot shows the data with the best-fit oscillated predicted Far spectrum super-imposed. The bottom right plot quotes the best fit values with their errors and shows the 68% and 90% confidence contours. The best fit values of Δm^2 , $\sin^2 2\theta$ and the normalization all agree with the generated values.

Figure 6 shows the results from 500 pseudo experiments with no sources of systematic errors, but with the data points statistically fluctuated. The top left plot shows the best fit value of Δm^2 for each pseudo experiment, the top middle plot shows the best fit value of $\sin^2 2\theta$, and the top right plot shows the best fit value of the overall normalization. The middle row shows histograms of the error obtained for each of the three fit parameters, left shows the error in Δm^2 , middle shows the error on $\sin^2 2\theta$, and the right shows the error on the normalization. The bottom left plot shows how many sigma the best fit value of Δm^2 was from the generated value, the bottom middle plot shows the number of sigma $\sin^2 2\theta$ was from the generated value, while the bottom right shows the number of sigma the best fit value of the normalization was from the true value. The histograms each only have 310 entries, indicating that the fits from 190 pseudo runs either failed to converge, or returned a value of $\sin^2 2\theta$ greater than 2. Furthermore, we note that the mean best fit value is larger than the input value. To understand the high failure rate of fits, several single failures were studied in detail. Figure 7 shows a characteristic failed fit. In this case, the fit fails due to the unfortunate statistical spread of the points; however, if $\sin^2 2\theta$ is bounded to be in the physical region, the fit converges. When $\sin^2 2\theta$ is limited to be in the physical region, 90% of the fits converge.

As an attempt to understand why the mean best fit values of the parameters are higher than the input values, 500 pseudo experiments were run using 10 times the statistics for each run. The summary plots for the increased number of events is shown in Figure 8. In these runs with increased statistics, all but two of the pseudo experiments converged and returned reasonable best fit values. Furthermore, the means of the best fit values agree with the generated values, indicating that the bias in the mean fit values seen from the 1×10^{20} pseudo runs stem from the low statistics samples.

Figure 9 shows the average value of Δm^2 obtained when the fake data is oscillated with different values of Δm^2 for 1×10^{20} protons on target and $\sin^2 2\theta$ =0.9. Figures 10 and Figures 11 show the mean best fit values of $\sin^2 2\theta$ and the normalization respectively. For low generated Δm^2 and 1×10^{20} protons on target, the average best fit of Δm^2 tends to be larger than the generated value. For larger values of generated Δm^2 , we tend to get best fit values of Δm^2 slightly lower than the generated value. The best fit of $\sin^2 2\theta$ does not seem to vary much with the generated value of Δm^2 , but the best fit value of the normalization tends to match the generated value better for higher generated Δm^2 .

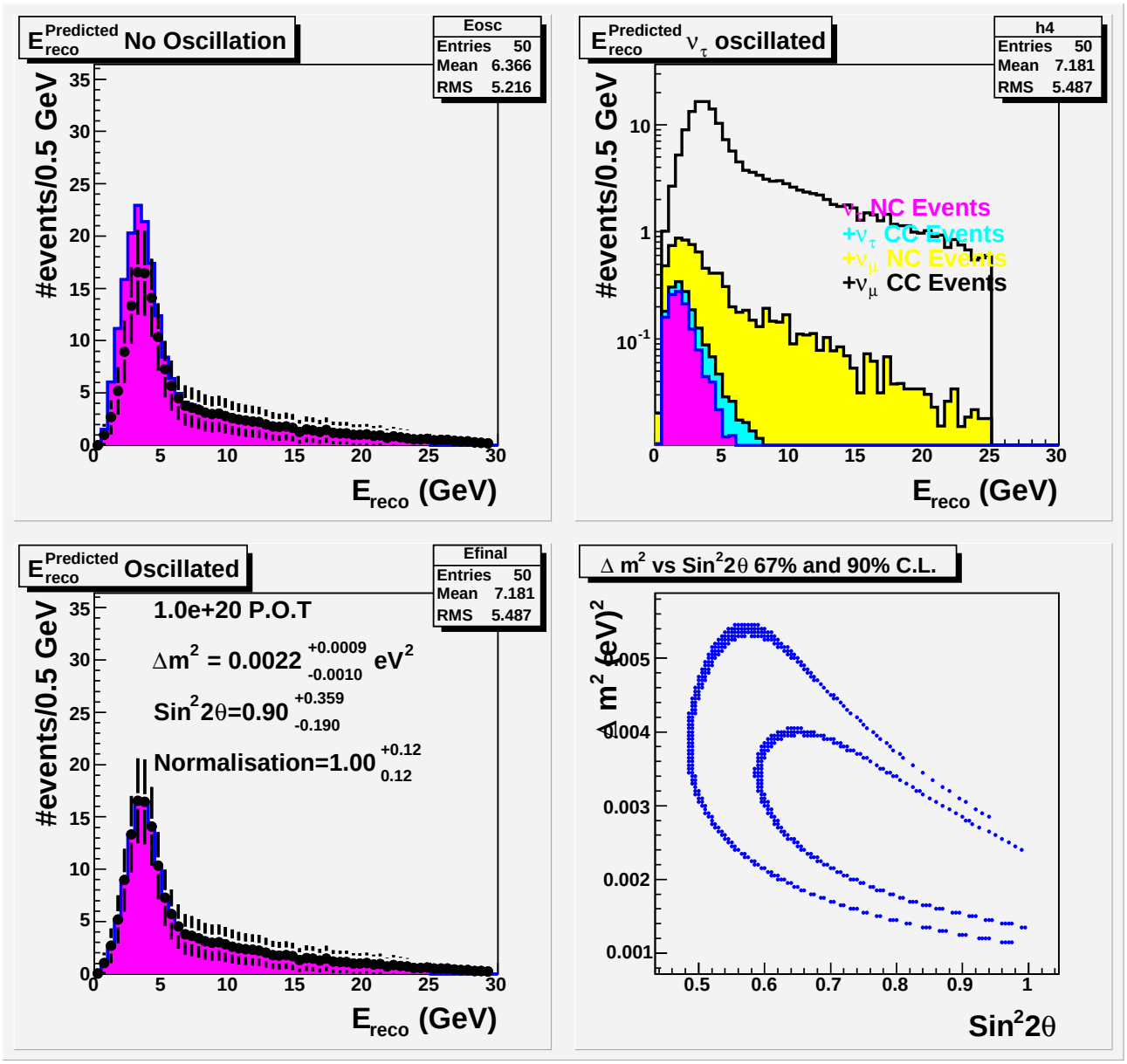


Figure 5: Results of a smoothed run with no sources of systematic errors included. Top left shows the predicted far spectrum with no oscillations in blue, and the fake data spectrum in black. The fake data was drawn from the same underlying distribution as the Monte Carlo, but oscillated with Δm^2 =0.0022 eV^2 and $\sin^2 2\theta$ = 0.9. Top right shows the different components of the spectrum. Bottom left shows the fake data spectrum with the predicted spectrum from the best fit superimposed and quotes the best fit parameters with their errors. Bottom right shows the 68% and 90% confidence regions

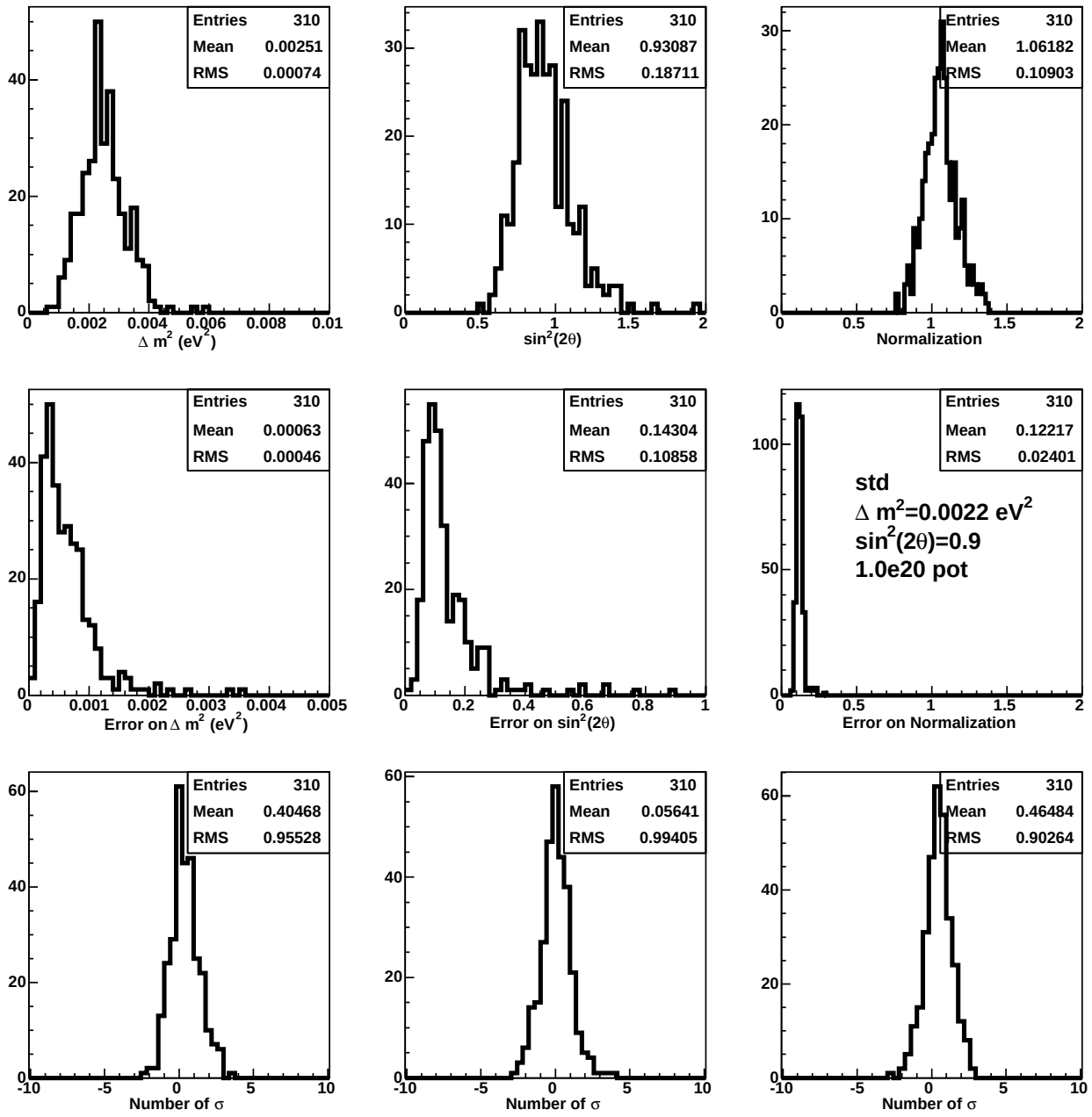


Figure 6: The top left plot shows the best fit value of Δm^2 for each pseudo experiment, the top middle plot shows the best fit value of $\sin^2 2\theta$, and the top right plot shows the best fit value of the overall normalization. The middle row shows histograms of the error obtained for each of the three fit parameters, left shows the error in Δm^2 , middle shows the error on $\sin^2 2\theta$, and the right shows the error on the normalization. The bottom left plot shows how many sigma the best fit value of Δm^2 was from the generated value, the bottom middle plot shows the number of sigma $\sin^2 2\theta$ was from the generated value, while the bottom right shows the same for the normalization best fit value. These are for pseudo experiments with 1×10^{20} pot, Δm^2 =0.0022 eV^2 and $\sin^2 2\theta$ =0.90.

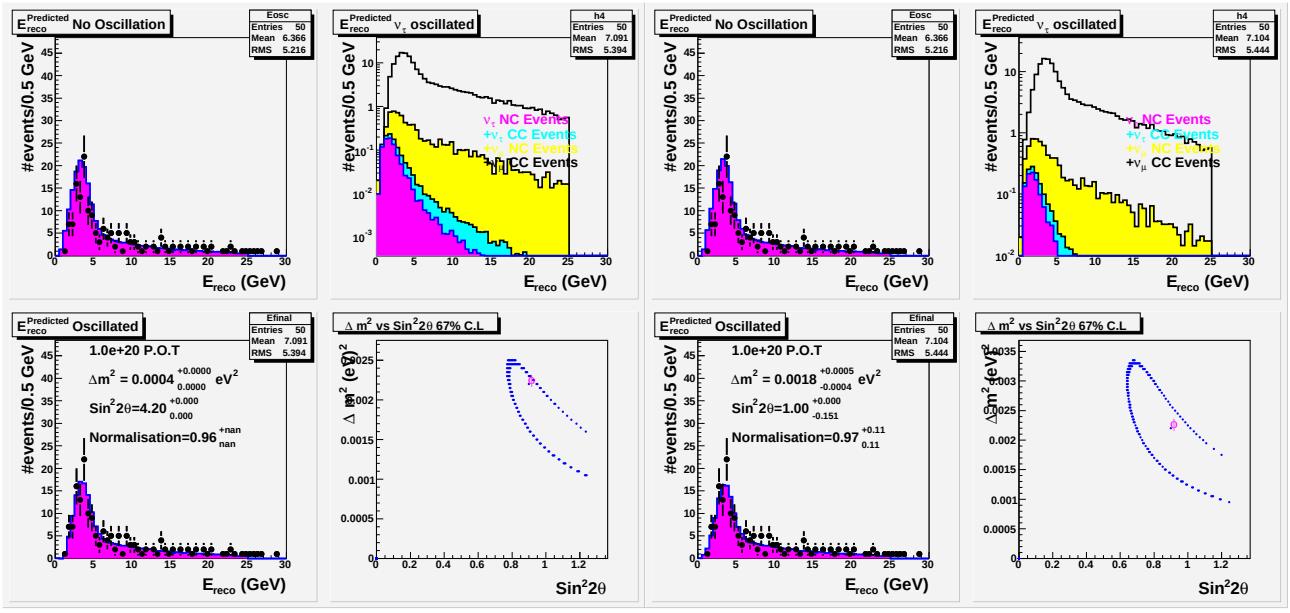


Figure 7: Two plots showing a fit failure (left) and the second fit when $\sin^2 2\theta$ is bounded to be in the physical region (right).

3.3 Investigating sources of systematic errors

A number of different sources of systematic errors were investigated. Monte Carlo was modified in the ways described below, then fake data samples were generated from the modified Monte Carlo with statistics corresponding to 1×10^{20} protons on target. Five-hundred pseudo experiments were performed on each of the modified fake data sets.

- **Cross Section Parameter Variations** To study the effect of changes in the cross section parameters, the LE Monte Carlo was reweighted using the MCReweight+NeugenInterface packages to account for 50% changes in qe_ma and res_ma, both individually and together. The fake data was generated using the reweighted Monte Carlo sample. The standard LE Monte Carlo was used to evaluate the Far/Near ratio. Even with large changes to these cross section parameters, the best fit values of Δm^2 , $\sin^2 2\theta$ and the normalization are on average within the one σ errors of the generated values.

- **Intranuke** Variations in the effect of Intranuke were explored by generating the fake data set from a Monte Carlo sample in which the reconstructed shower energy was increased by 10% in both detectors. Once again, the best fit values of the parameters are consistent with the generated values.

- **Calibration Errors** Errors in the Calibration were explored by generating the fake data set from a Monte Carlo sample in which the Far Detector reconstructed neutrino energy was multiplied by 80%, 90%, 110%, and 120%. The results from the 500 pseudo experiments indicate that

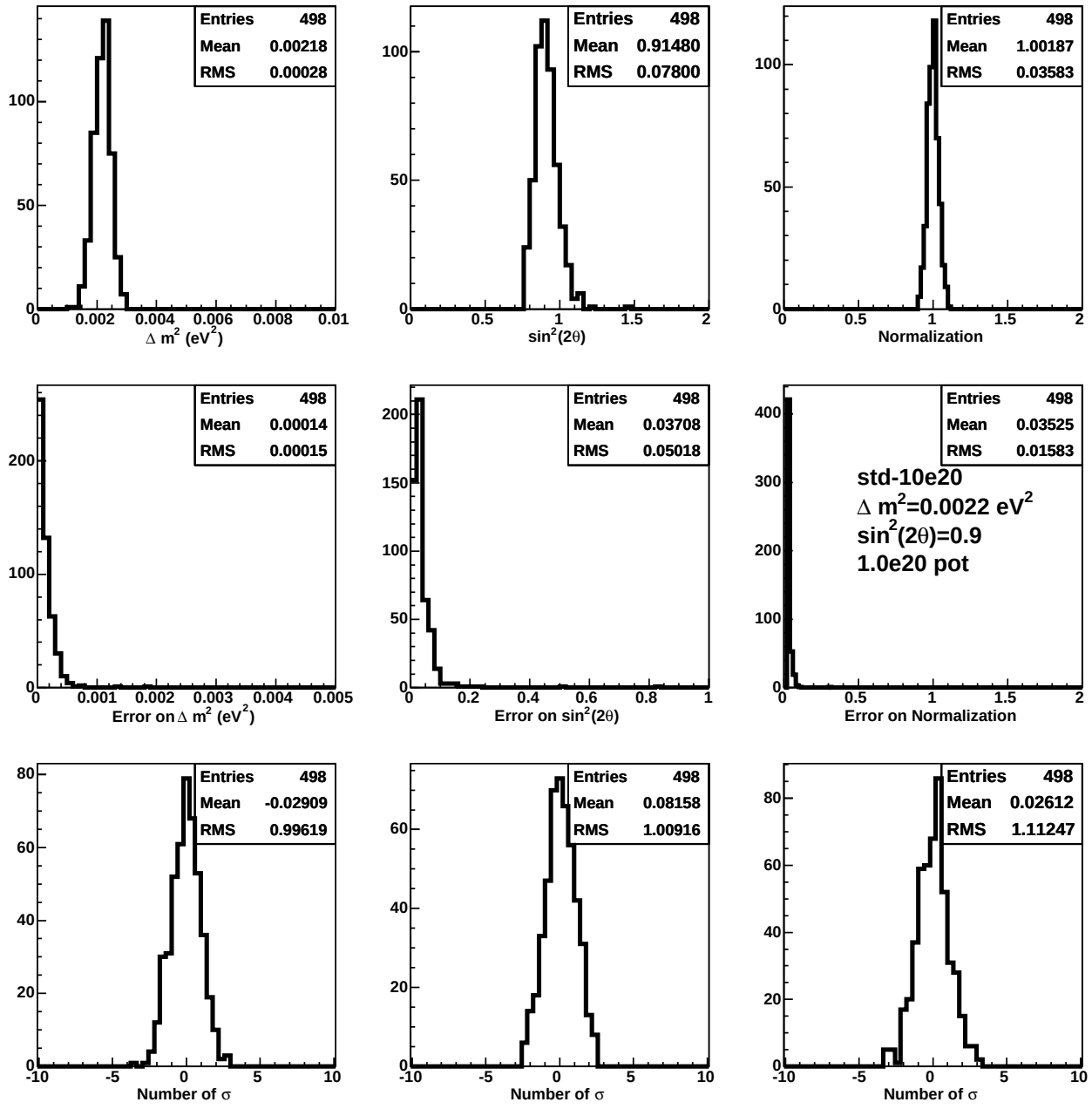


Figure 8: The top left plot shows the best fit value of Δm^2 for each pseudo experiment, for 10×10^{20}, the top middle plot shows the best fit value of $\sin^2 2\theta$, and the top right plot shows the best fit value of the overall normalization. The middle row shows histograms of the error obtained for each of the three fit parameters, left shows the error in Δm^2 , middle shows the error on $\sin^2 2\theta$, and the right shows the error on the normalization. The bottom left plot shows how many sigma the best fit value of Δm^2 was from the generated value, the bottom middle plot shows the number of sigma $\sin^2 2\theta$ was from the generated value, while the bottom right shows the same for the normalization best fit value. These are for pseudo experiments with Δm^2 =0.0022 eV^2 and $\sin^2 2\theta$ =0.90.

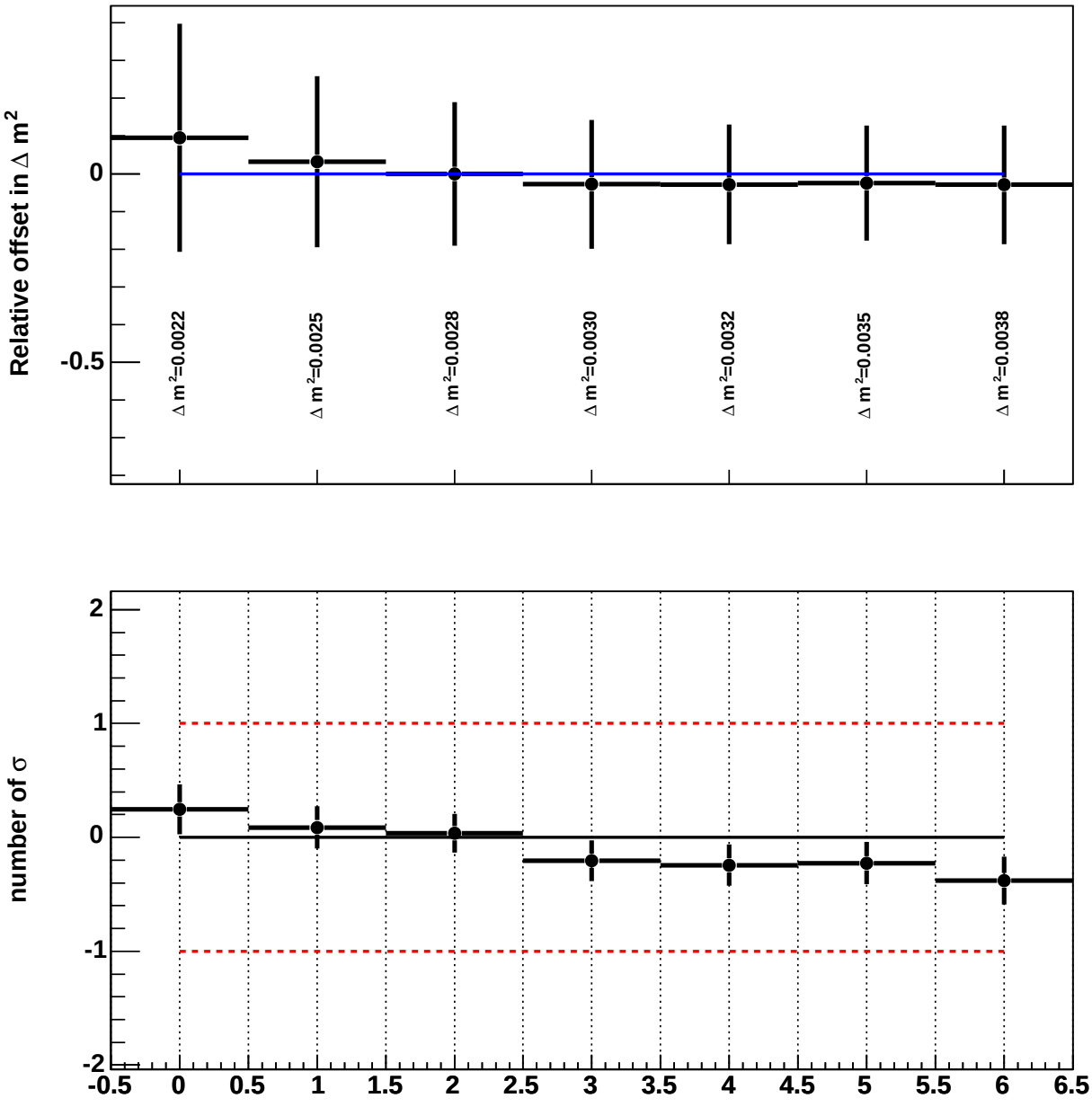


Figure 9: The top plot shows the relative difference between the average best fit value of Δm^2 and the generated value for different values of generated Δm^2 . The error bars indicate the spread of the distribution. The bottom plot shows the number of sigma the best fit value of Δm^2 is away from the generated value for the different values of generated Δm^2 . These are for pseudo experiments with 1×10^{20} pot and $\sin^2 2\theta$ =0.90.

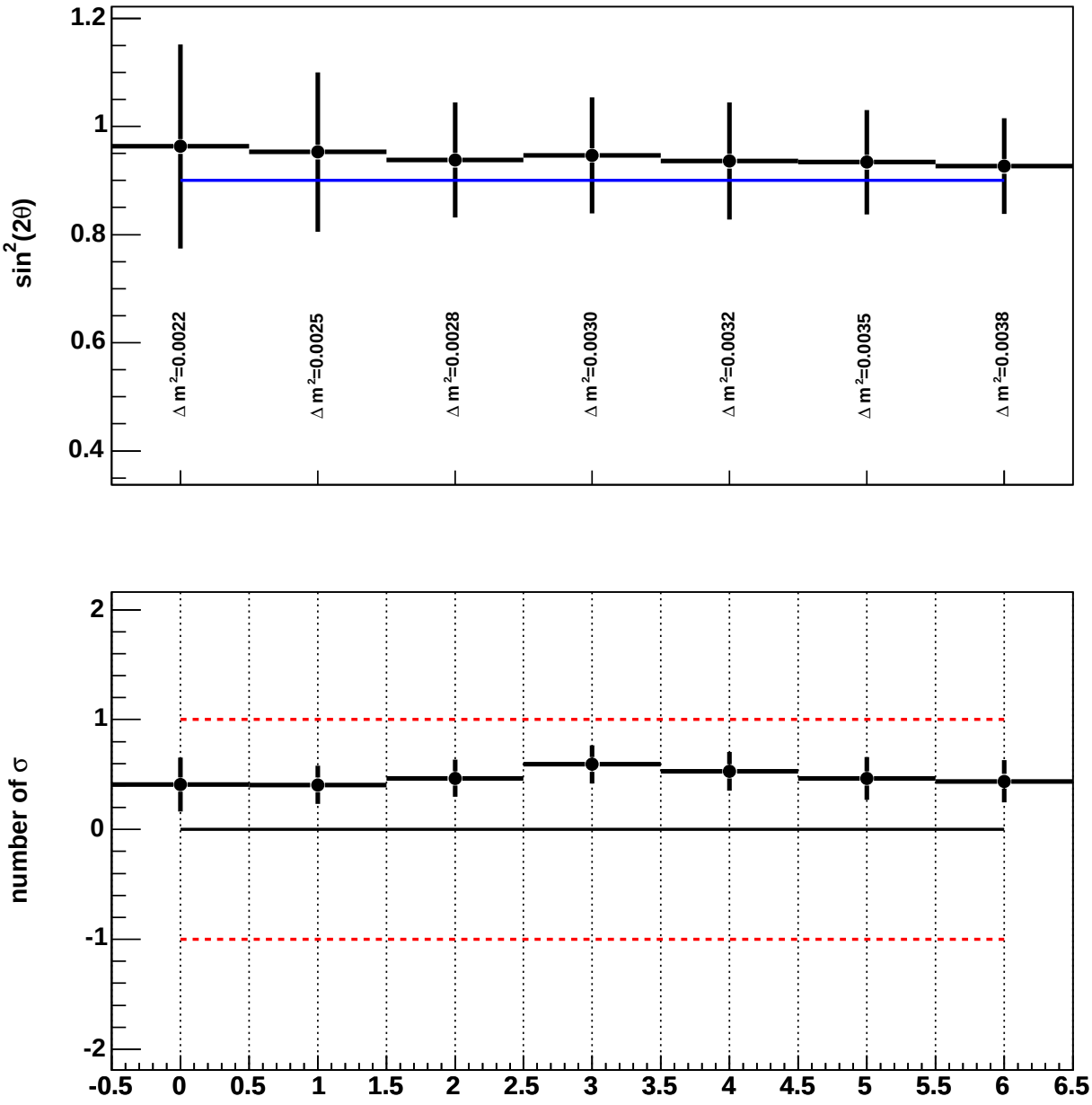


Figure 10: The top plot shows the average best fit value of $\sin^2 2\theta$ for different values of generated Δm^2 . The error bars correspond to the spread of the distribution. The bottom plot shows the number of sigma the best fit value of $\sin^2 2\theta$ is from the generated value of $\sin^2 2\theta$ for different values of generated Δm^2 . These are for pseudo experiments with 1×10^{20} pot and $\sin^2 2\theta$ =0.90.

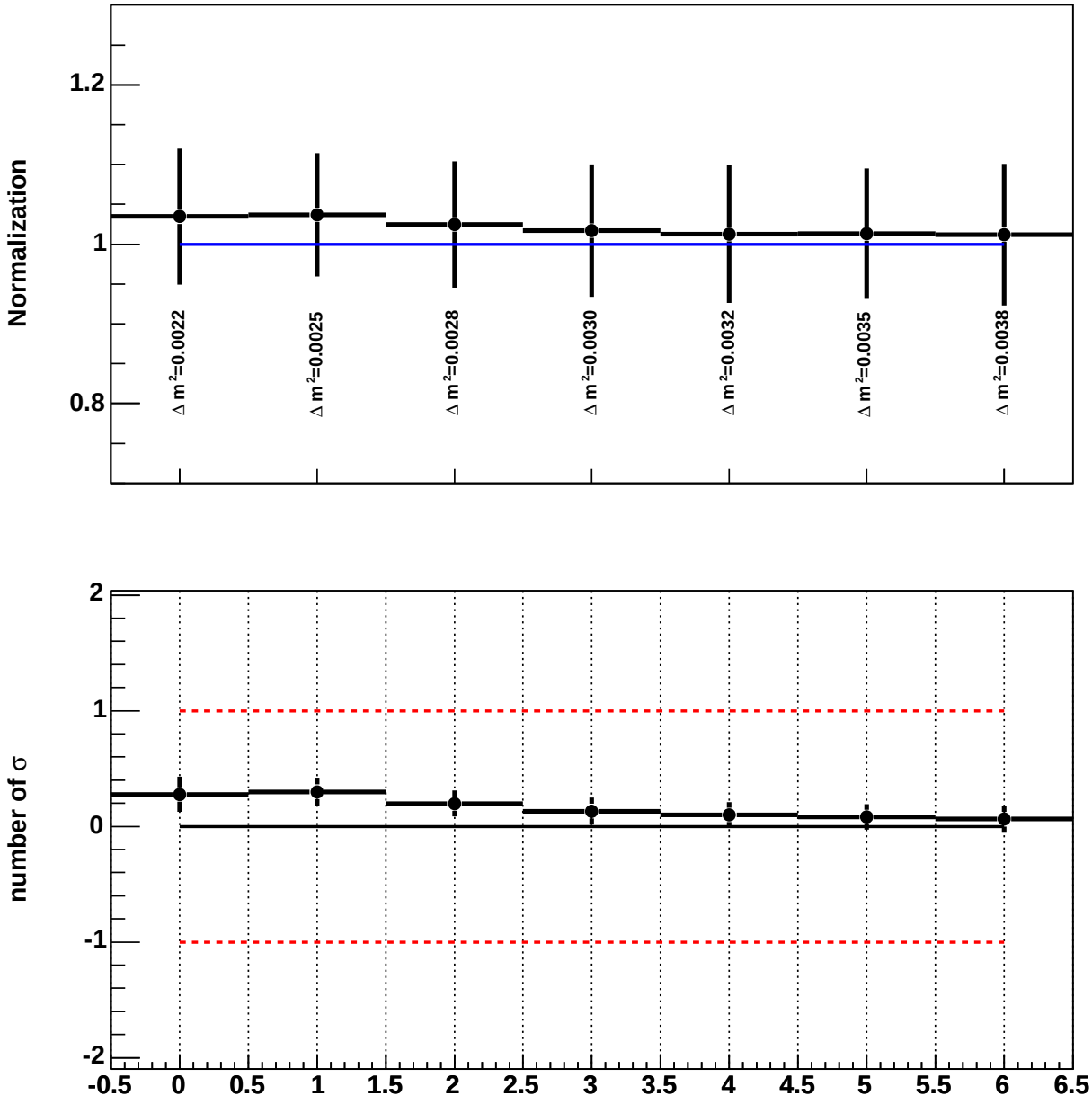


Figure 11: The top plot shows the average best fit value of $\sin^2 2\theta$ for different values of the generated normalization. The error bars correspond to the spread of the distribution. The bottom plot shows the number of sigma the best fit value of the normalization is from the generated value for different values of generated Δm^2 . These are for pseudo experiments with 1×10^{20} pot and $\sin^2 2\theta$ =0.90.

calibration differences between the two detectors must be kept below 5% for the 1×10^{20} proton on target measurement.

- **Different Flux Predictions** Fake data were generated for a number of different beam configurations by reweighting the standard Monte Carlo to the different flux spectra by using histograms provided by Zarko. The spectra were reweighted to the LE10, LE10 170kA, MARS LE10, MARS LE10 170kA, and MARS LE10 200kA beams. Furthermore, the standard LE beam was weighted up and down by the beam systematic errors on the F/N ratio. Even when the fake data is reweighted to the different beam configurations, the average best fit values of Δm^2 and $\sin^2 2\theta$ are consistent with the generated values.

- **Proton on Target Normalization Errors** The fake data spectra were scaled to 90% and 110% of the true value, then the fit was performed. This scaling is absorbed into the best fit value of the normaliztion in the fit. The average best fit values of Δm^2 and $\sin^2 2\theta$ are consistent with the generated values.

- **Neutral Current contamination** The fake data samples were taken from distributions in which the number of neutral current background events were doubled. The average best fit of all parameters are consistent with the generated values.

- **ND data-MC 'unknown' differences** In another study, the first 7 bins of reconstructed neutrino energy were increased by 10% , but no changes were made to the Far Detector reconstructed energy spectrum. This modification was meant to mimic the effect of detector differences such as PMT after pulsing. Again, with this modification, the average best fit values of Δm^2 , $\sin^2 2\theta$ and the normalization agree with the generated values. Finally, pseudo experiments were performed in which the fake data were taken from the standard LE Monte Carlo, but the predicted spectrum came from multiplying the F/N ratio by the measured Near spectrum with the beam in the LE-10 position. Even with substantial differences in the Near spectrum propagated to the Far predicted spectrum, but not the Far fake data spectrum, the average best fit values of all the fit parameters agree with the generated values.

Appendix A shows fits and contours to the smoothed distributions for some of the systematic studies. Appendix B shows distributions from the pseudo experiments plots for each study. An overall summary of the results are shown in Figures 12, 13, and 14. These figures each have two plots: the top plot shows the mean best fit value for each parameter for each of the systematic studies shown. The vertical line indicates the generated value, and the error bars on the points represents the spread of the distribution. The lower plot shows the mean number of sigma the best fit value was from the generated value. Figure 12 summarizes the results for the best fit value of Δm^2 , Figure 13 summarizes the results for the best fit value of $\sin^2 2\theta$, and Figure 14 summarizes the results for the best fit values of the normalization.

We also looked at the effects of some of the above modifications on a larger data set. Figures 15 16, and 17 show the summary of results for experiments with 10 times the statistics. From these plots, we see that even 5% relative calibration errors begin to cause larger than 1 σ deviations from the true value of $\sin^2 2\theta$ for higher statistics samples.

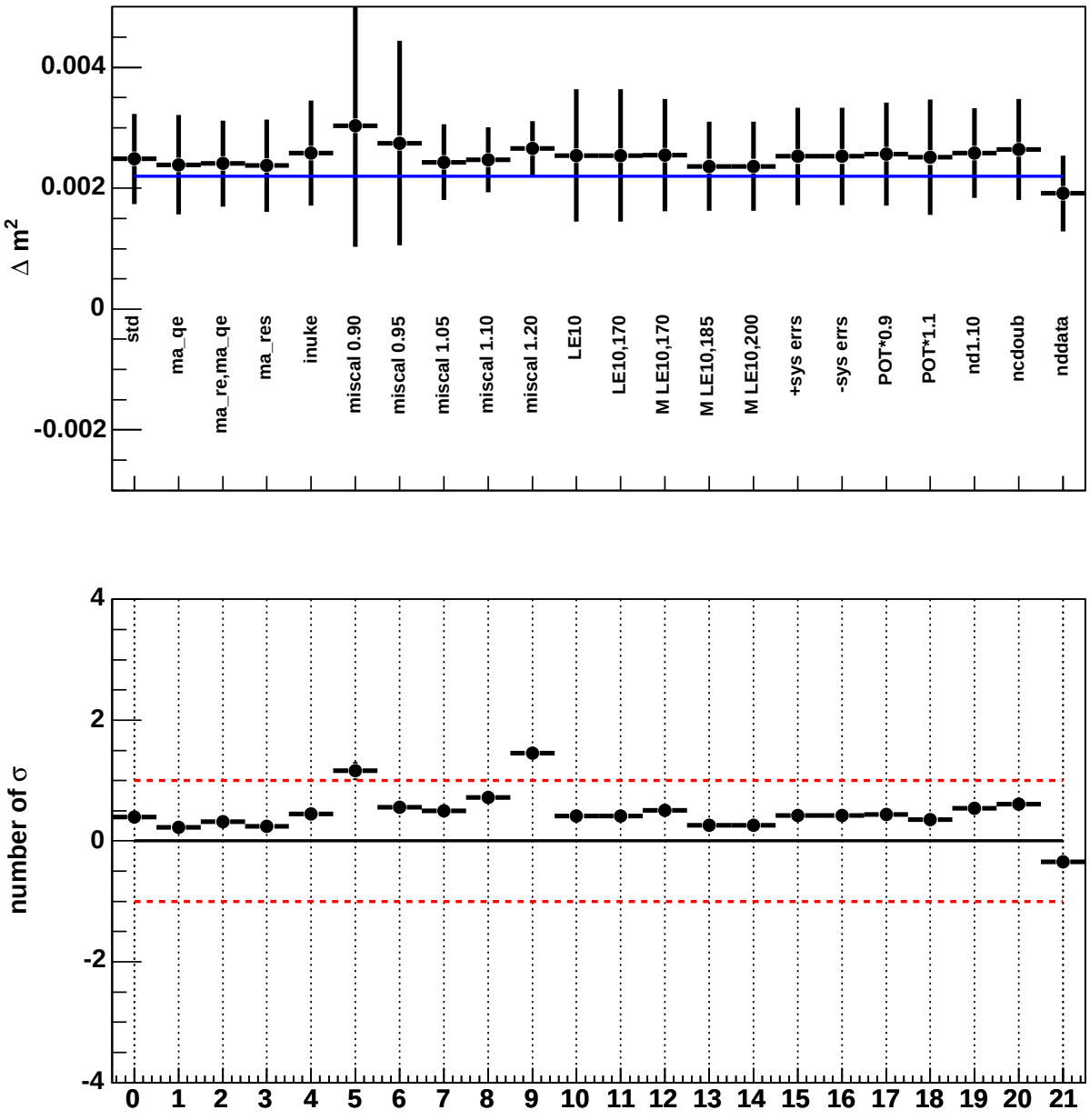


Figure 12: Results of the systematics study on the parameter measurement of Δm^2 for 1×10^{20} pot. Top plot shows the average best fit value of Δm^2 . The vertical line indicates the generated value. The error bars represent the spread of the distribution. The bottom plot shows the mean number of σ the best fit value is from the generated value of Δm^2 . The pseudo experiments were generated with Δm^2 =0.0022 eV^2 and $\sin^2 2\theta$ =0.90.

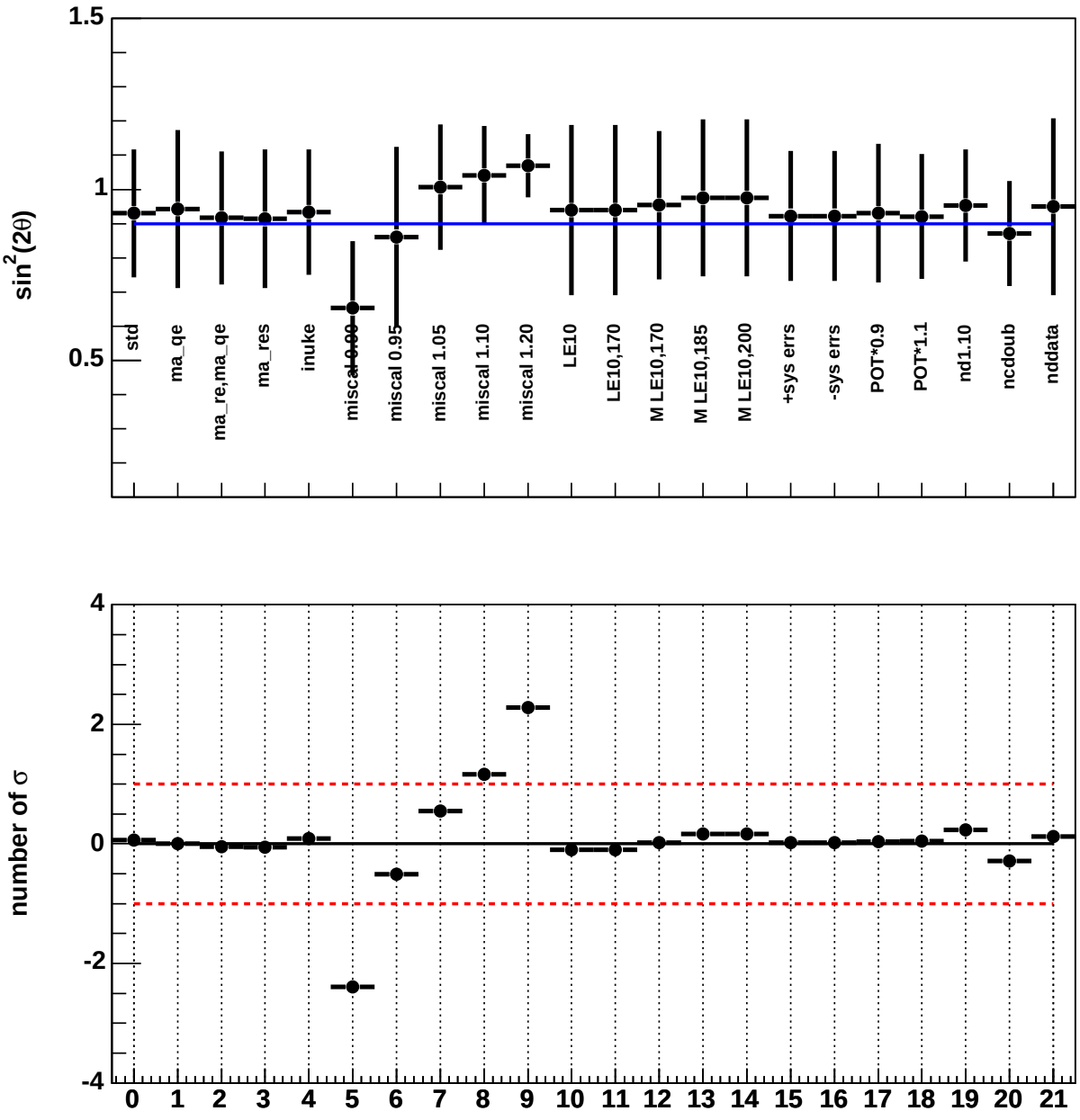


Figure 13: Results of the systematics study on the parameter measurement of $\sin^2 2\theta$ for 1×10^{20} pot. Top plot shows the average best fit value of Δm^2 . The vertical line indicates the generated value. The error bars represent the spread of the distribution. The bottom plot shows the mean number of σ the best fit value is from the generated value of $\sin^2 2\theta$. The pseudo experiments were generated with Δm^2 =0.0022 eV^2 and $\sin^2 2\theta$ =0.90.

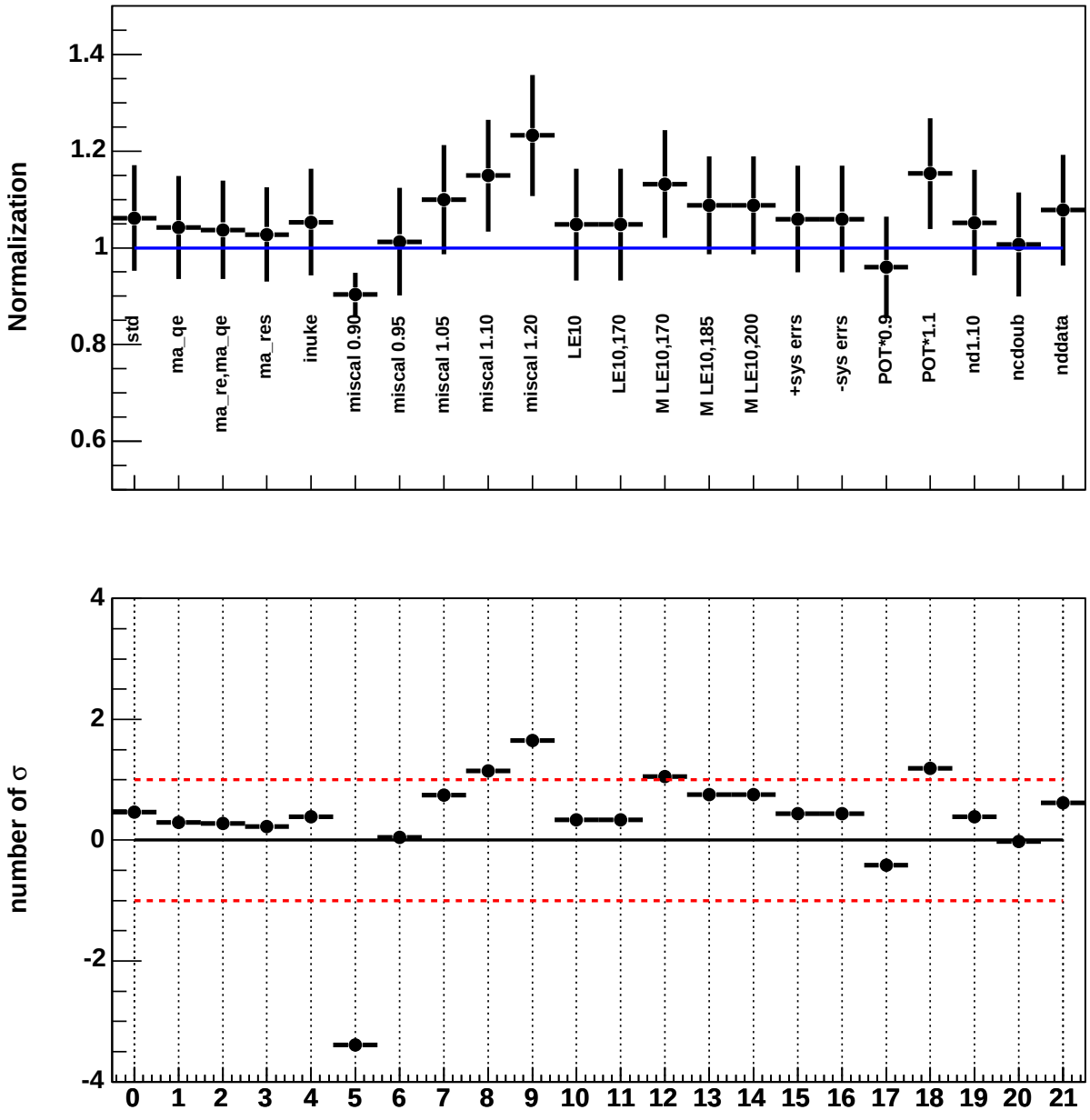


Figure 14: Results of the systematics study on the parameter measurement of the normalization for 1×10^{20} pot. Top plot shows the average best fit value of the normalization. The vertical line indicates the generated value. The error bars represent the spread of the distribution. The bottom plot shows the mean number of σ the best fit value is from the generated value of the normalization. The pseudo experiments were generated with Δm^2 =0.0022 eV^2 and $\sin^2 2\theta$ =0.90.

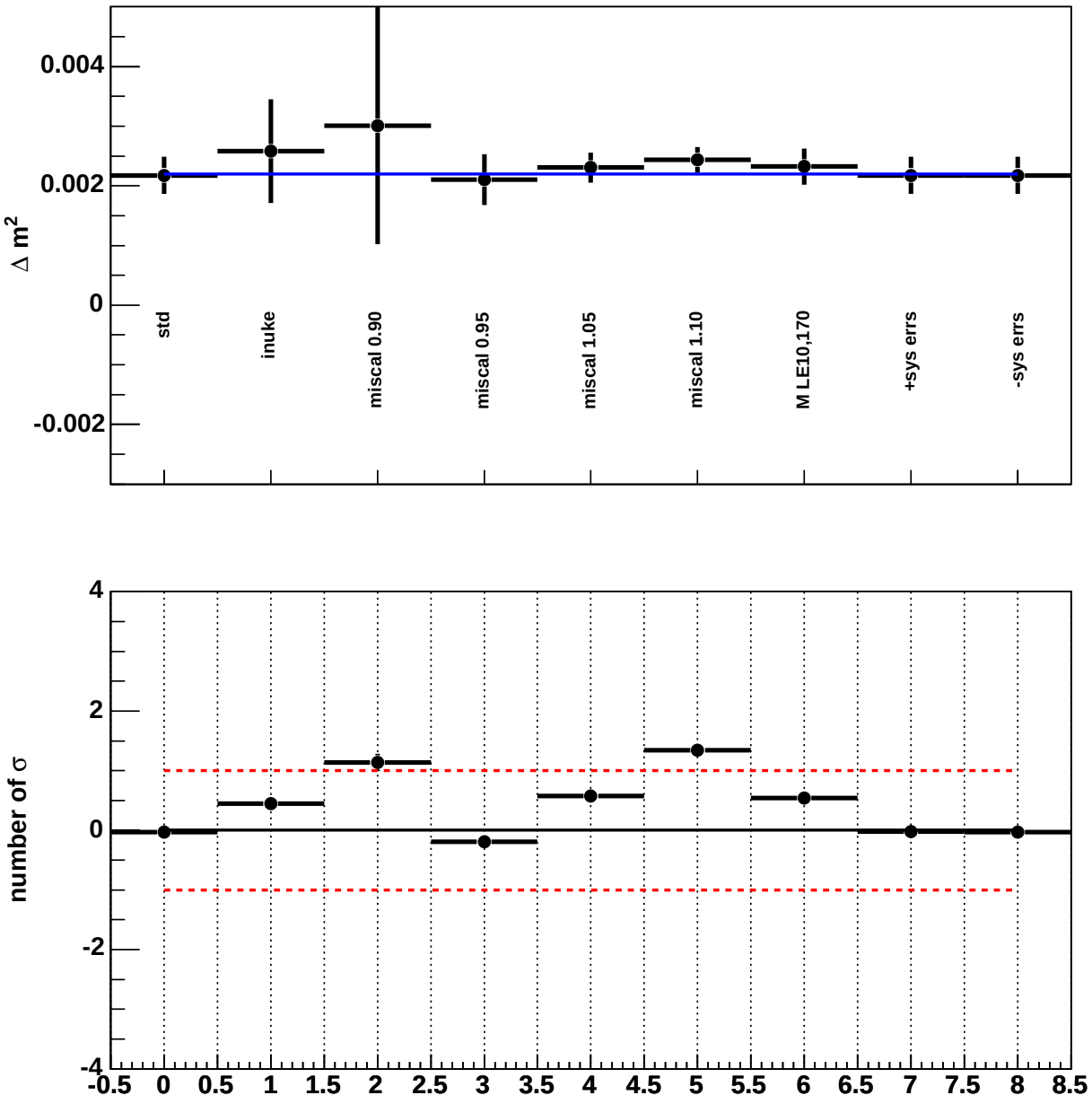


Figure 15: Results of the systematics study on the parameter measurement of Δm^2 with 10×10^{20} pot. Top plot shows the average best fit value of Δm^2 . The vertical line indicates the generated value. The error bars represent the spread of the distribution. The bottom plot shows the mean number of σ the best fit value is from the generated value of Δm^2 . The pseudo experiments were generated with Δm^2 =0.0022 eV^2 and $\sin^2 2\theta$ =0.90.

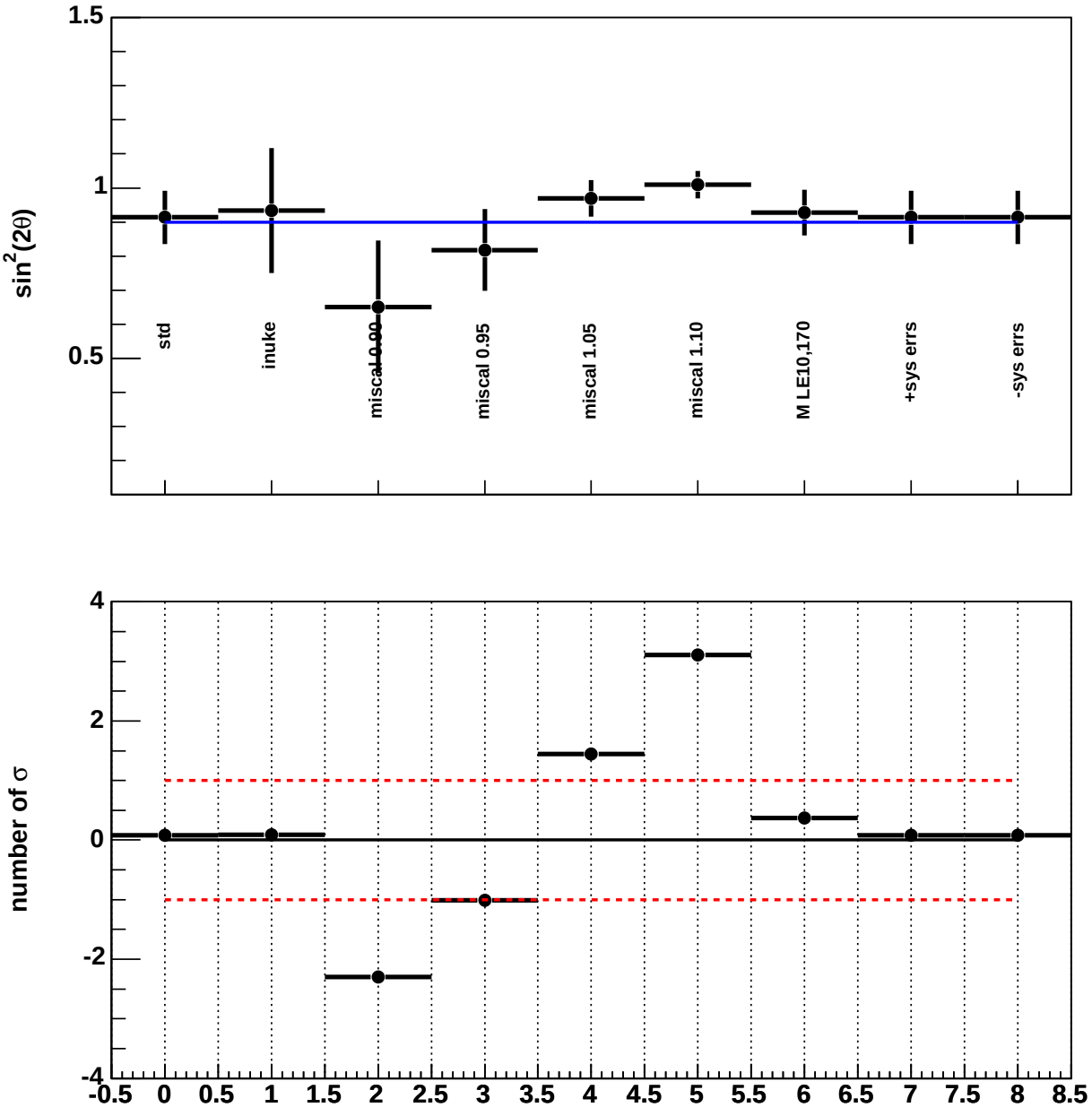


Figure 16: Results of the systematics study on the parameter measurement of $\sin^2 2\theta$ with 10×10^{20} pot. Top plot shows the average best fit value of $\sin^2 2\theta$. The vertical line indicates the generated value. The error bars represent the spread of the distribution. The bottom plot shows the mean number of σ the best fit value is from the generated value of $\sin^2 2\theta$. The pseudo experiments were generated with Δm^2 =0.0022 eV^2 and $\sin^2 2\theta$ =0.90.

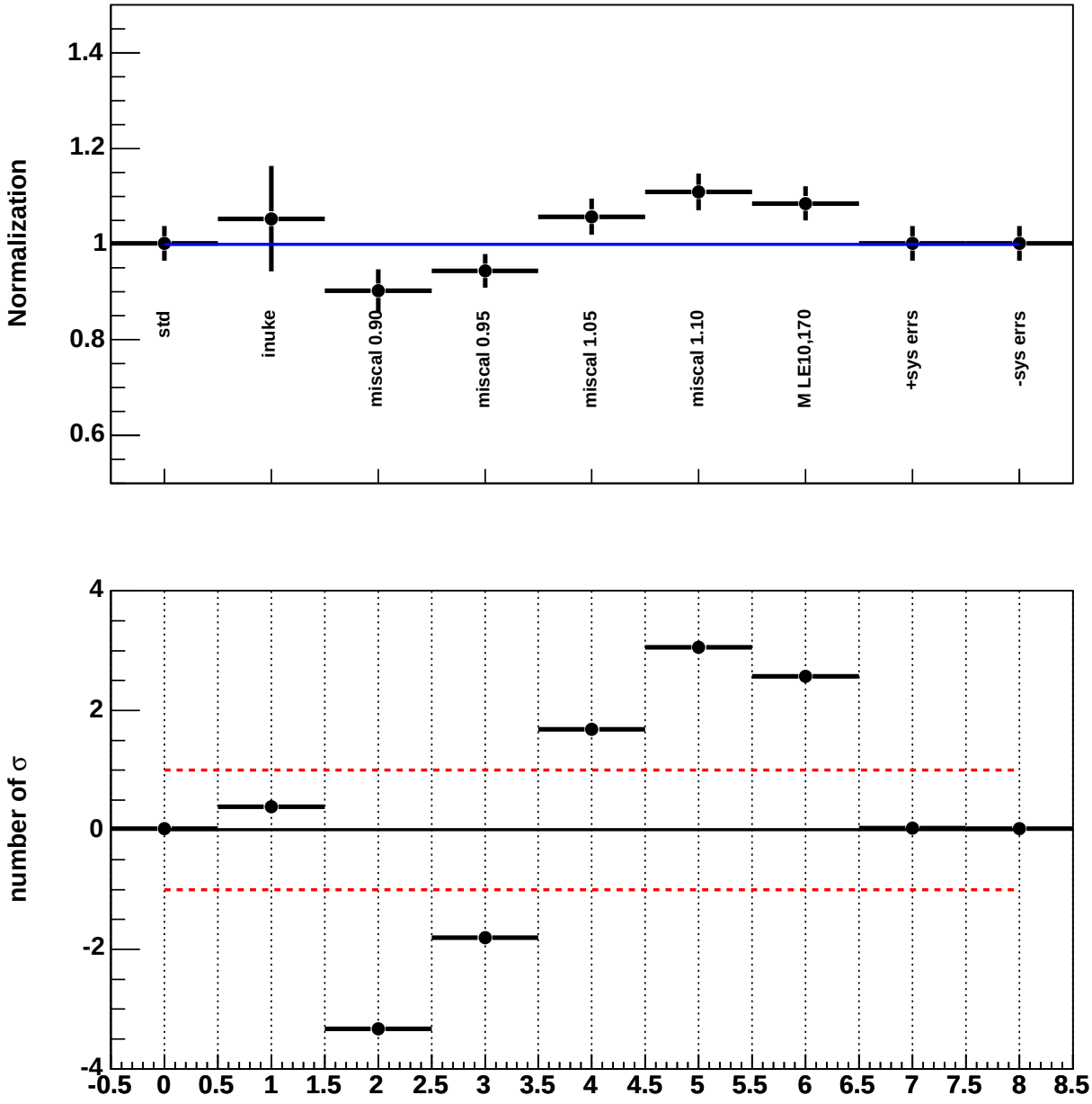


Figure 17: Results of the systematics study on the parameter measurement of the normalization, with 10×10^{20} pot. Top plot shows the average best fit value of the normalization. The vertical line indicates the generated value. The error bars represent the spread of the distribution. The bottom plot shows the mean number of σ the best fit value is from the generated value of the normalization.

4 The Matrix Method

The ratio method has a draw back in that any differences between data and Monte Carlo in a given energy bin will be propagated to the same energy bin the in the Far Detector spectrum. If the difference between data and Monte Carlo arises from cross section differences, this is the appropriate way to propagate those differences; however, differences in the spectra caused by the underlying pion parent flux would cause differences in the Far Detector spectrum in a different neutrino energy bin than the difference appears in the Near Detector. Thus, we are investigating a complementary method of predicting the Far Detector spectrum. This involves the Matrix Transport Method, first put forward by Szleper and Para [1], to transport the Near Detector spectrum to a predicted Far Detector spectrum. This method of transporting a measured Near Detector spectrum to the Far Detector exploits the correlation of the two spectra resulting from the fact that both spectra come from decays of the same underlying distribution of parent particles. For each bin in neutrino energy in the ND, the parent pions of those neutrinos can be traced and in turn, the daughter neutrinos of those pions which reach the Far Detector can be identified. For example, a single bin in neutrino energy in the ND will translate into a distribution of bins in the FD where the connection between the two is the position and P_t of the parent pions and the angular acceptance for the neutrinos in the two detectors.

The matrix is constructed by using the GNUMI flux files to create a histogram of far neutrino energy vs. near neutrino energy, weighted by the parent importance weight times the probability that a neutrino coming from the decay of this parent will hit the center of the Far Detector. Then, each bin of true near neutrino energy is divided by the number of events in the Near Detector with that energy. Figure 18 shows the matrix.

This matrix produces a flux at the Far Detector, given a Near Detector flux. Of course, what is measured is a reconstructed event spectrum at each detector, that is modulated by selection efficiencies and has background contamination. Thus, before multiplying by the matrix, one must first subtract off the backgrounds, then convert the Near Detector reconstructed energy spectrum to a true neutrino event spectrum by using the reco vs. true histograms described above. Then, the spectrum is corrected for selection efficiencies. The resulting spectrum is divided by the cross sections at the center of each bin to derive a flux. This flux is multiplied by the matrix to derive a Far Detector flux. In the case of no oscillations, the far flux is multiplied by the cross section to produce a Far Detector event spectrum, then it is multiplied by the selection efficiencies. Finally, the true spectrum is converted to a reconstructed spectrum by using the 2-d reco vs. true histogram in the Far Detector to derive a predicted, reconstructed neutrino event spectrum in the Far Detector.

In the case of oscillations, once the Far Detector flux is derived, the oscillation probability is calculated for each true energy bin. Two histograms are then made, one multiplied by the oscillation probability, P_{ν_μ}, represents the ν_μ flux, and another multiplied by $1 - P_{\nu_\mu}$ represents the ν_τ flux. The ν_μ histogram is multiplied by the total CC, ν_μ cross section, while the ν_τ histogram is multiplied by the total CC ν_τ cross section. These histograms are each multiplied by the appropriate selection efficiencies for ν_μ 's and ν_τ 's, individually converted into reconstructed neutrino histograms, then summed to give an oscillated spectrum. Figure 19 shows a schematic diagram of the steps involved in the matrix method.

Figure 20 shows the performance of the matrix method. The top left plot shows the true Near

[1] M.Szleper and A.Para, NuMI-B-781 (2001)

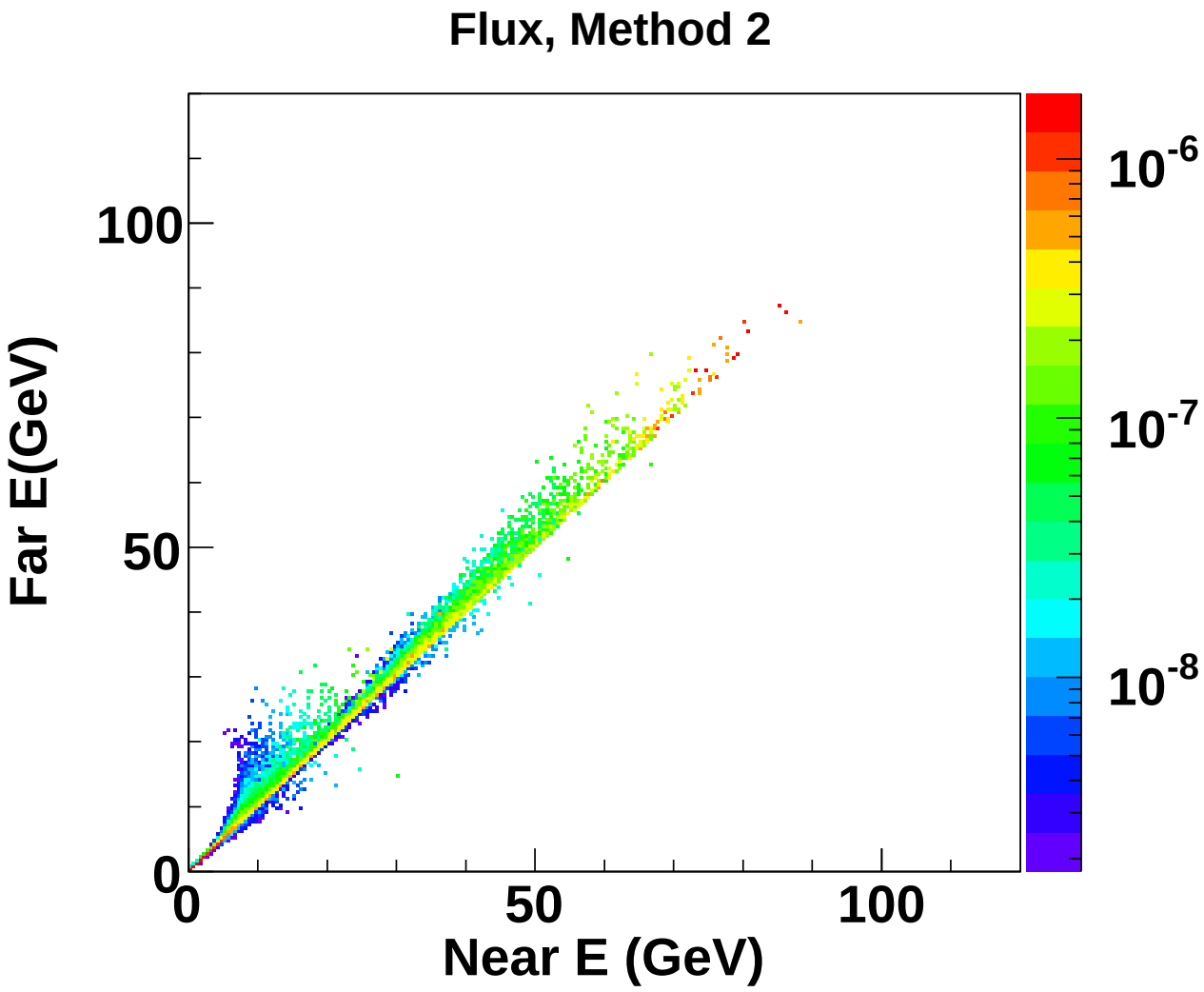


Figure 18: The Matrix; Far neutrino energy vs. Near neutrino energy

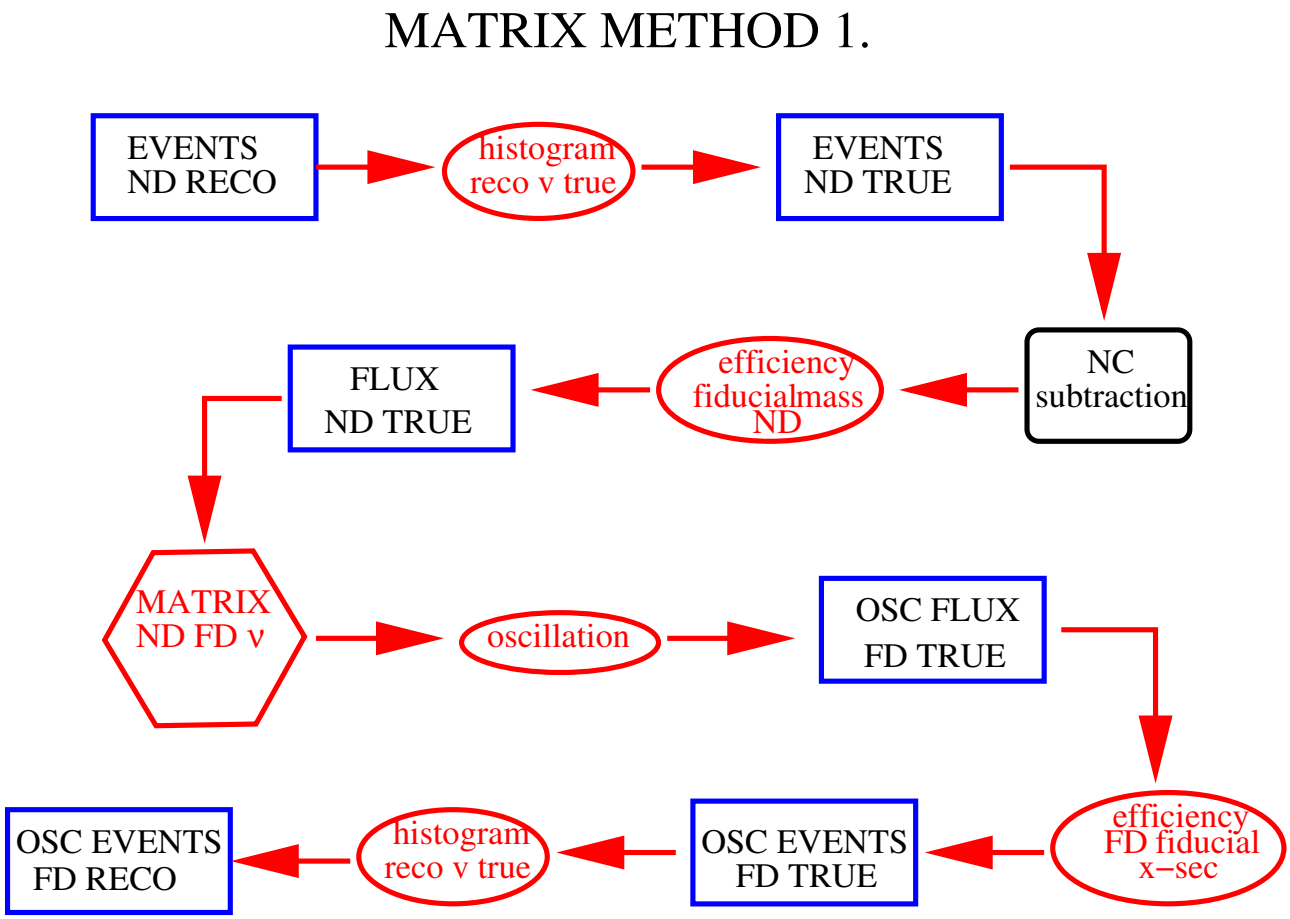


Figure 19: A schematic diagram of the steps involved in the matrix method.

Detector spectrum from the LE GMINOS Monte Carlo sample, for true CC, ν_μ events with true neutrino interaction vertices within some well defined fiducial volume. The top right plot shows the true Far Detector spectrum from the LE GMINOS Monte Carlo sample, for true CC, ν_μ events with true neutrino interaction verities within some well defined fiducial volume. The bottom left plot shows the predicted Far Detector spectrum from the matrix method superimposed on the Far Detector LE GMINOS spectrum. The predicted spectrum is scaled by the ratio of protons on target used to make the Near Detector spectrum divided by the number of protons on target to make the Far Detector spectrum times the ratio of the fiducial masses of the two detectors. The bottom right plot shows the ratio of the true spectrum divided by the predicted spectrum as a function of true neutrino energy. In these plots, the neutrino weights for the matrix are recalculated to account for neutrino vertices spread throughout a 0.5 m radius (the GNUMI weights are calculated for the center of each detector). The ratio is nearly flat with energy out to about 20 GeV, however, it is centered at about 1.05, indicating that there are about 5% more events in the GMINOS spectrum than in the predicted spectrum. This same 5% is apparent just when comparing the GMINOS spectrum to the spectrum obtained from multiplying the flux times the cross sections, indicating some as yet not understood discrepancy beween the GNUMI and GMINOS spectra. We note that the agreement between the matrix predicted Far spectrum and the GMINOS Far spectrum is better using the Carrot Monte Carlo and the v18 fluxes, and will revisit the matrix method as time allows. Figure 21 shows the comparison of the GMINOS Monte Carlo with the matrix predicition for the reconstructed energy. The agreement, although not perfect, is reasonable and constitutes mostly a scale factor which is taken into account in the fitting. The ratio of reconstructed energy is for the two methods is also shown in this figure along with the F/N ratio as calculated by the matrix method and given by GMINOS.

Many of the same tests carried out using the ratio method were revisited using the matrix method. For the pseudo experiments using the matrix method, the fake data were statistically fluctuated using random numbers from Poisson distributions instead of Gaussians as was done in the ratio method. The level of agreement for 1e20 p.o.t when there are no systematic effects present is shown in Figure 22 both for the smoothed distributions and for 500 pseudo runs. The number of entries is less than 500 in these plots. This reflects the efficiency of the fit and is a characteristic of the particular random fluctuation for particular pseudo experiments. Although these fits fail, it is clearly possible to change bin sizes in order to allow them to succeed, but this has not been attempted in an automated way. Plots from the different systematic studies are shown in Appendix C. In Figure 23 the summary of the oscillation parameter sensitivity is shown for each systematic effect for the parameter Δm^2 and its average error and $\sin^2 2\theta$ and its average error for both the matrix transport method and for comparison, the F/N ratio transport method. In Figure 24 the same summary is shown but with the results of the fits from the pseudo runs overlaid in red. This gives an impression of the level of uncertainty that is introduced from the combination of a systematic and a statistical effect.

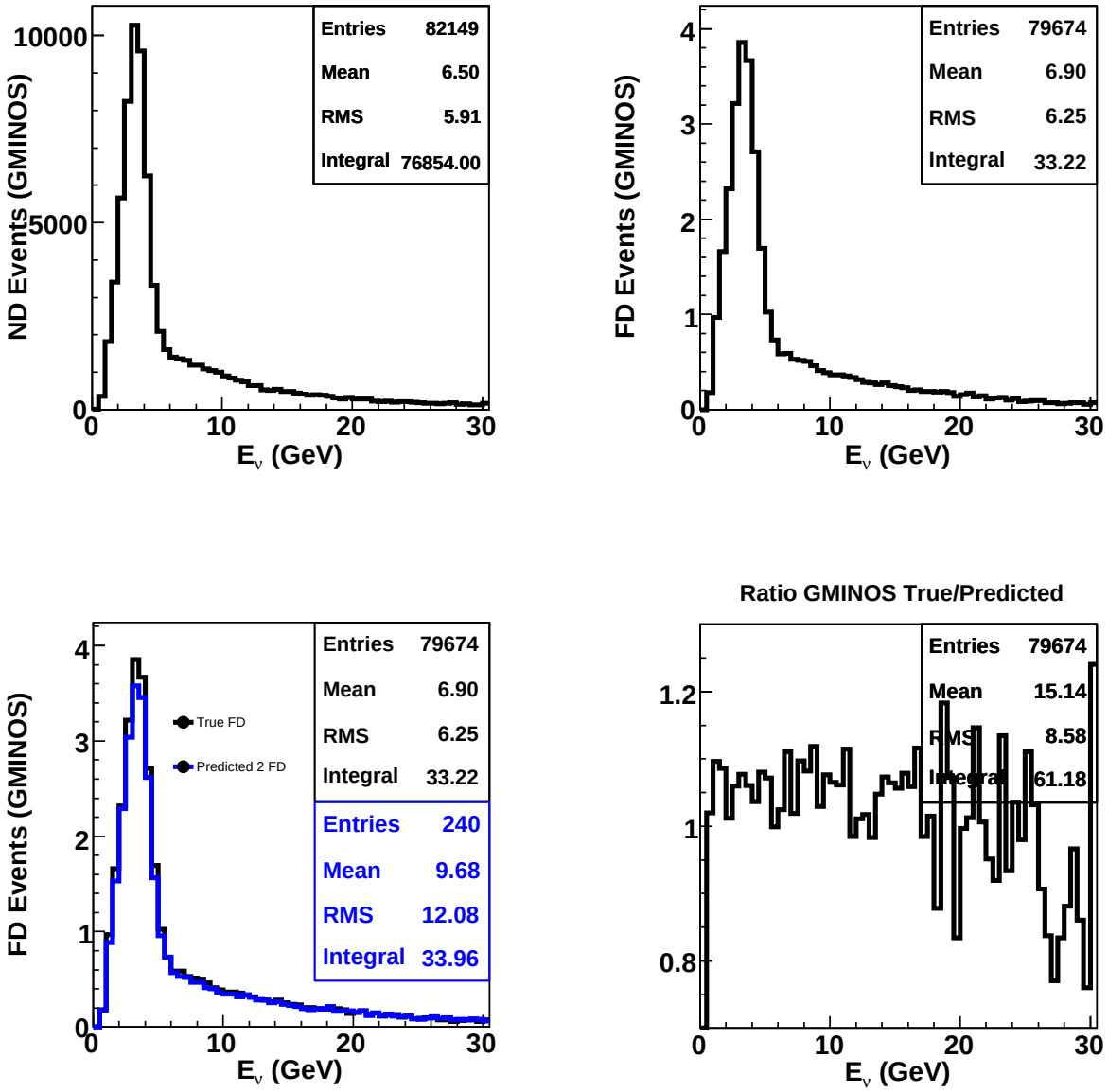


Figure 20: Top left shows the GMINOS true ND spectrum. Top right shows the true GMINOS FD spectrum. Bottom left shows the true FD spectrum in black and the matrix method FD predicted spectrum in blue. Bottom right shows the ratio of the true GMINOS spectrum over the predicted spectrum.

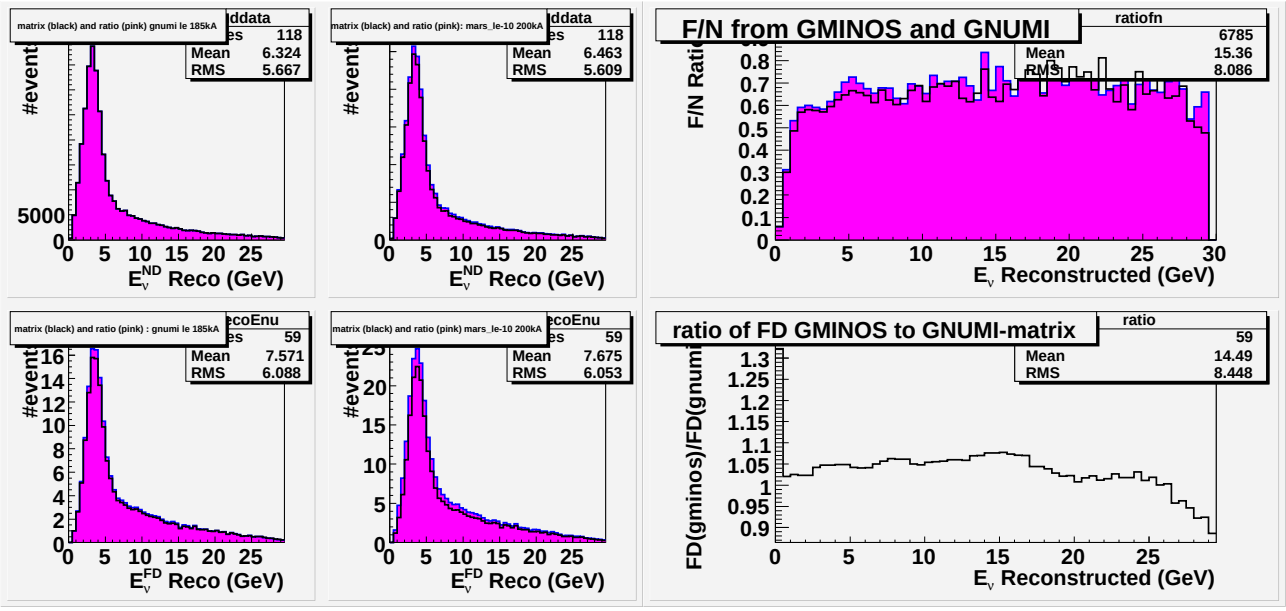


Figure 21: Left pad shows the GMINOS true ND spectrum (pink) overlayed with the matrix predicted spectrum for the standard gnumi le 185kA (left) (ND top, FD bottom) and for the mars le-10 200kA (right). The right pad shows the F/N ratio for the two methods (top) and the ratio of the FD reconstructed spectra for the two methods (bottom)

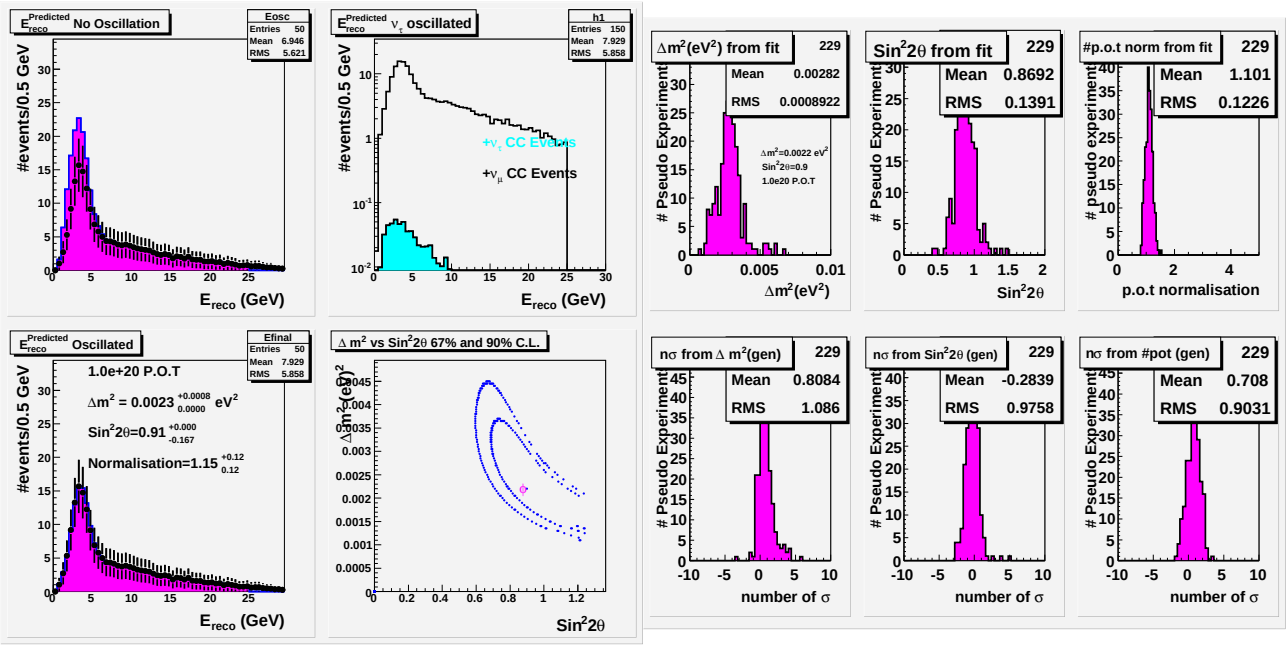


Figure 22: Sensitivity plot for the standard Monte Carlo data set with the generated oscillation parameters Δm^2 =0.0022 and $\sin^2 2\theta$ =0.9 and p.o.t = 1e20 (left) and results of 500 pseudo runs to measure the oscillation parameters Δm^2 and $\sin^2 2\theta$ and pot with no systematic effects included (right).

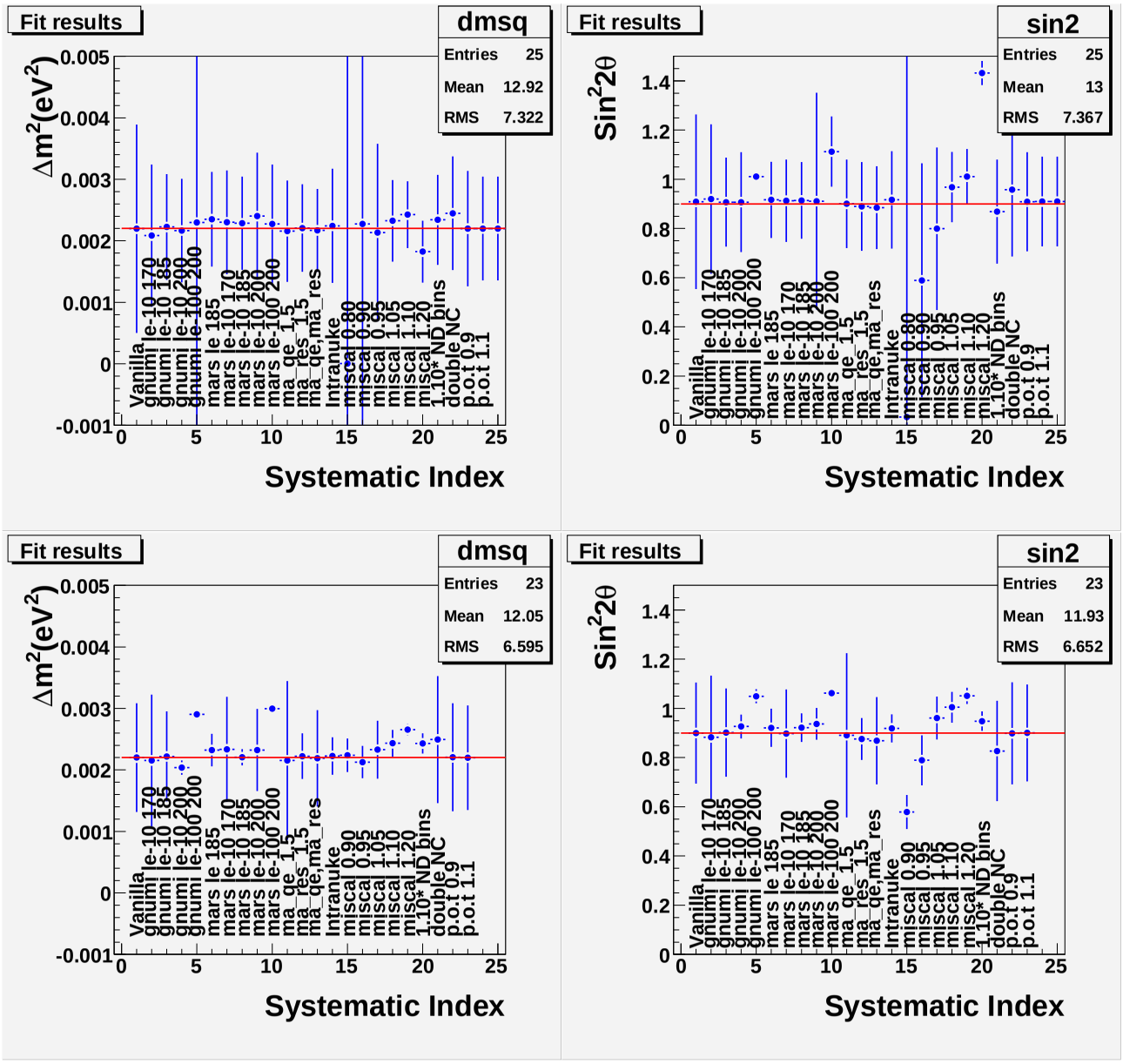


Figure 23: Results of the systematics study on the parameter measurement of Δm^2 and $\sin^2 2\theta$ using the matrix transport method (top) and for the F/N ratio transport method (bottom) for comparison. These plots show the best fit value for the fits to the smoothed spectra (no statistical fluctuations included).

5 Conclusion

We have investigated a simple approach to predicting the non-oscillated spectrum at the far detector, relying on the F/N ratios in either the reconstructed or true neutrino energy. This transport method has then been used as a tool to study the effects of systematic errors on the parameter measurement. At the level of 1e20 p.o.t only a calibration error of greater than 5% would cause any significant perturbation of the parameter measurement.

The matrix method is significantly more robust to changes in the beam modeling compared to the ratio method, but more sensitive to changes in the ND detector response or systematics such as NC background uncertainty. The combination of these methods will allow us to tie down the correct parameters with fits carried out in both ways. The results of 500 pseudo runs show a problem in that only about half of the experiments produce results that converge easily with the possible combinations of statistical fluctuations.This may well be due to the 5% disagreement between the GMINOS prediction and the matrix for the standard le 185kA beam. Once this discrepancy is resolved, this study can be repeated.

A Appendix: Contours from Systematic Studies Using the Ratio Method

Figures 25- 27 show the fits to a smoothed data set with 1×10^{20} protons on target, for many of the systematics studies performed. In all of the plots, top left shows the predicted far spectrum with no oscillations in blue, and the fake data spectrum in black. The fake data was oscillated with Δm^2 =0.0022 eV^2 and $\sin^2 2\theta$ = 0.9. Top right shows the different components of the spectrum. Bottom left shows the fake data spectrum with the predicted spectrum from the best fit superimposed and quotes the best fit values and their errors. The bottom right shows the 68% and 90% confidence regions.

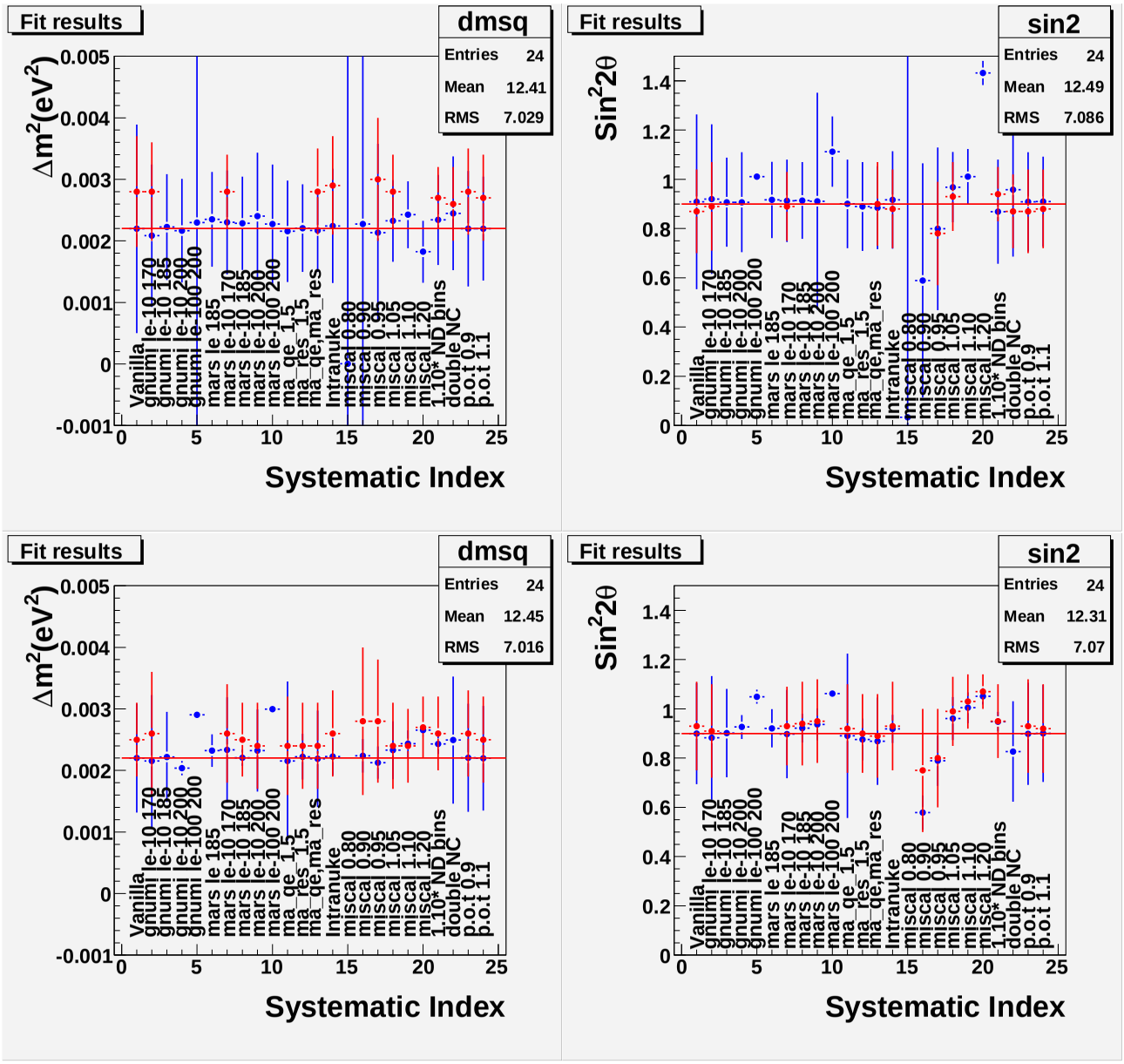


Figure 24: Results of the systematics study on the parameter measurement of Δm^2 and $\sin^2 2\theta$ using the matrix transport method (top) and for the F/N ratio transport method (bottom) for comparison with the mean best fit results from the 500 pseudo runs overlaid in red.

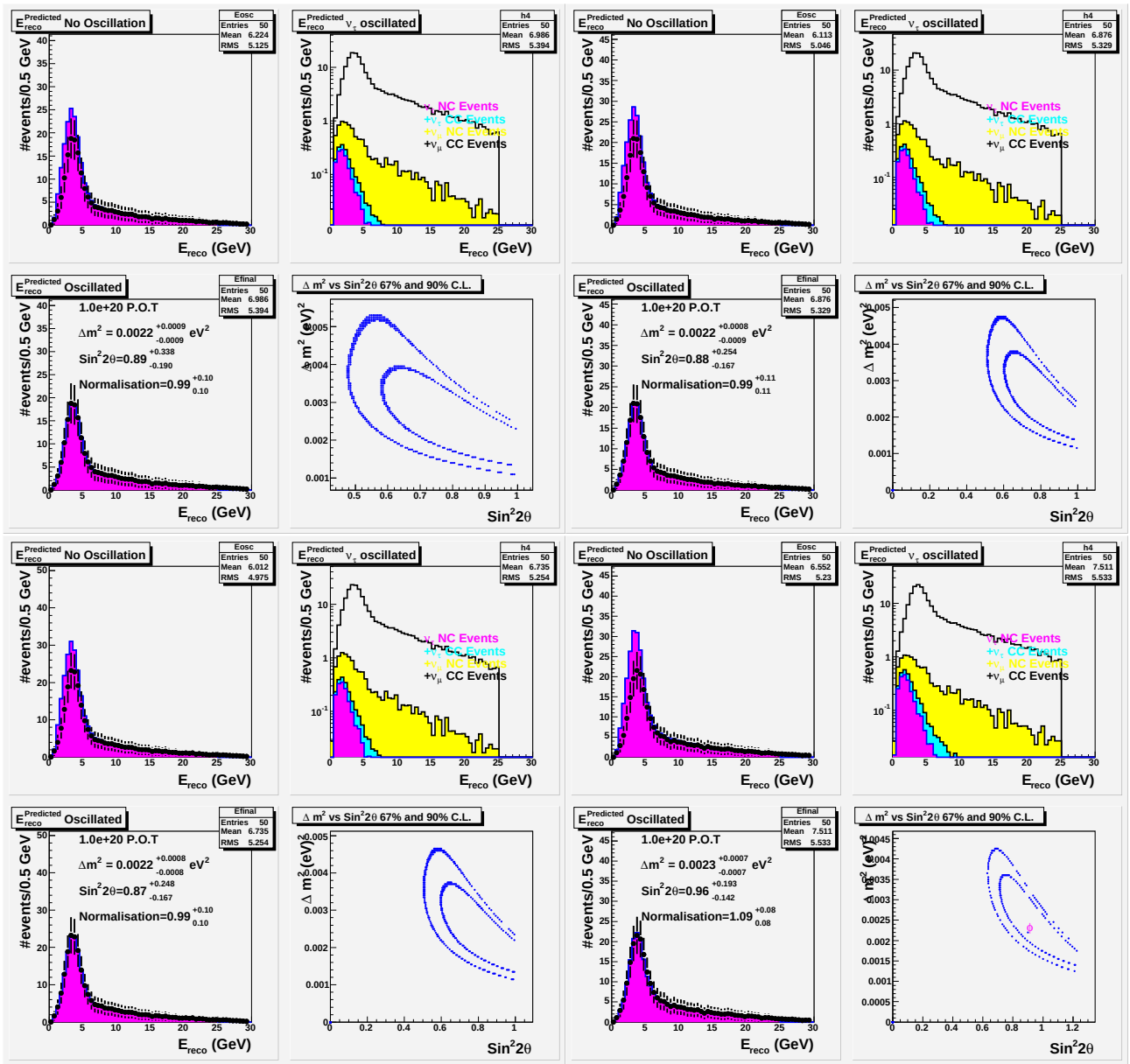


Figure 25: Contours for study in which ma_qe was changed to 1.5 times the default (top left), ma_res changed to 1.5 times the default (top right), ma_qe and ma_res both changed to 1.5 times the default (bottom left), shower energy multiplied by 1.10 (bottom right)

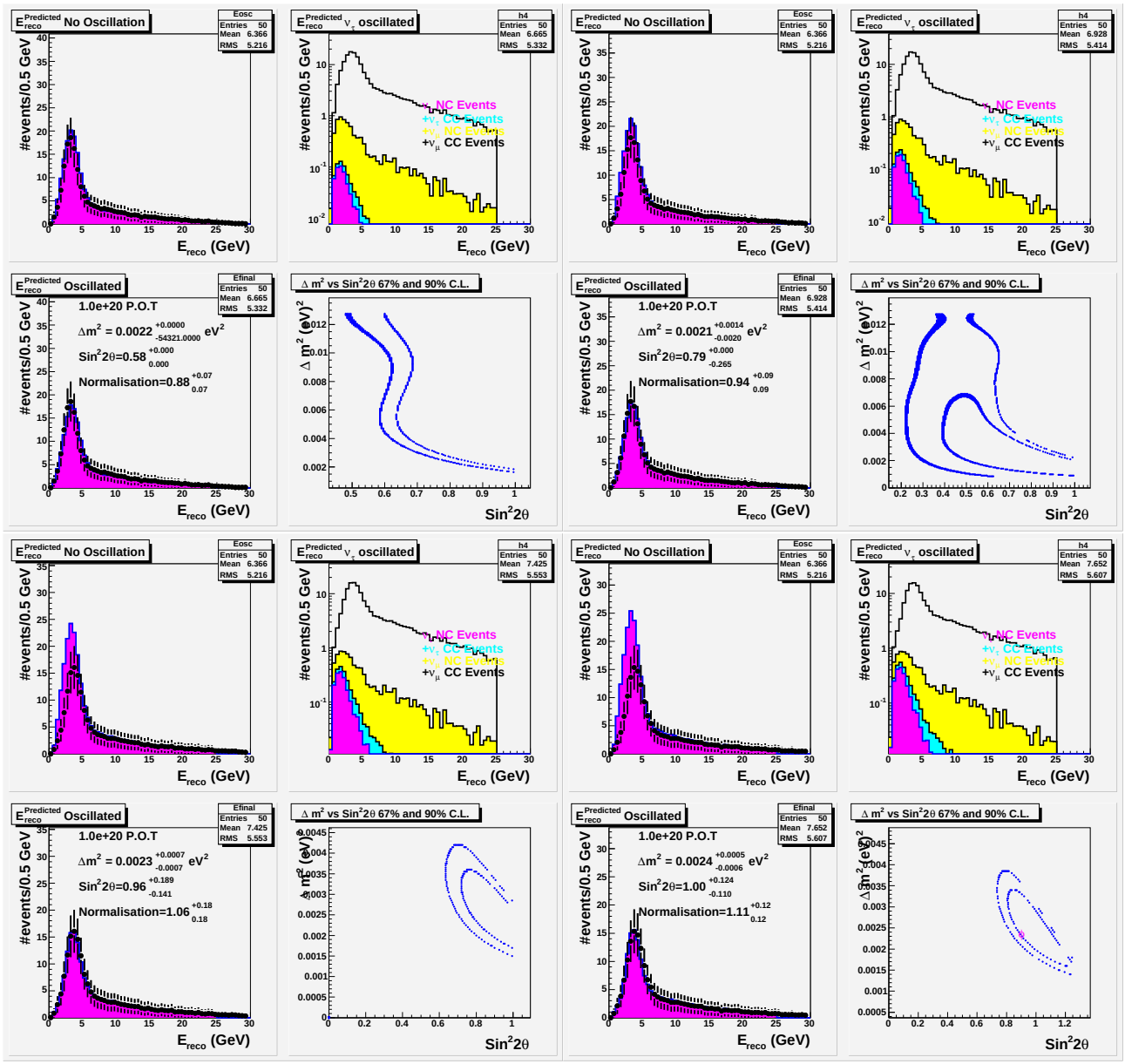


Figure 26: Contours for study in which the neutrino energy in the Far Detector was multiplied by 0.90 (top left). Note that the allowed region is below the drawn contours. The error bars likely indicate that the data is not well described by the fitting function. Contours for Far Detector neutrino energy multiplied by 0.95 (top right), 1.05 (bottom left) and 1.10 (bottom right).

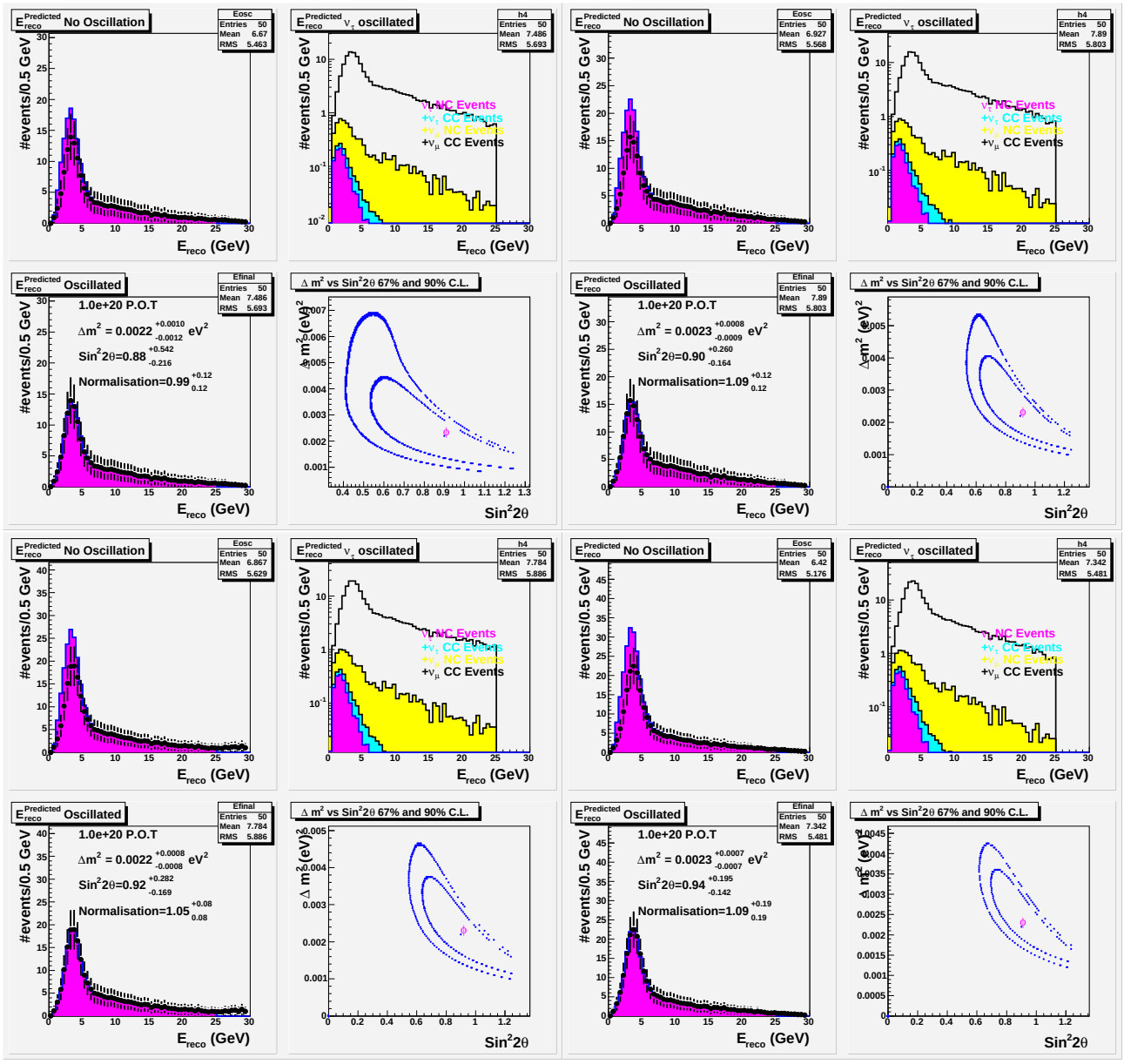


Figure 27: Contours for study in which the MC was reweighted to the LE10, 170kA flux spectra (top left), study in which the MC was reweighted to the MARS LE10, 170kA flux spectra (top right), study in which the MC was reweighted to the MARS LE10, 185kA flux spectra (bottom left), study in which the MC was reweighted to the MARS LE10, 200kA flux spectra (bottom right).

B Appendix: Summary of Pseudo experiments for Systematic Studies Using the Ratio Method

Figures 28- 47 show the summary of the pseudo experiments done for many of the systematic studies. In each of the following, the top left plot shows the best fit value of Δm^2 for each pseudo experiment, the top middle plot shows the best fit value of $\sin^2 2\theta$, and the top right plot shows the best fit value of the overall normalization. The middle row shows histograms of the error obtained for each of the three fit parameters, left shows the error in Δm^2 , middle shows the error on $\sin^2 2\theta$, and the right shows the error on the normalization. The bottom left plot shows how many sigma the best fit value of Δm^2 was from the generated value, the bottom middle plot shows the number of sigma $\sin^2 2\theta$ was from the generated value, while the bottom right shows the same for the normalization best fit value.

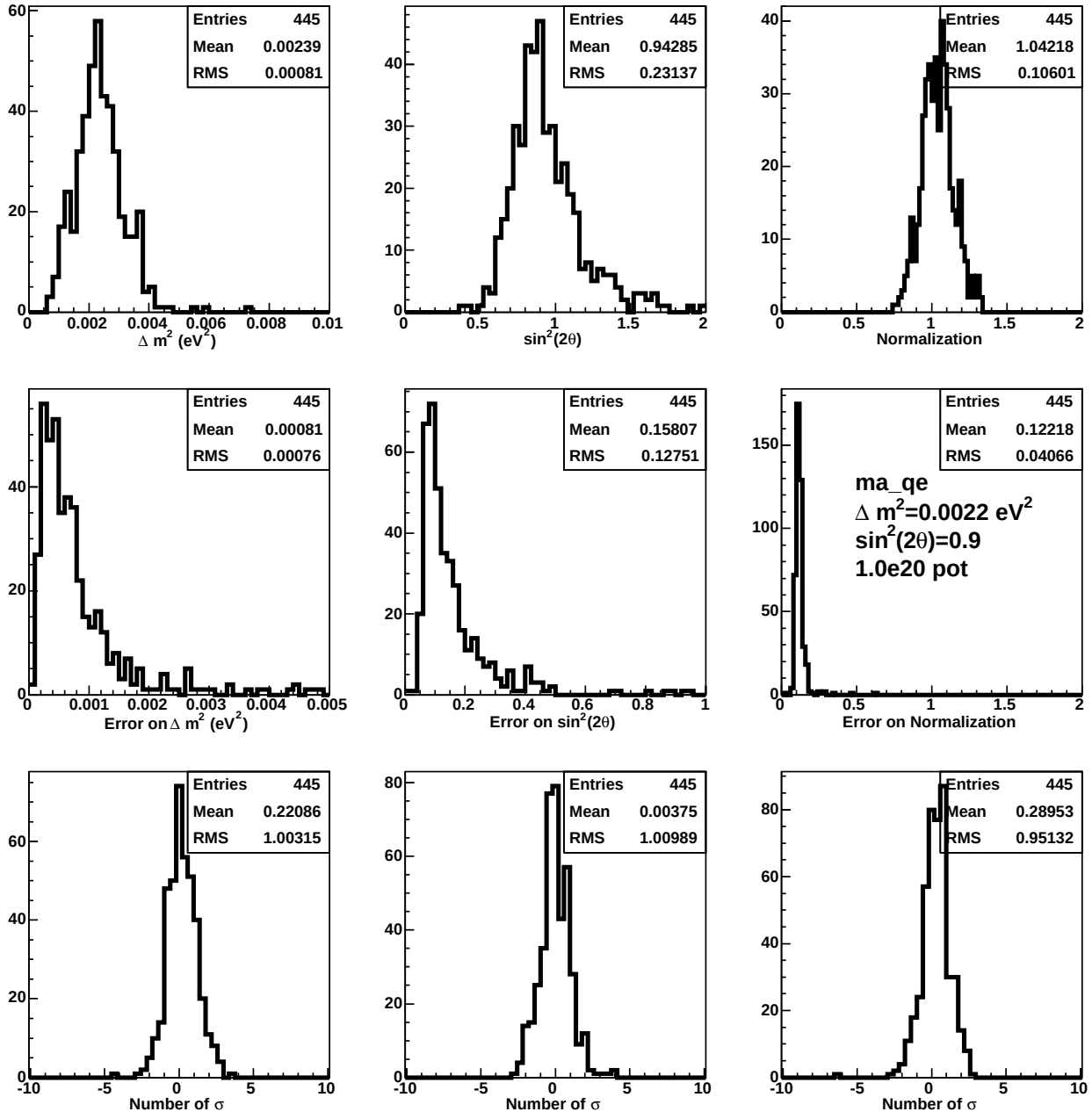


Figure 28: Pseudo experiment summary plots for the study in which ma_qe was changed to 1.5 times it's default value

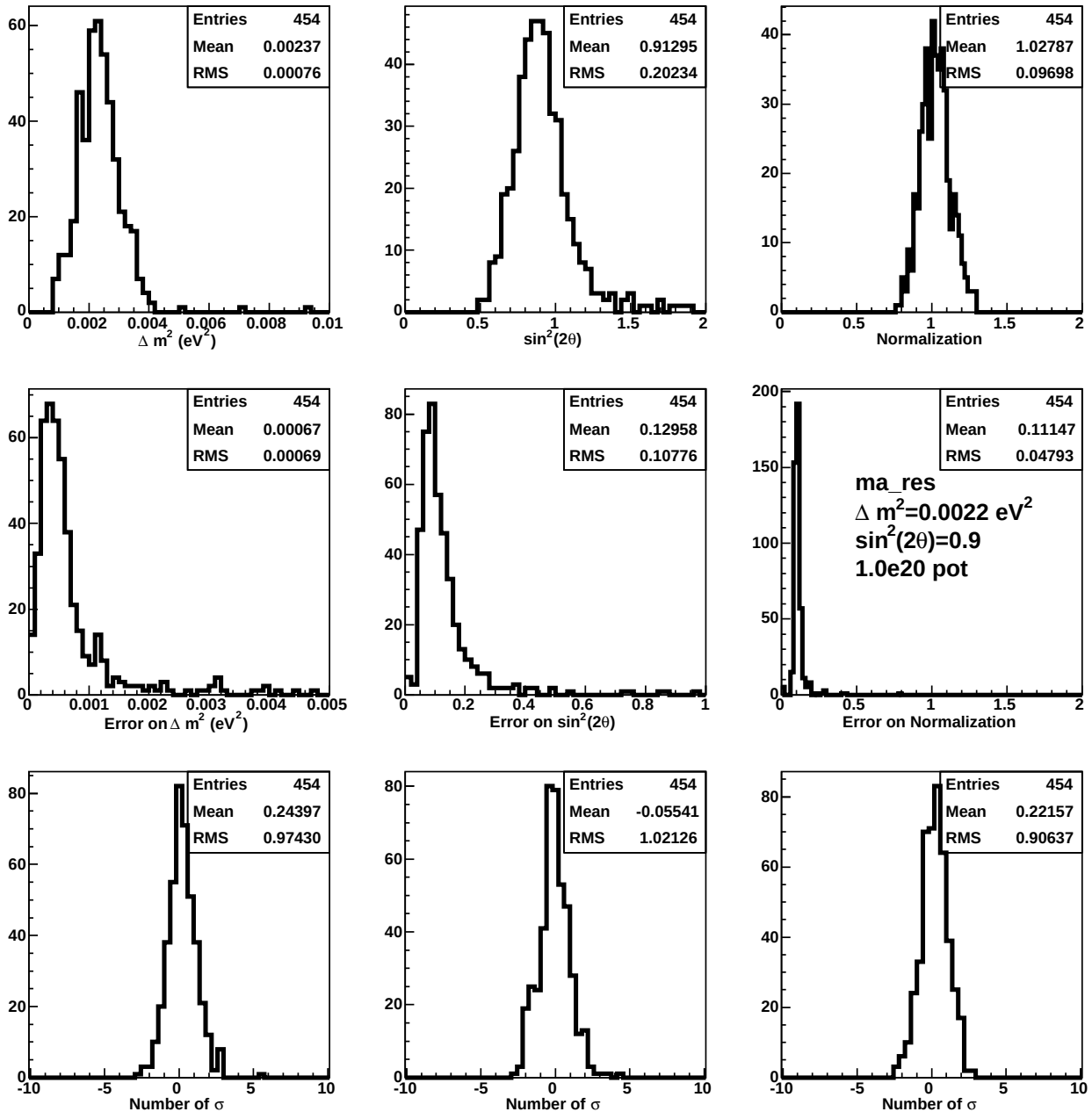


Figure 29: Pseudo experiment summary plots for the study in which ma_res was changed to 1.5 times it's default value

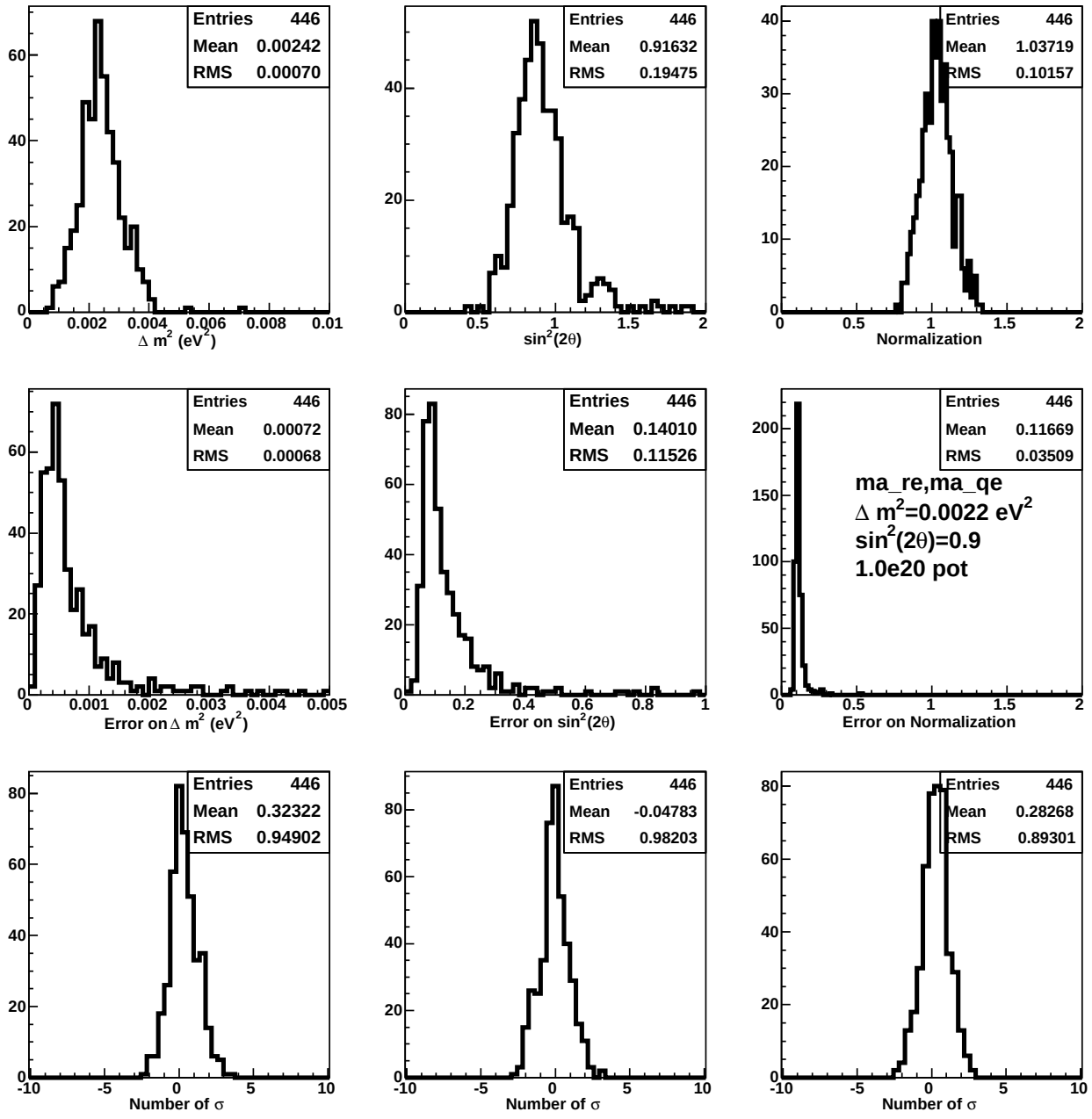


Figure 30: Pseudo experiment summary plots for the study in which ma_qe and ma_res were changed to 1.5 times the default values

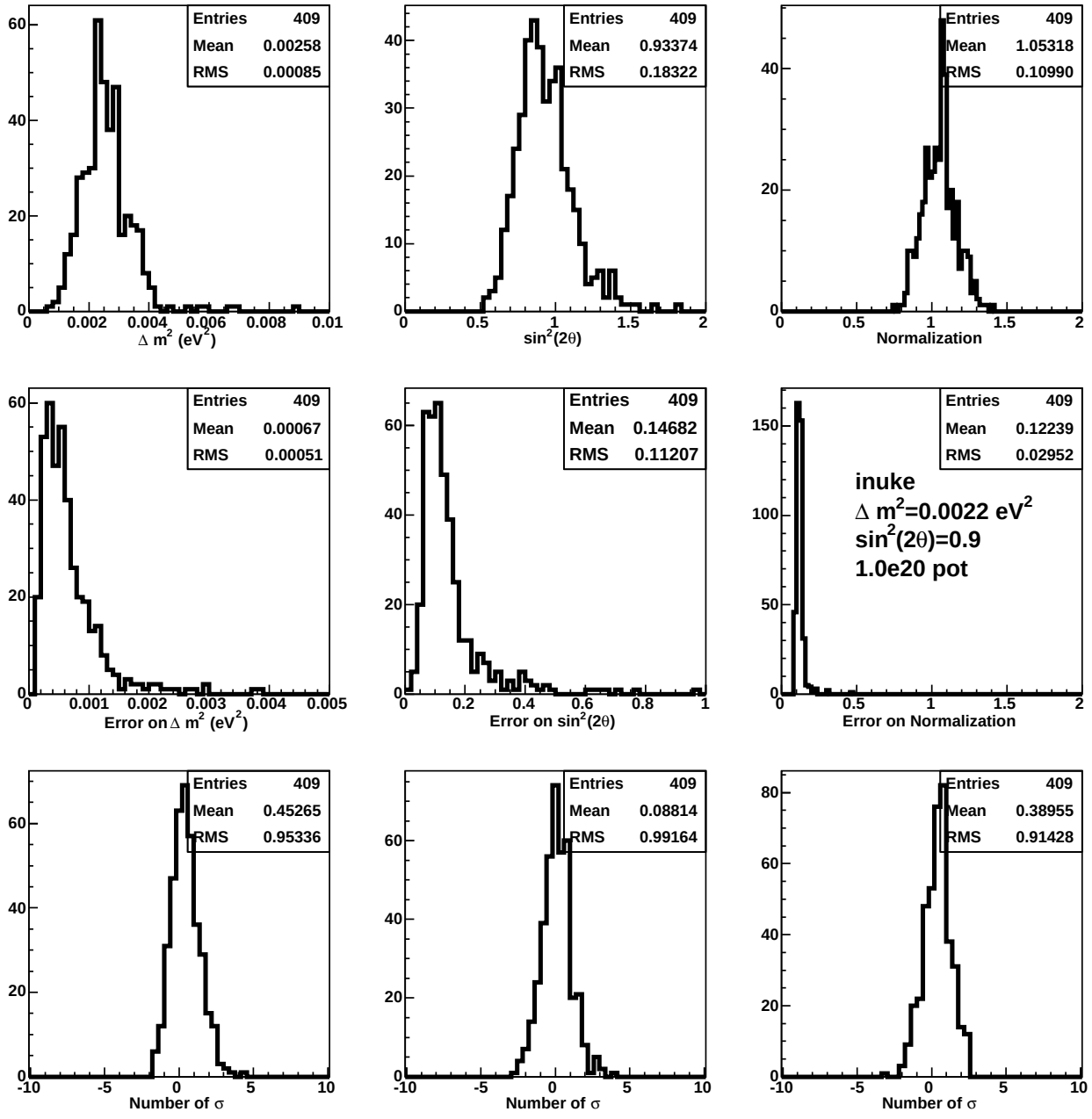


Figure 31: Pseudo experiment summary plots for the study in which the shower energy in both detectors was multiplied by 1.10

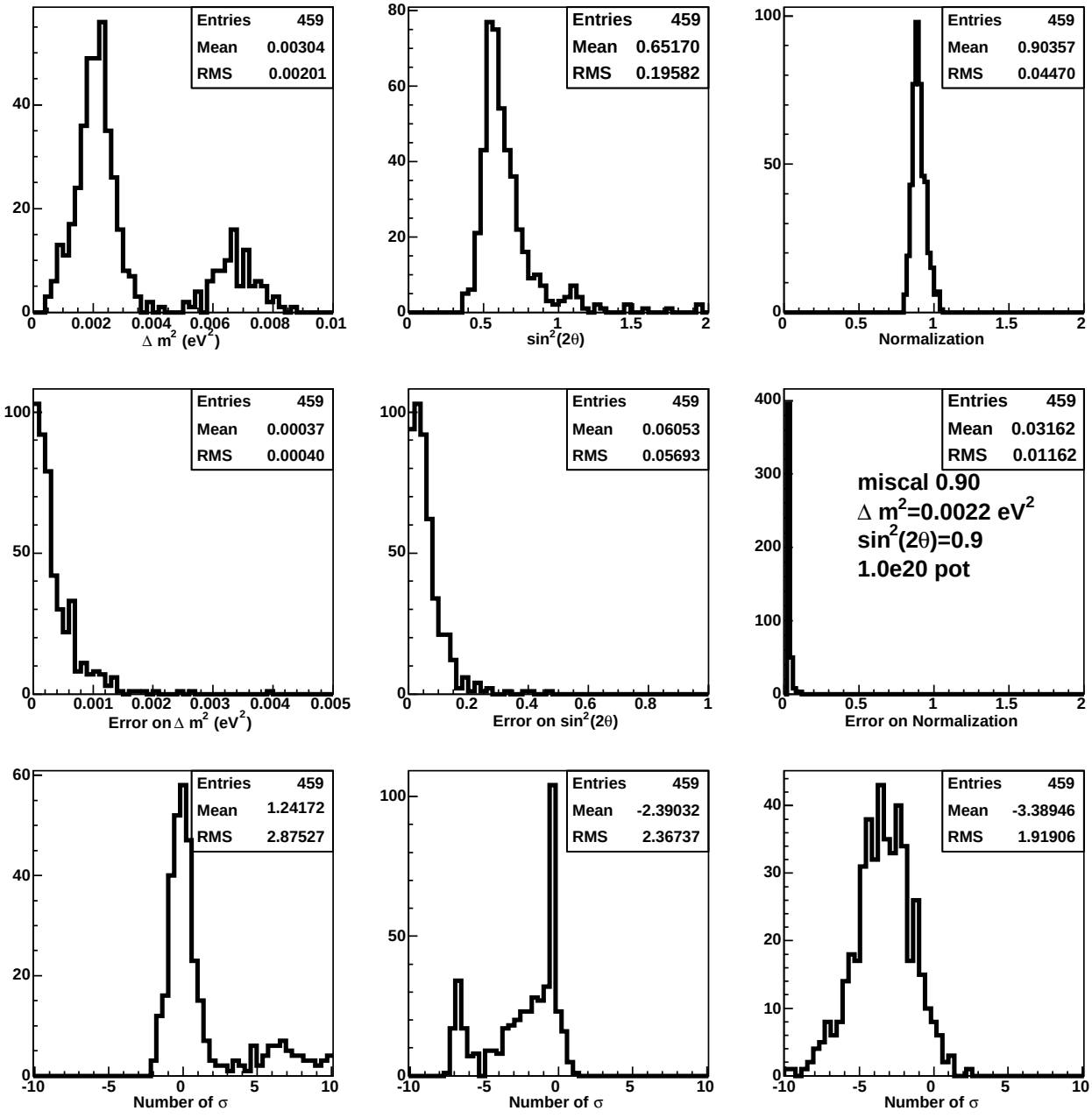


Figure 32: Pseudo experiment summary plots for the study in which the neutrino energy in the Far Detector was multiplied by 0.90.

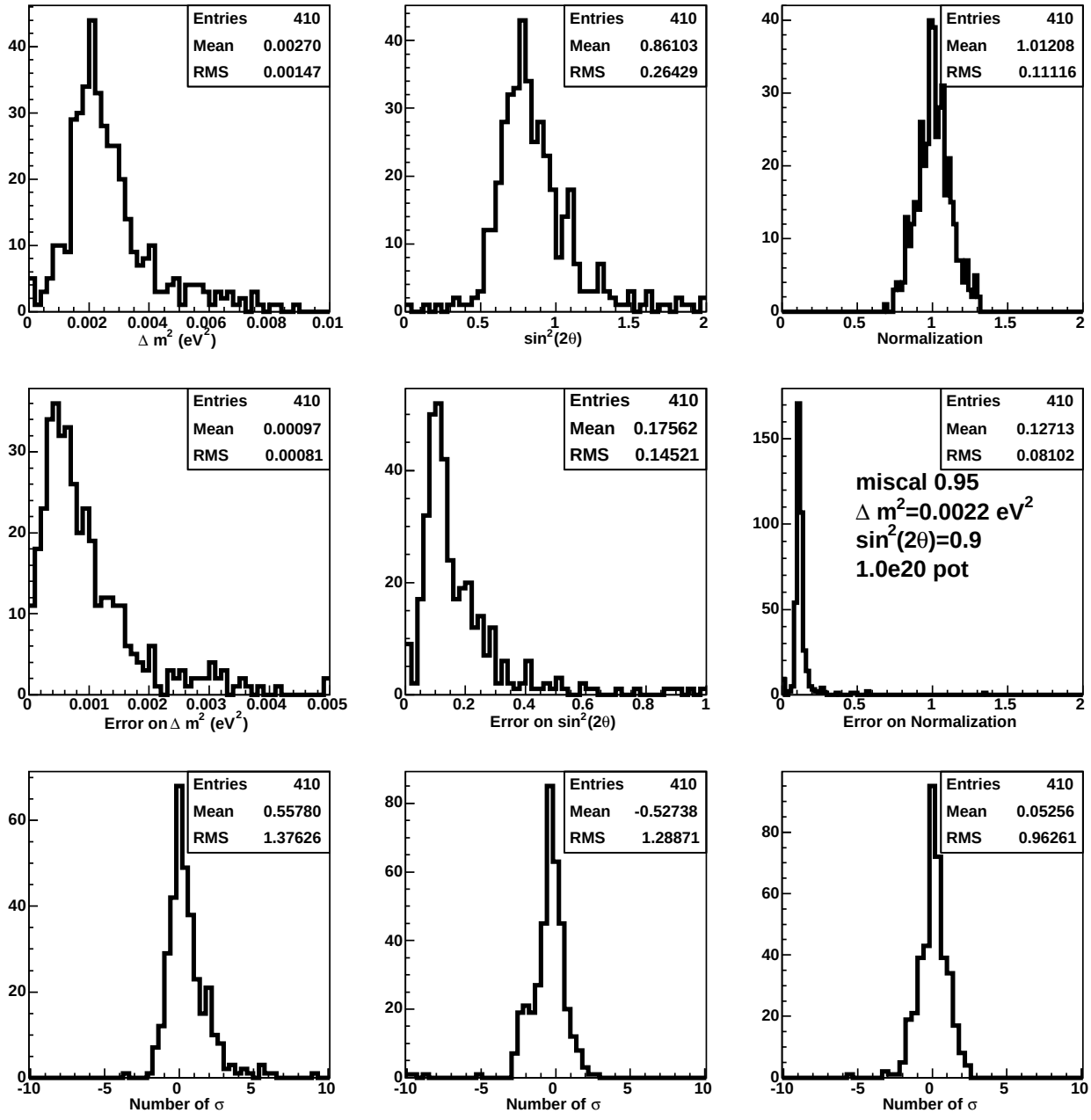


Figure 33: Pseudo experiment summary plots for the study in which the neutrino energy in the Far Detector was multiplied by 0.95

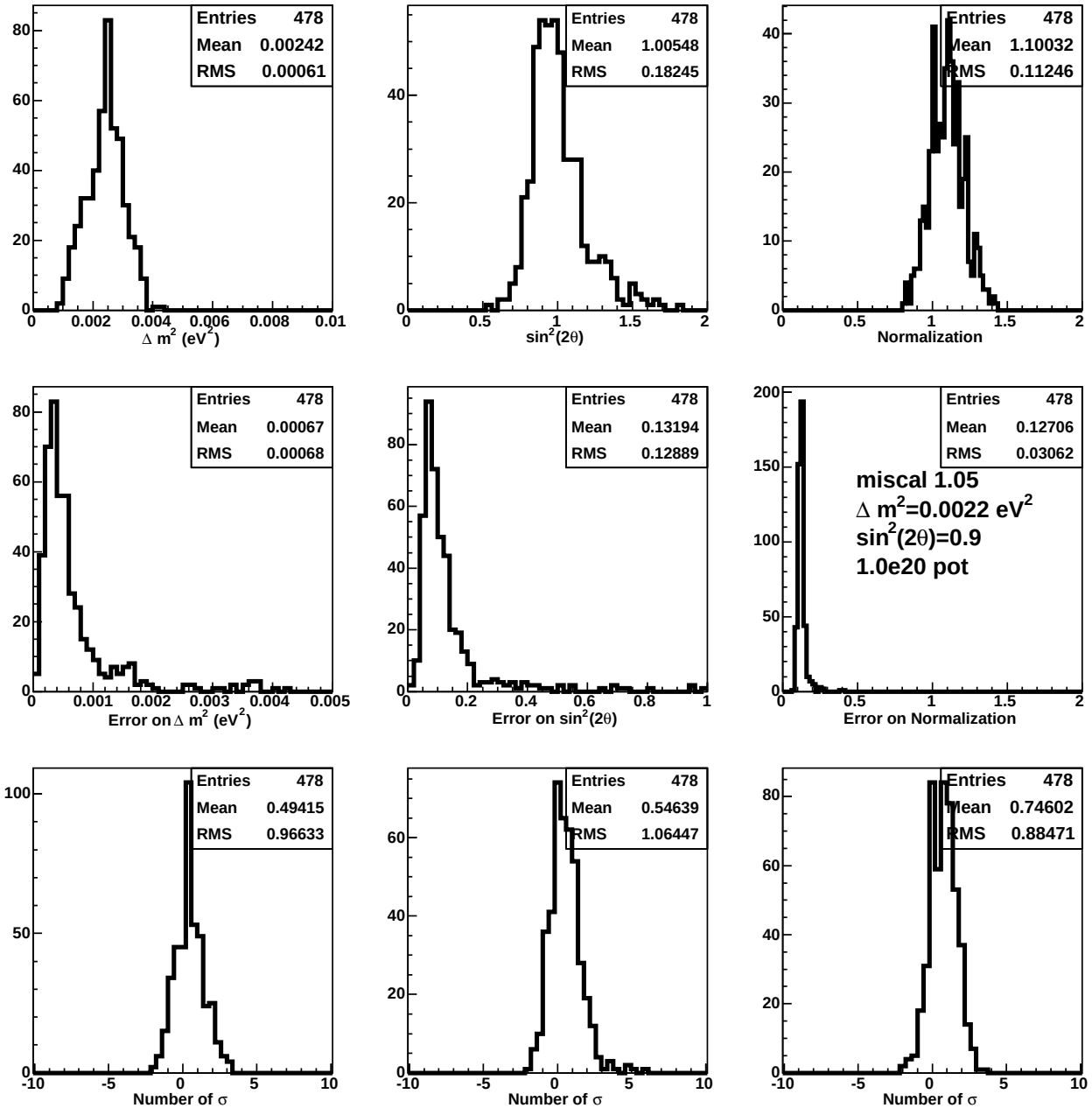


Figure 34: Pseudo experiment summary plots for the study in which the neutrino energy in the Far Detector was multiplied by 1.05

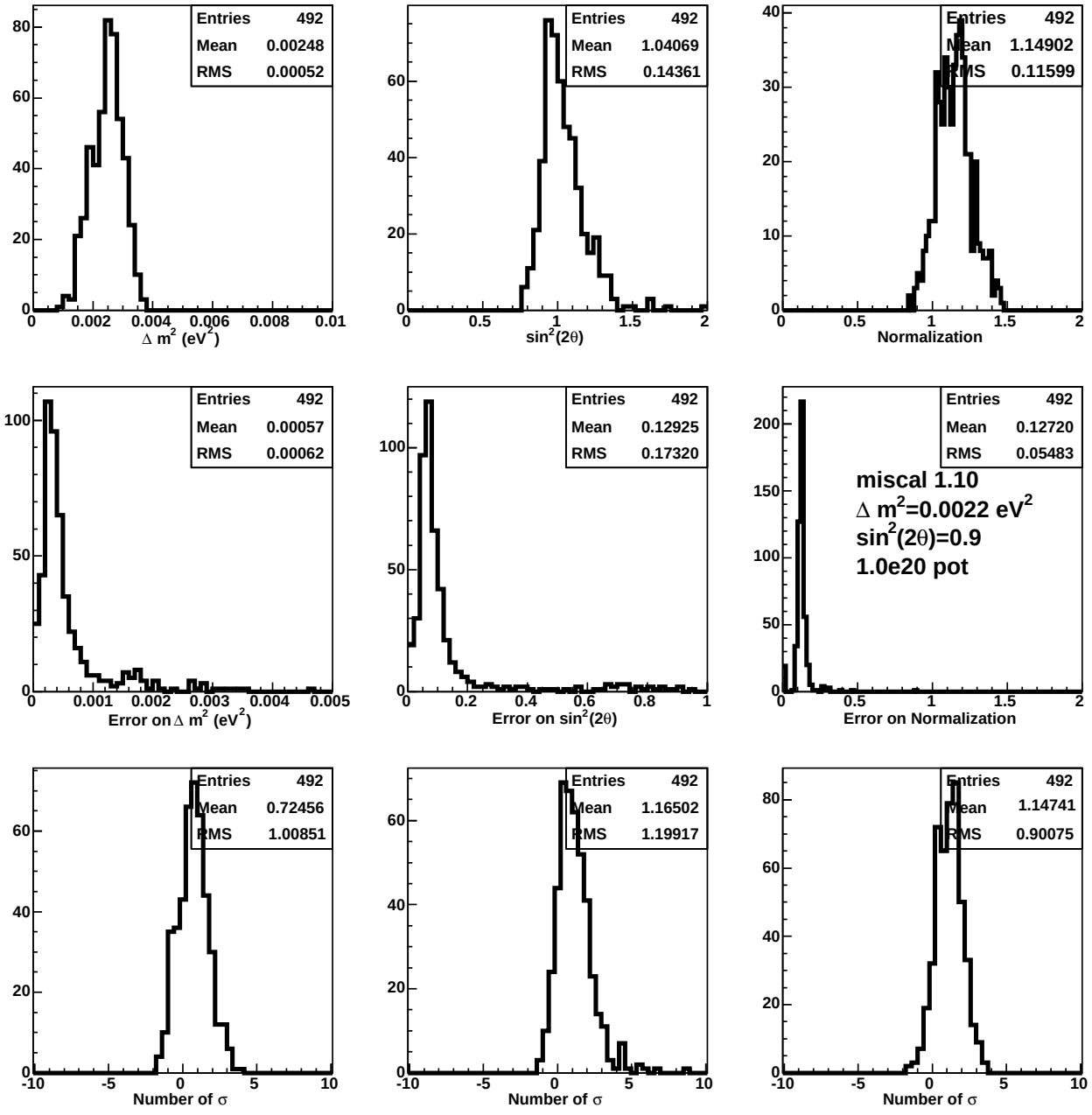


Figure 35: Pseudo experiment summary plots for the study in which the neutrino energy in the Far Detector was multiplied by 1.10

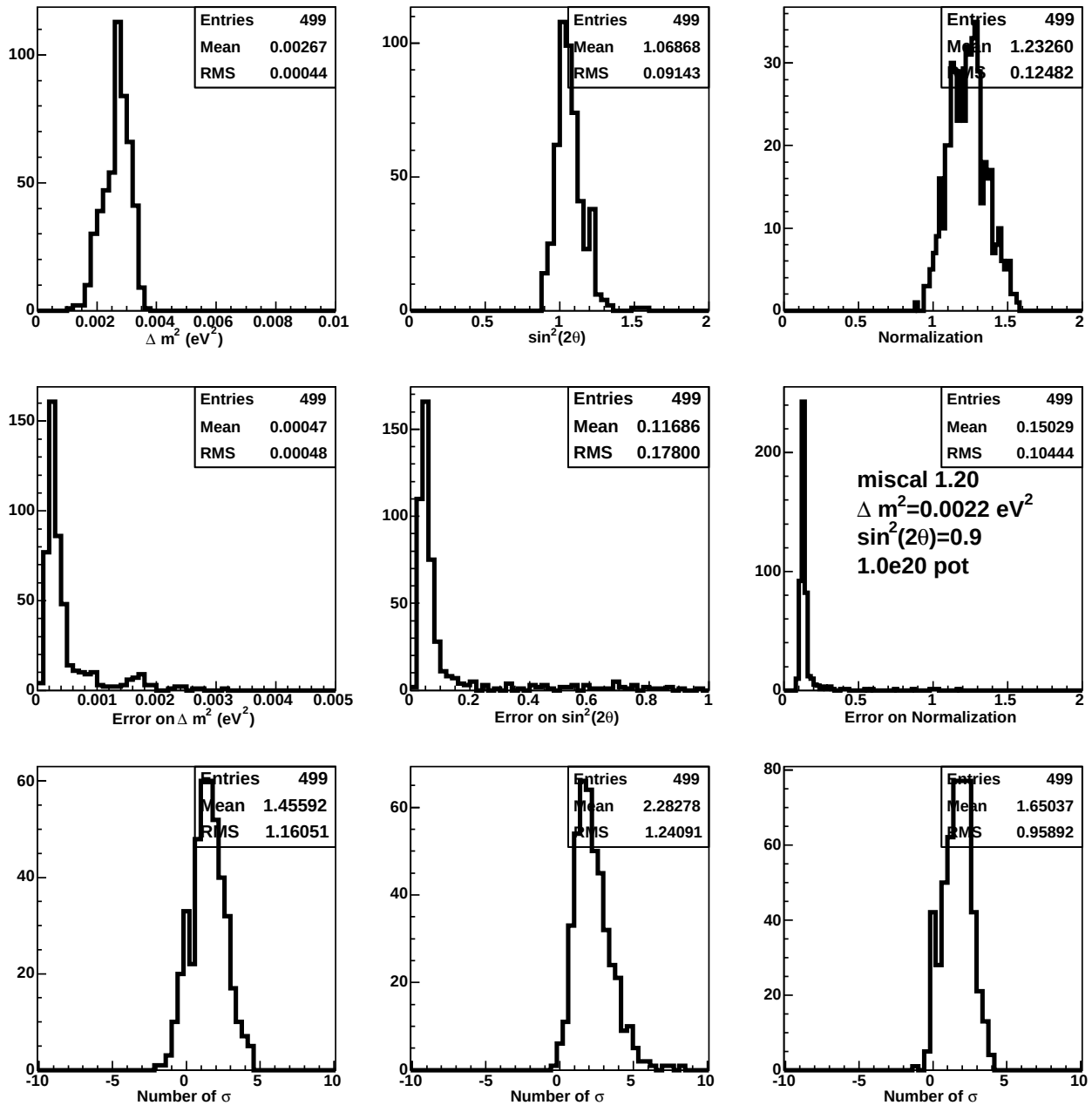


Figure 36: Pseudo experiment summary plots for the study in which the neutrino energy in the Far Detector was multiplied by 1.20

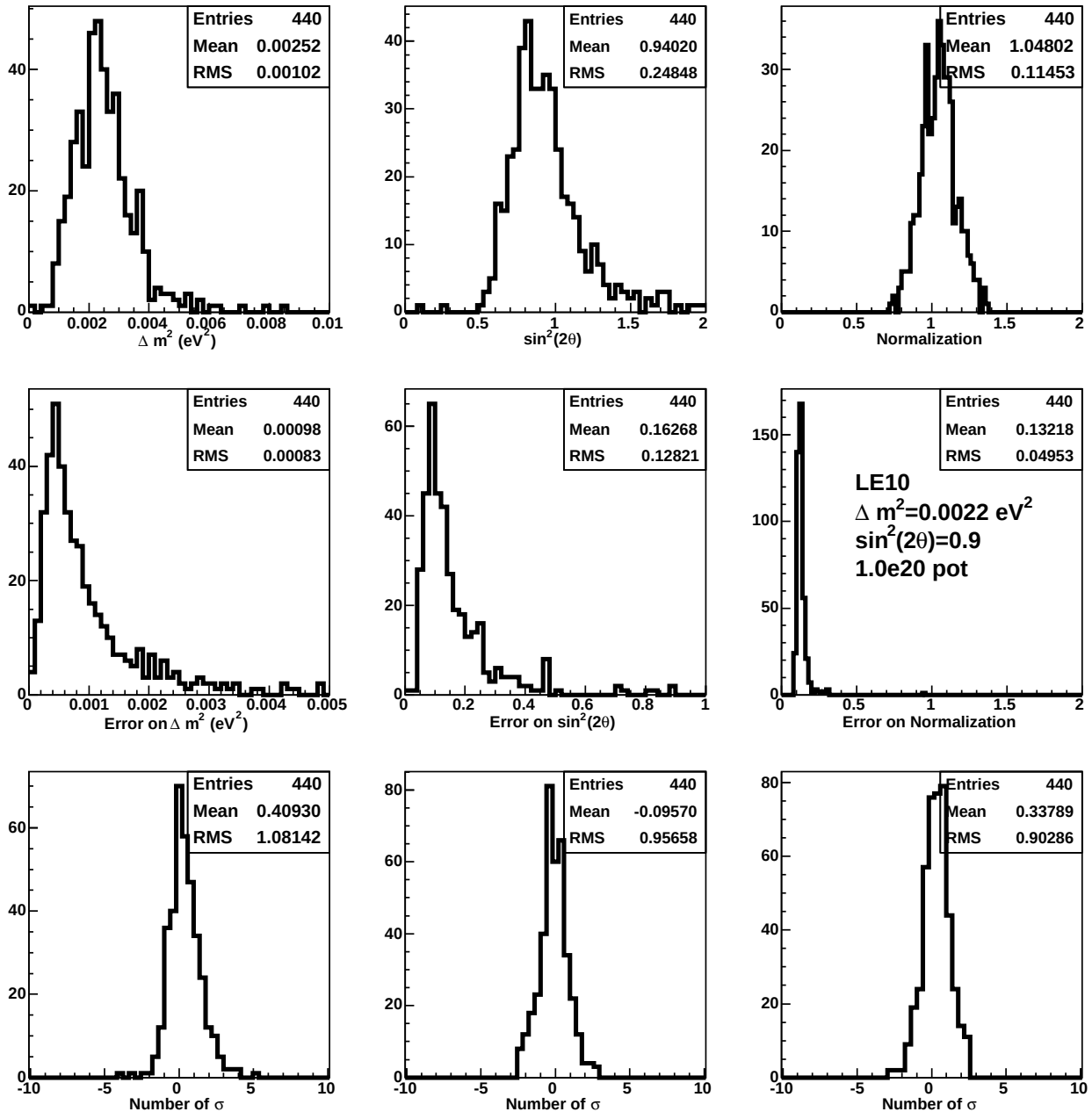


Figure 37: Pseudo experiment summary plots for the study in which the MC was reweighted to the LE10 beam

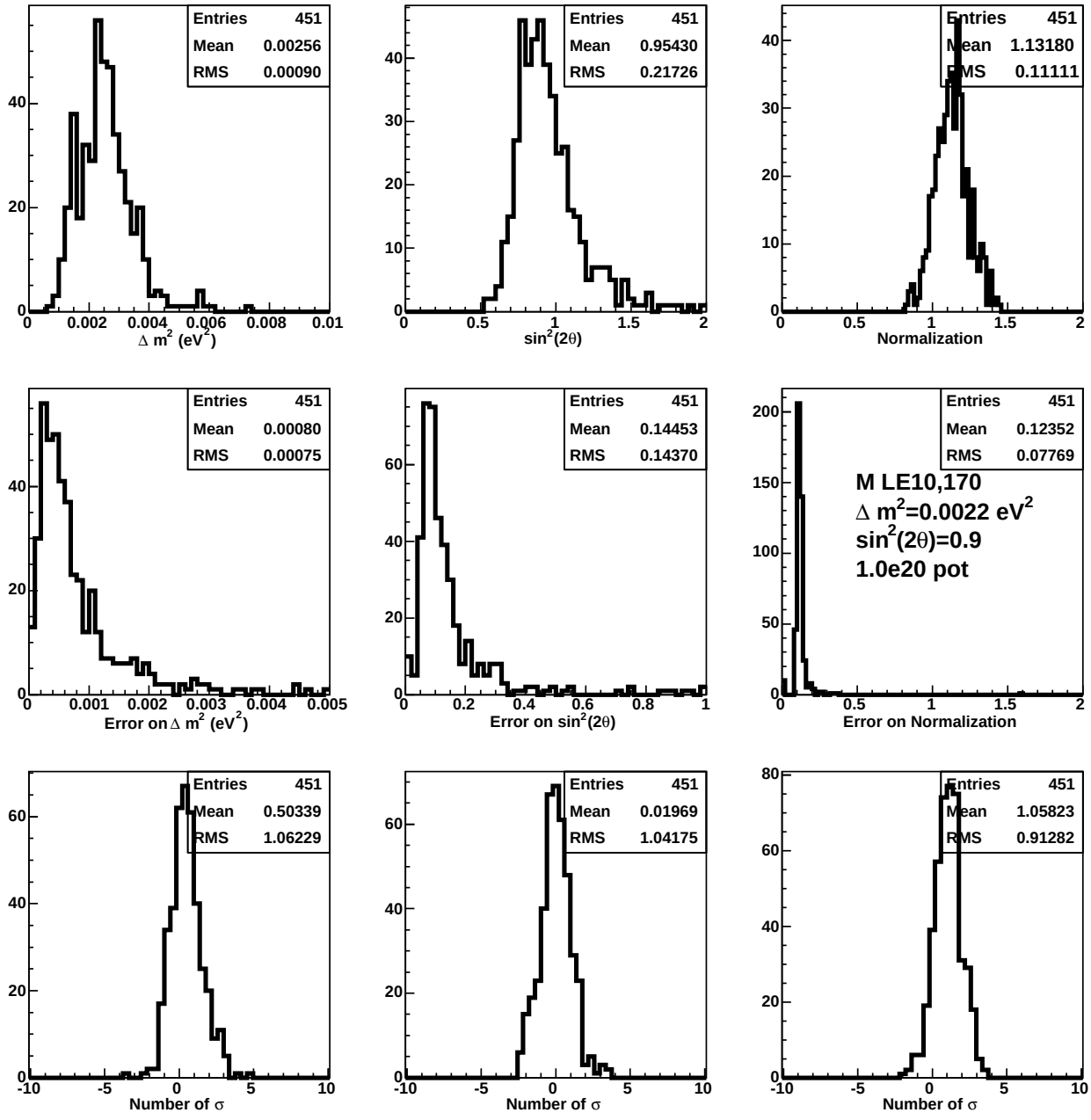


Figure 38: Pseudo experiment summary plots for the study in which the MC was reweighted to the mars LE10, 170 kA beam

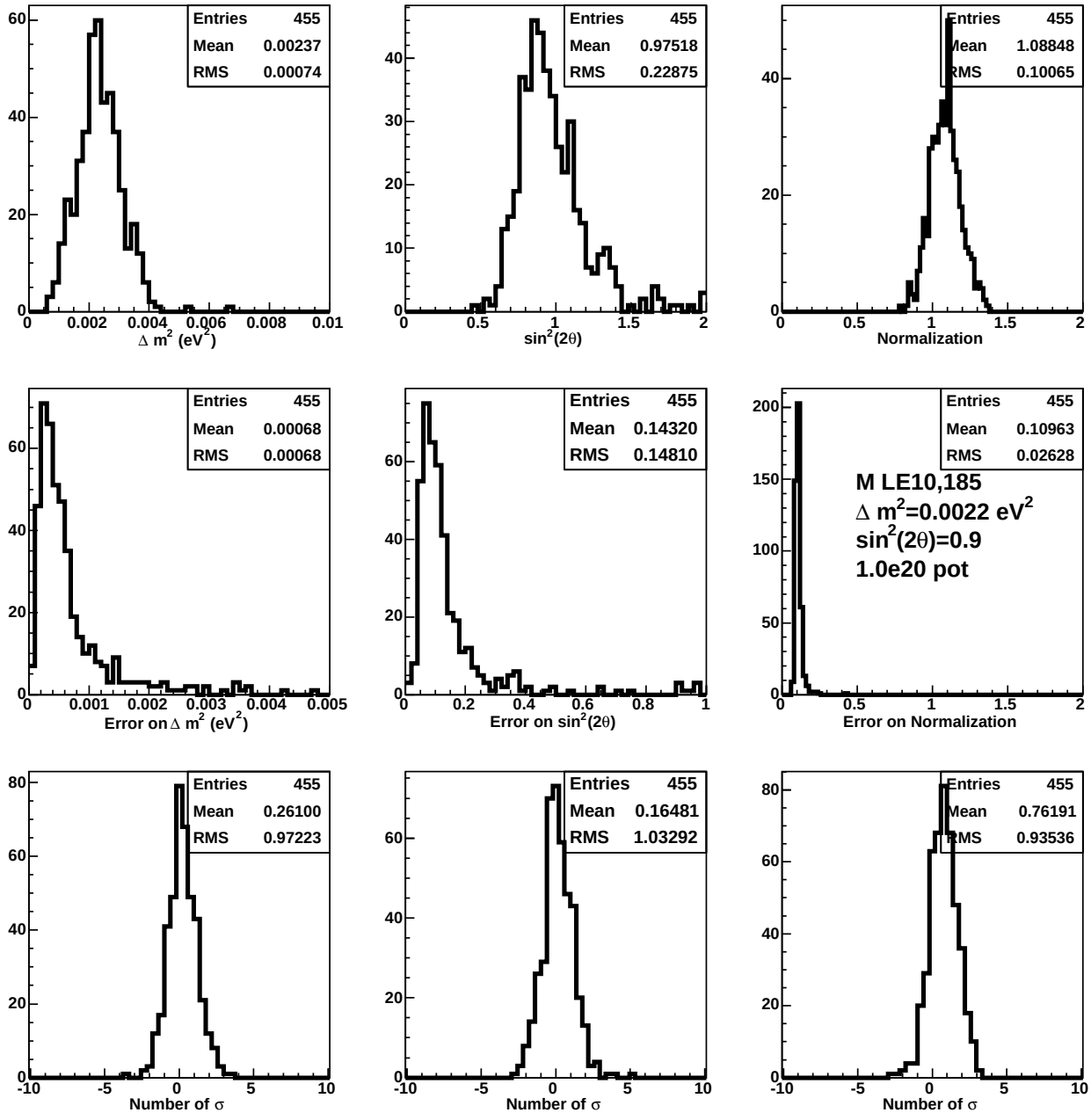


Figure 39: Pseudo experiment summary plots for the study in which the MC was reweighted to the mars LE10, 185 kA beam

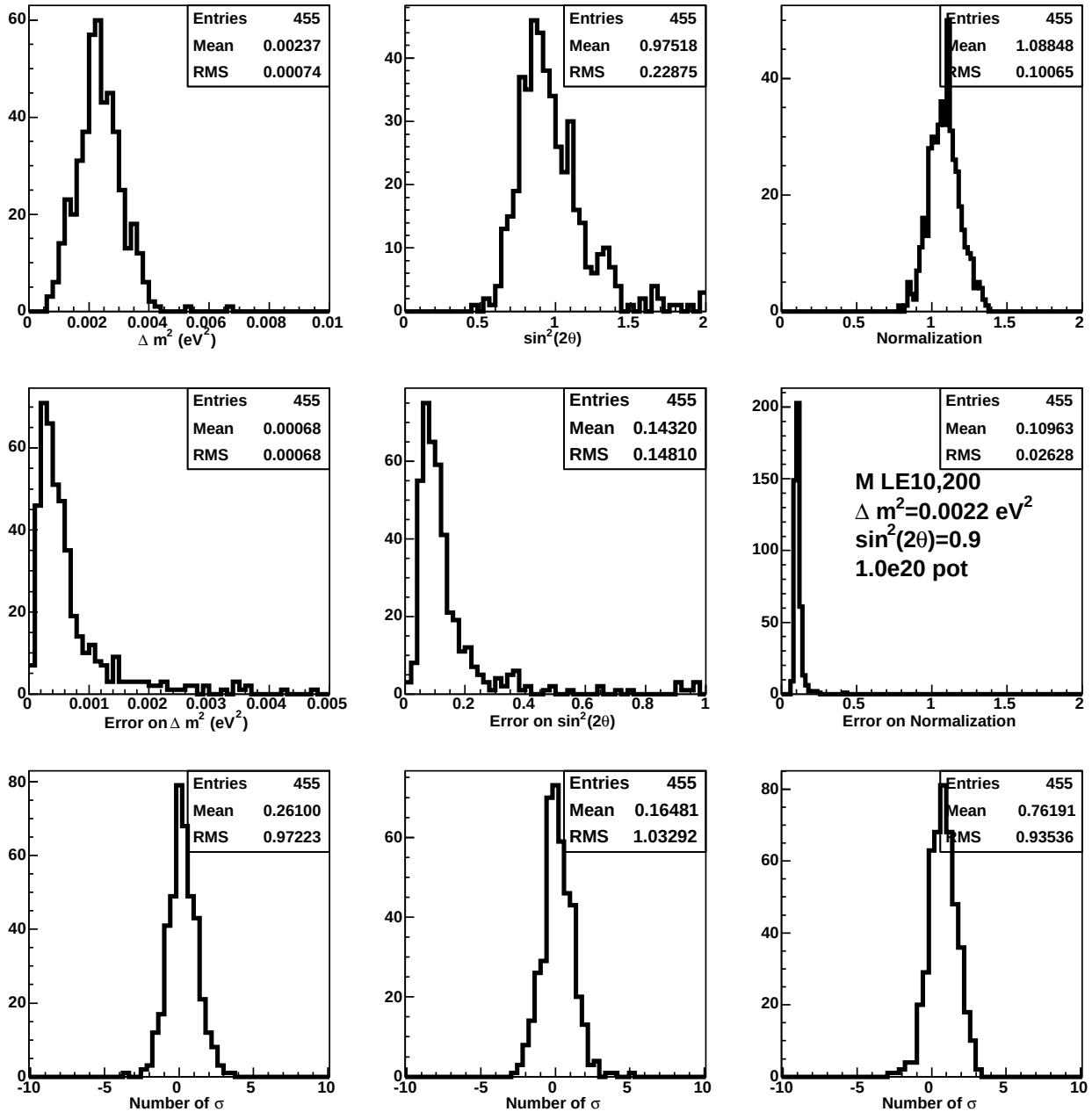


Figure 40: Pseudo experiment summary plots for the study in which the MC was reweighted to the mars LE10, 200 kA beam

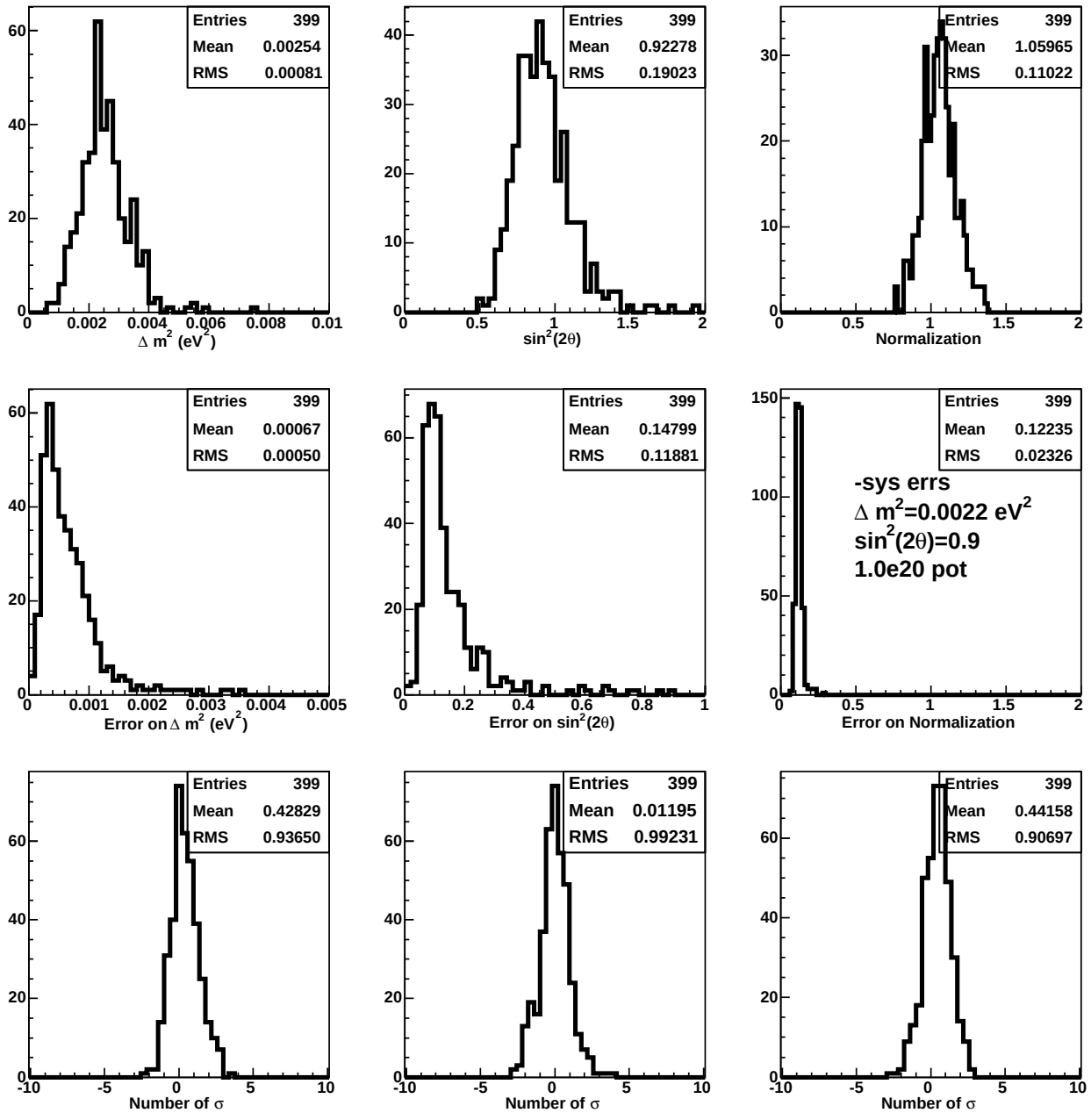


Figure 41: Pseudo experiment summary plots for the study in which the MC was reweighted down by the beam systematic errors on the F/N ratio

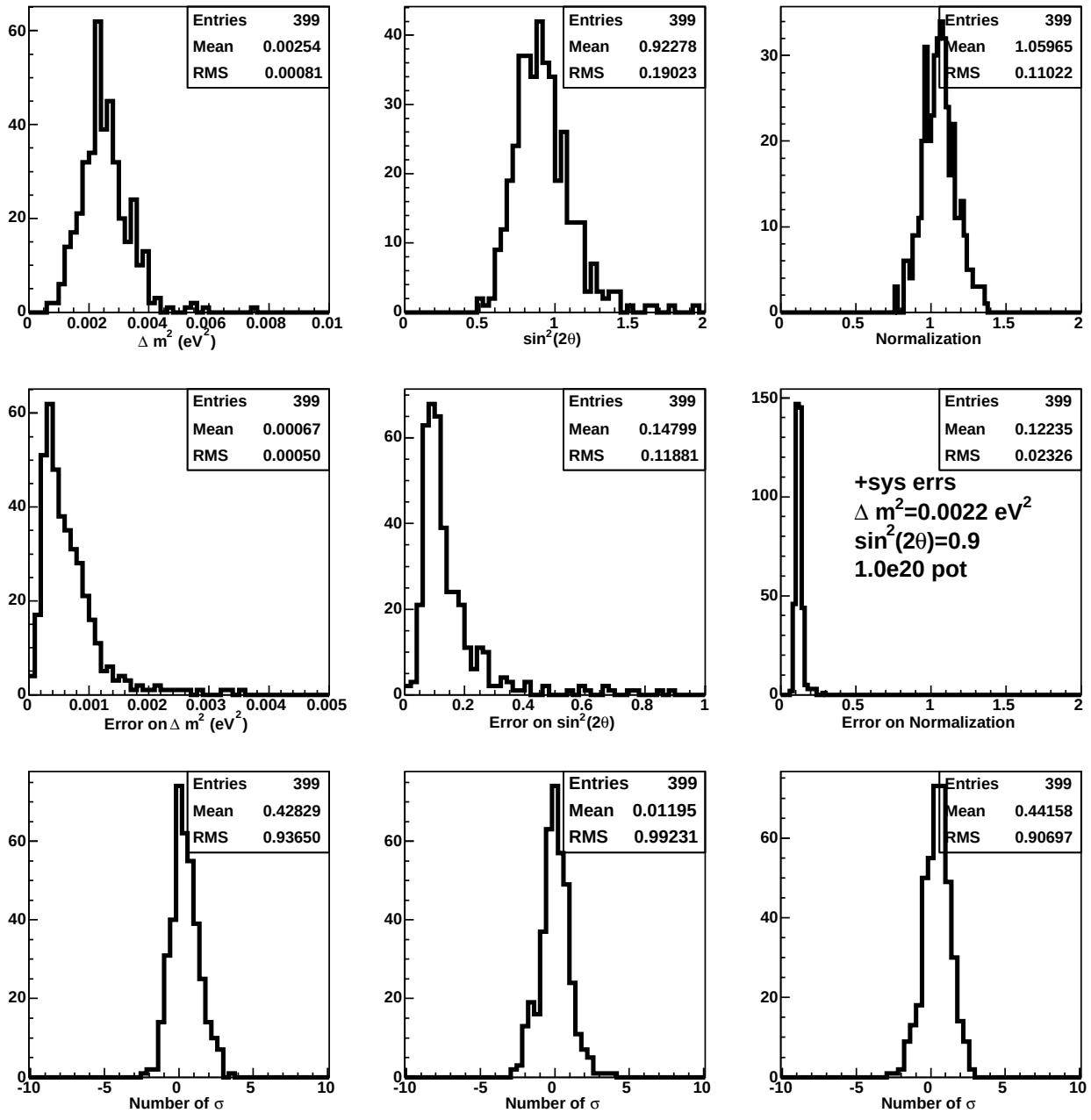


Figure 42: Pseudo experiment summary plots for the study in which the MC was reweighted down by the beam systematic errors on the F/N ratio

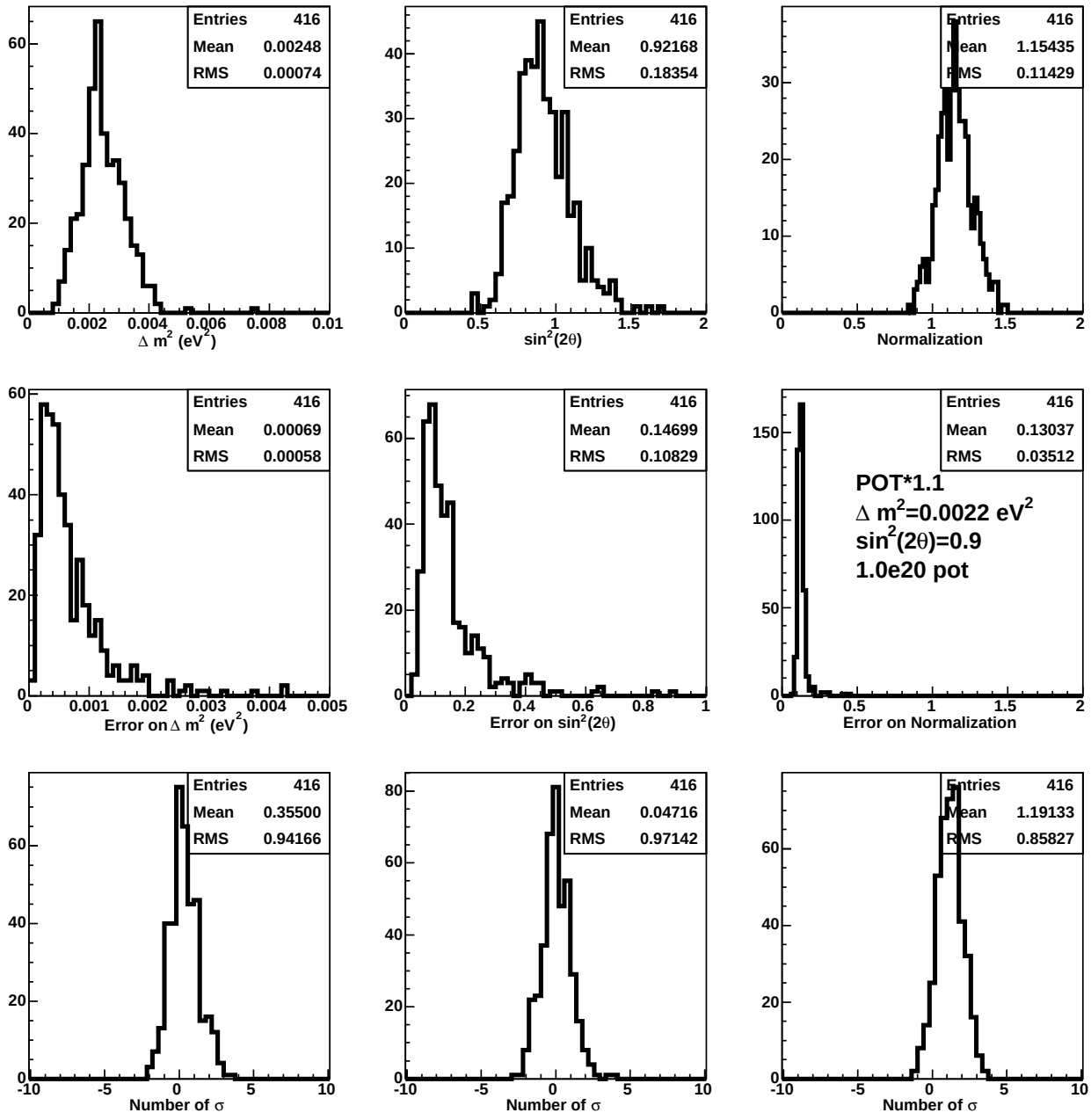


Figure 43: Pseudo experiment summary plots for the study in which the MC was scaled by 1.1

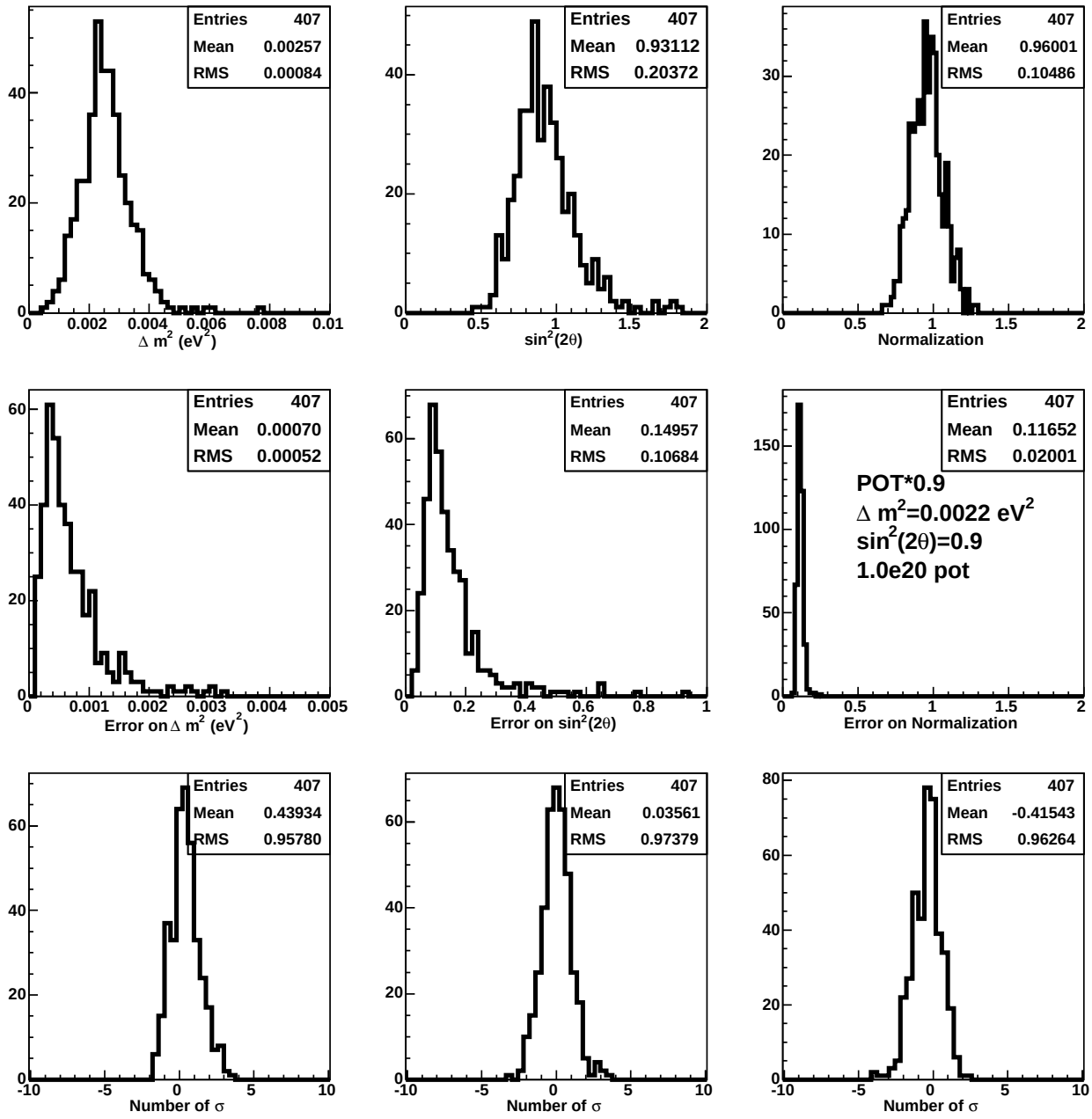


Figure 44: Pseudo experiment summary plots for the study in which the MC was scaled by 0.9

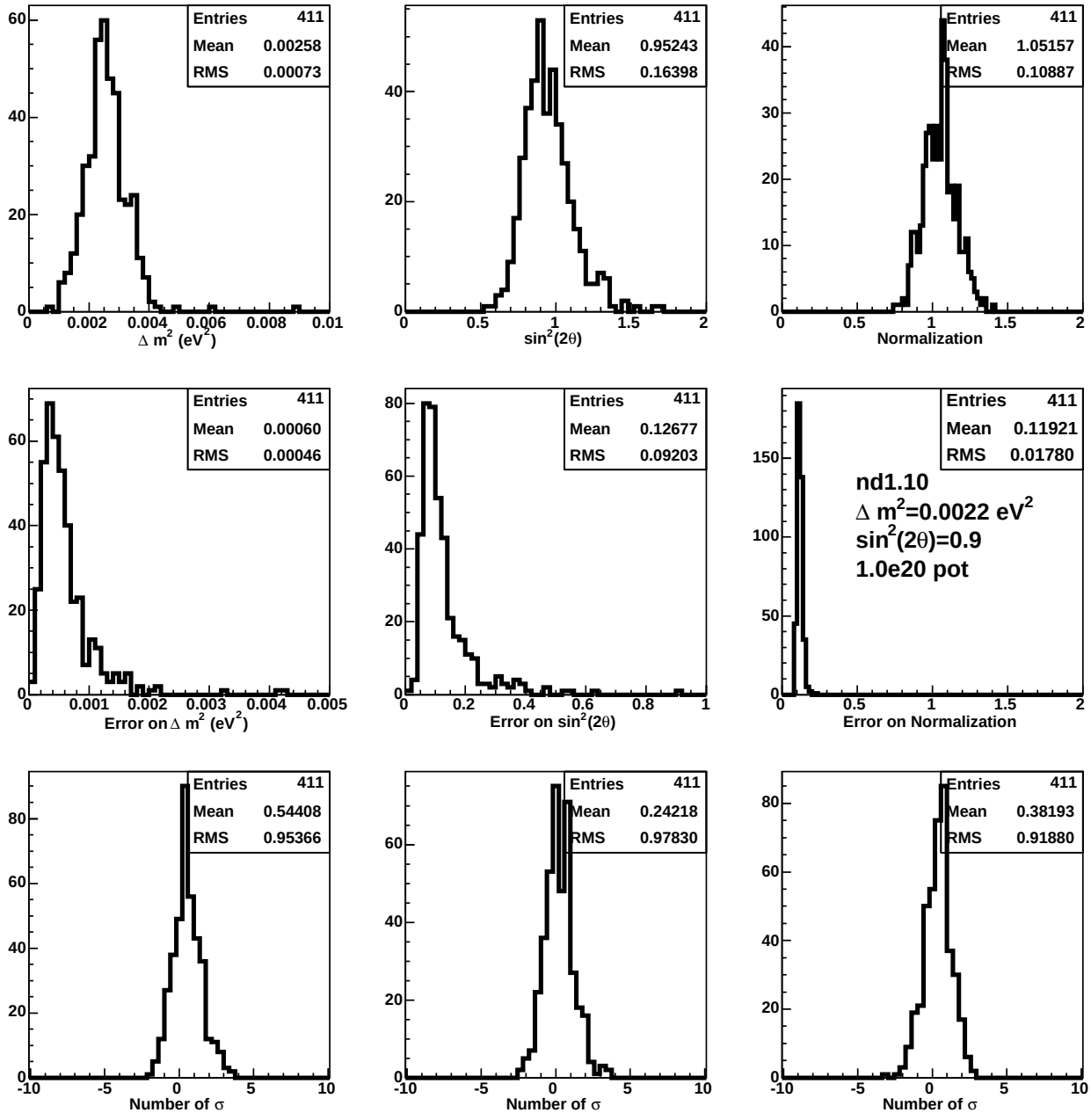


Figure 45: Pseudo experiment summary plots for the study in which the first 7 bins of the ND spectrum were scaled up by 10%

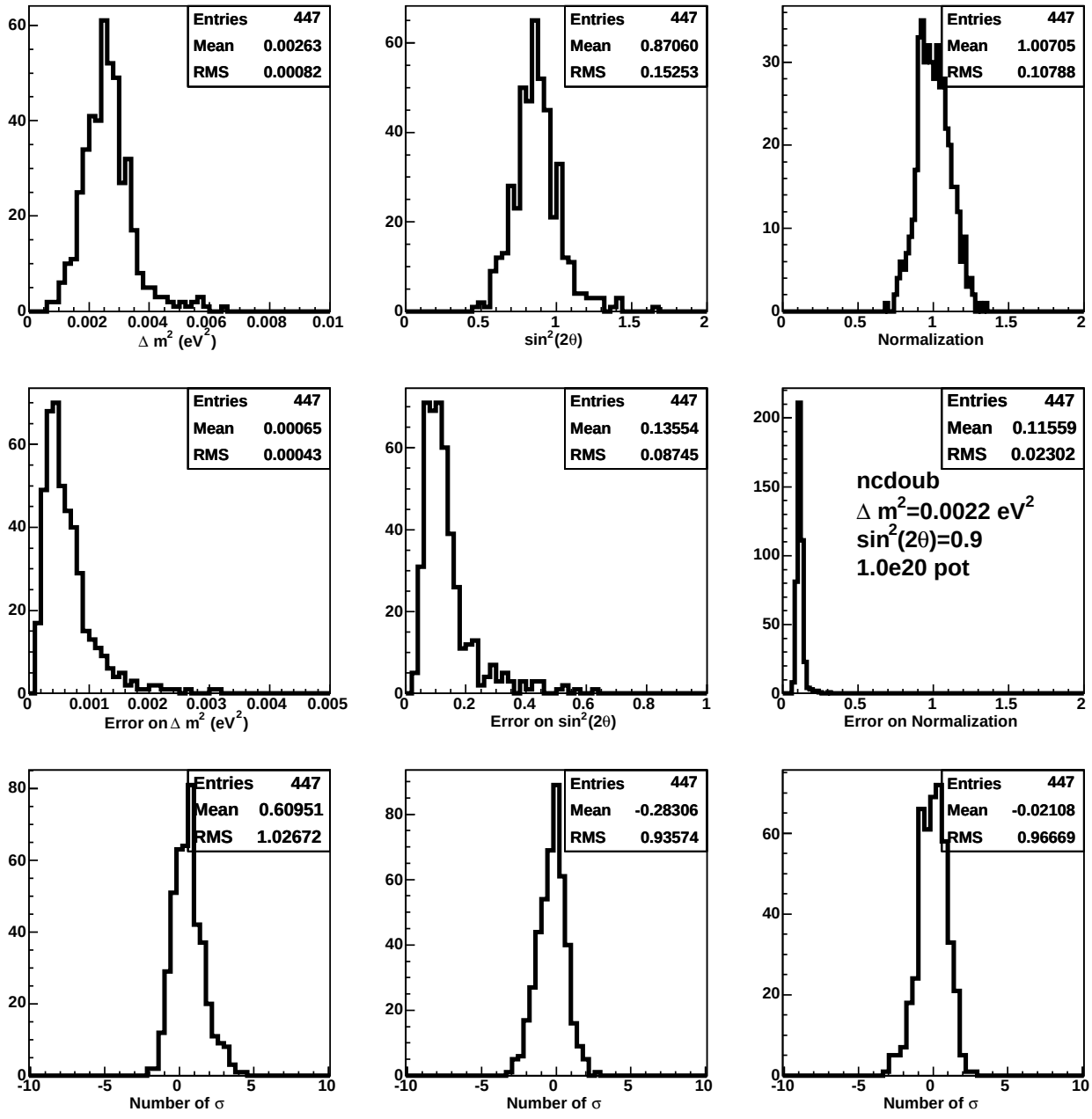


Figure 46: Pseudo experiment summary plots for the study in which the neutral current contamination was doubled

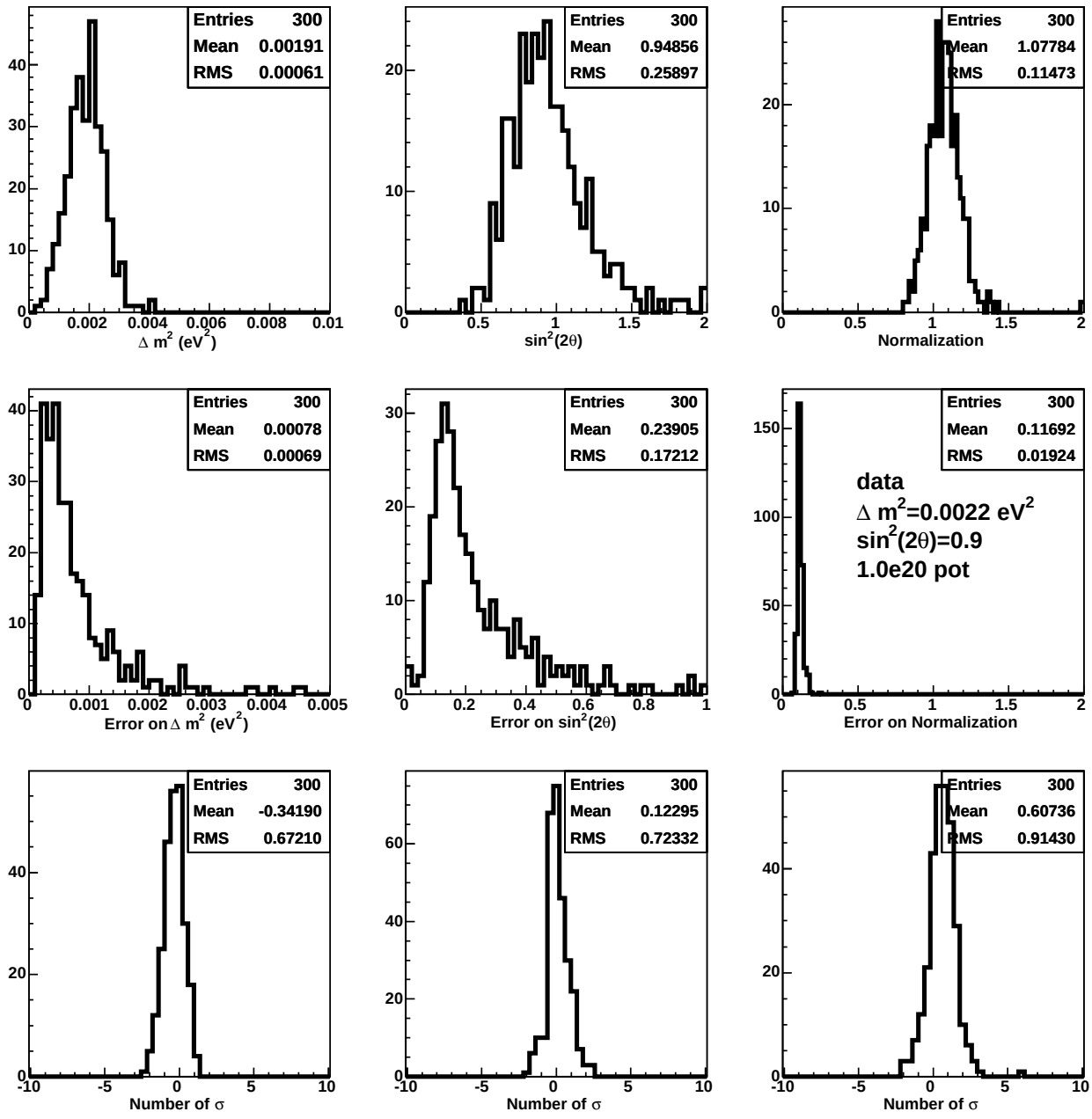


Figure 47: Pseudo experiment summary plots for the study in which the predicted Far spectrum was obtained by multiplying the measured ND data by the F/N ratio, but the fake data was taken from the standard LE MC.

C Appendix: Summary of Contours and Pseudo experiments for Systematic Studies Using the Matrix Method

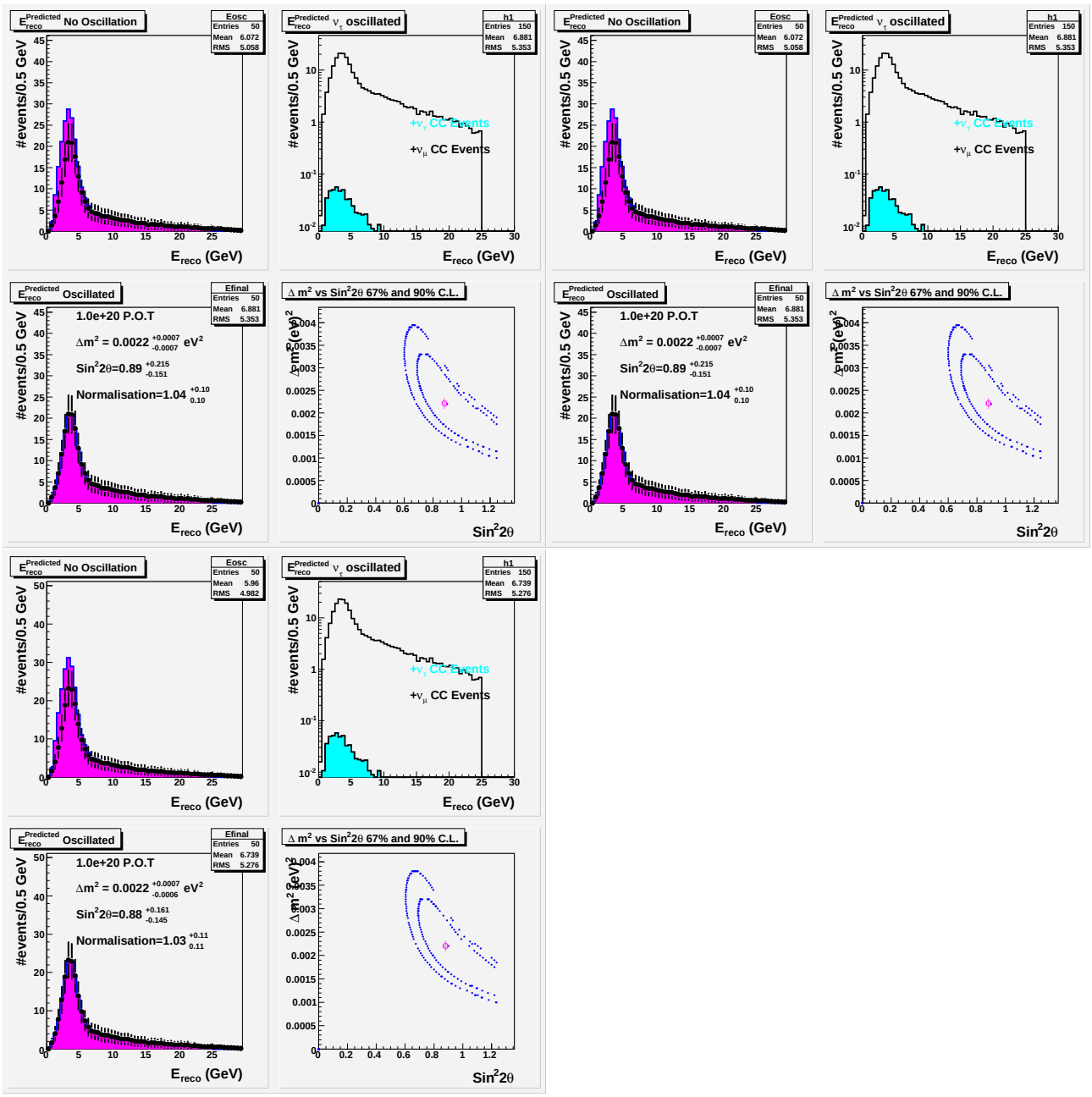


Figure 48: Sensitivity plots for changed ma-qe (top left), changed ma-res(top right), and changed ma-res and ma-qe (bottom left)

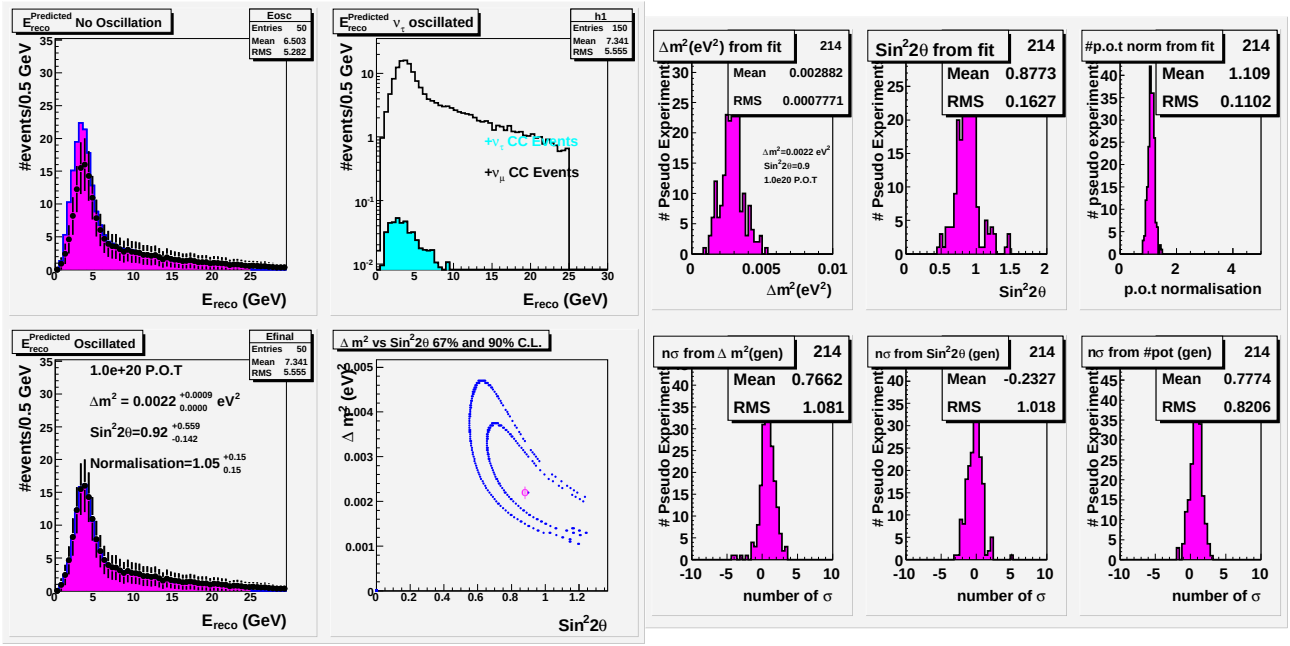


Figure 49: Sensitivity plots for changed shower response (faking intranuke) (left) and results of 500 pseudo runs (right)

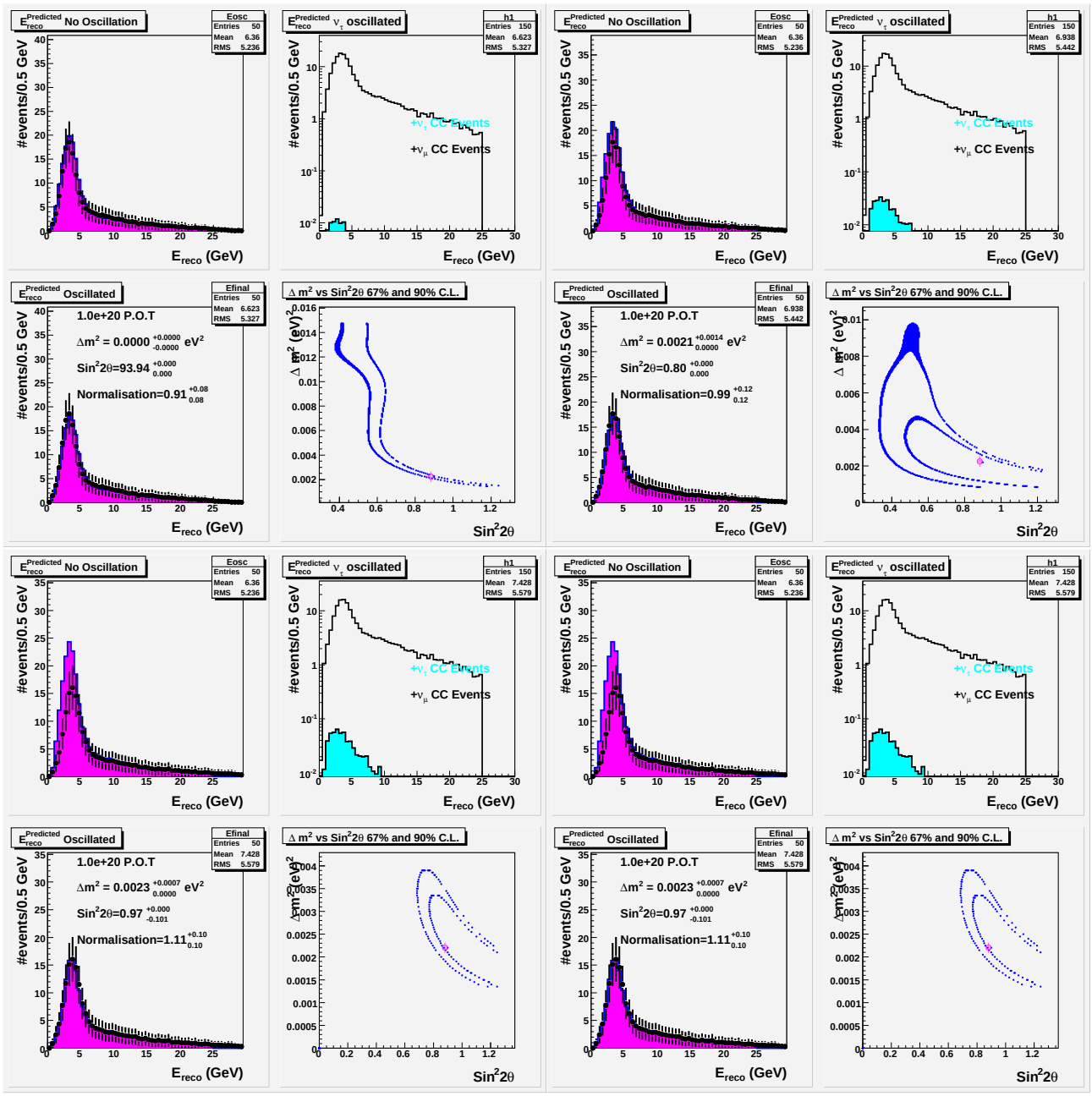


Figure 50: Sensitivity plots for different mis calibrations (F:N): 0.90 (left top), 0.95 (right top) 1.05 (left bottom) and 1.10 (right bottom).

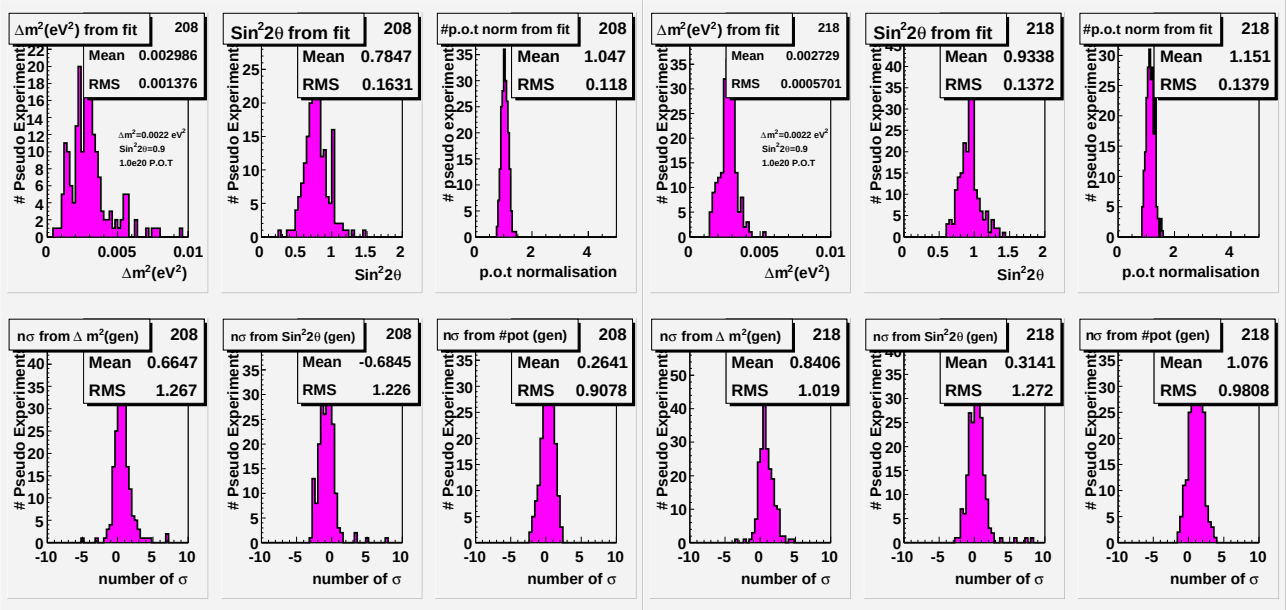


Figure 51: Results of 500 pseudo runs for 0.95 F:N miscalibration (left) and 1.05 F:N miscalibration (Right)

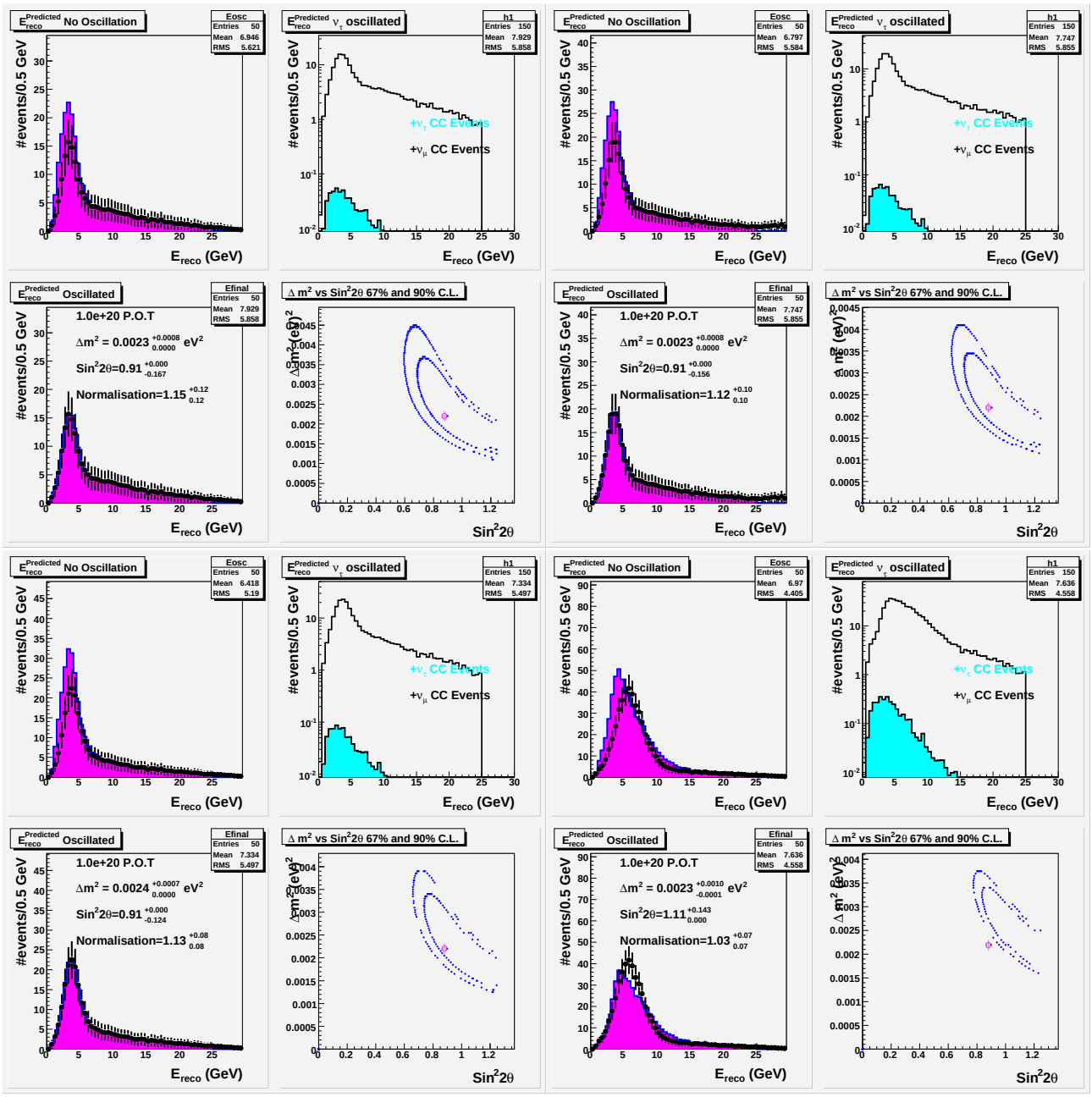


Figure 52: Sensitivity plots for different Mars beam configurations: le-10 170kA (left top), le-10 185kA (right top) le-10 200kA (left bottom) and le-100 200kA (right bottom).

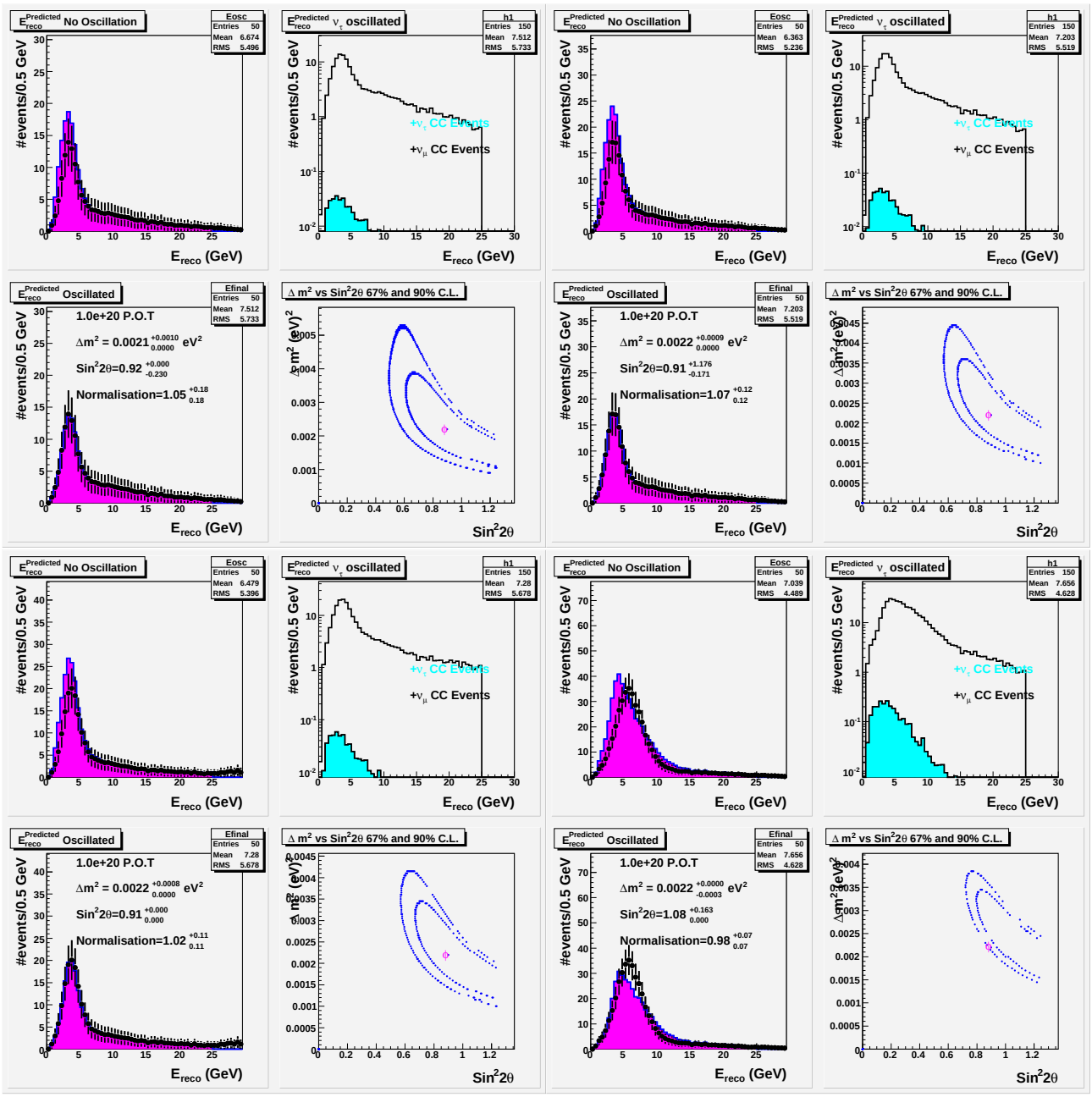


Figure 53: Sensitivity plots for different Fluka beam configurations: le-10 170kA (left top), le-10 185kA (right top) le-10 200kA (left bottom) and le-100 200kA (right bottom).

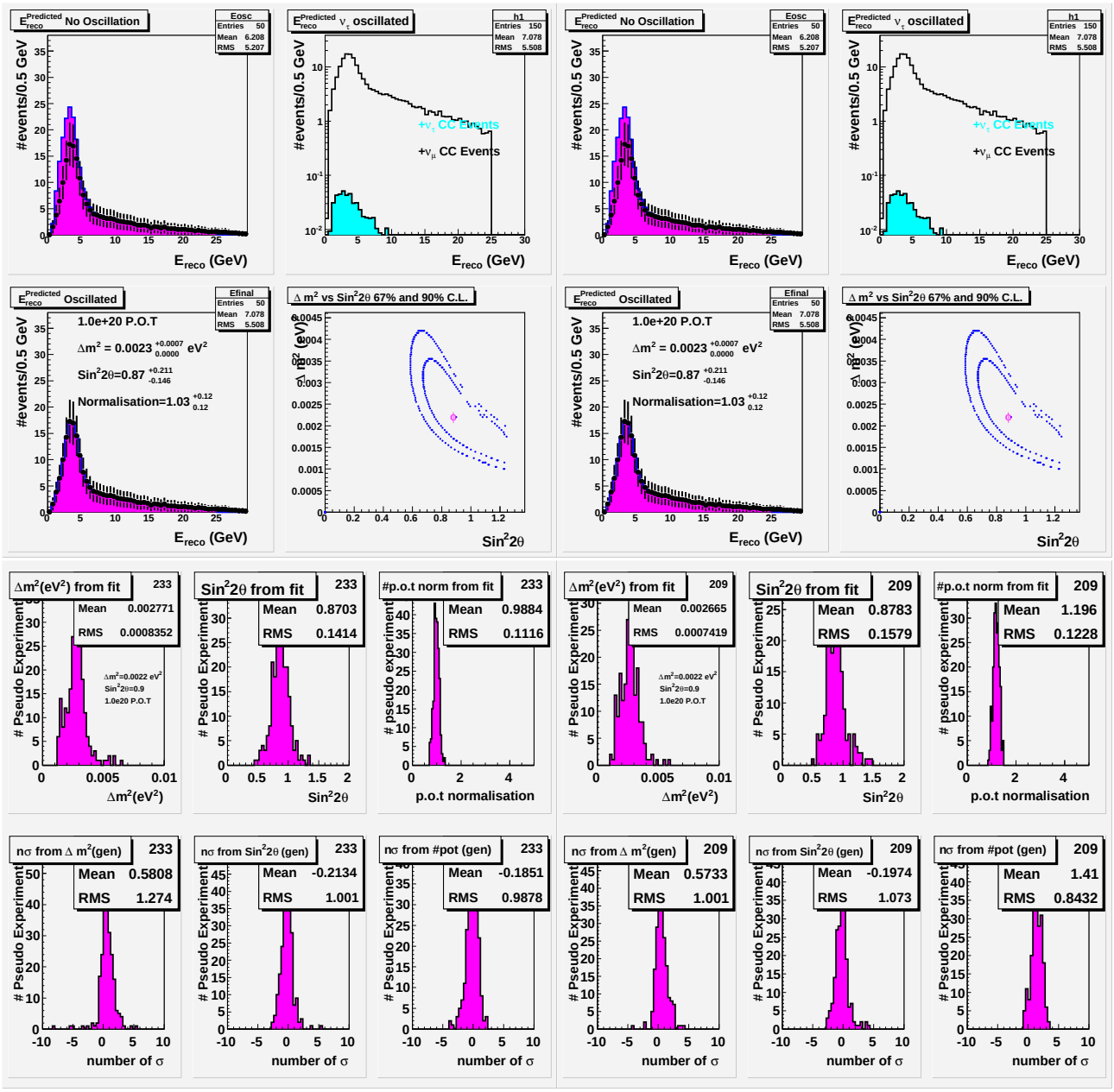


Figure 54: Sensitivity plot for the case of -10% (top left) and +10% (top right) p.o.t. The results of the corresponding 500 pseudo runs are shown in the bottom figures.

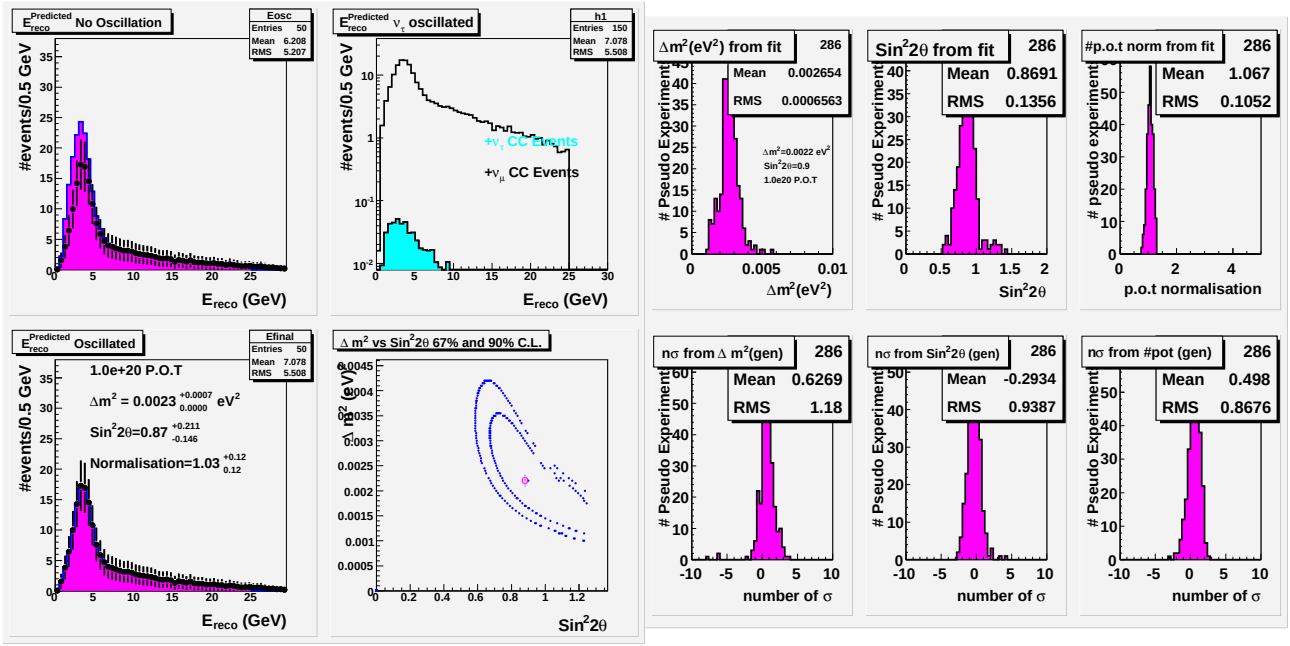


Figure 55: Sensitivity plot for the case of double the NC background than expected (left) and the results of 500 pseudo runs for the same case (right)

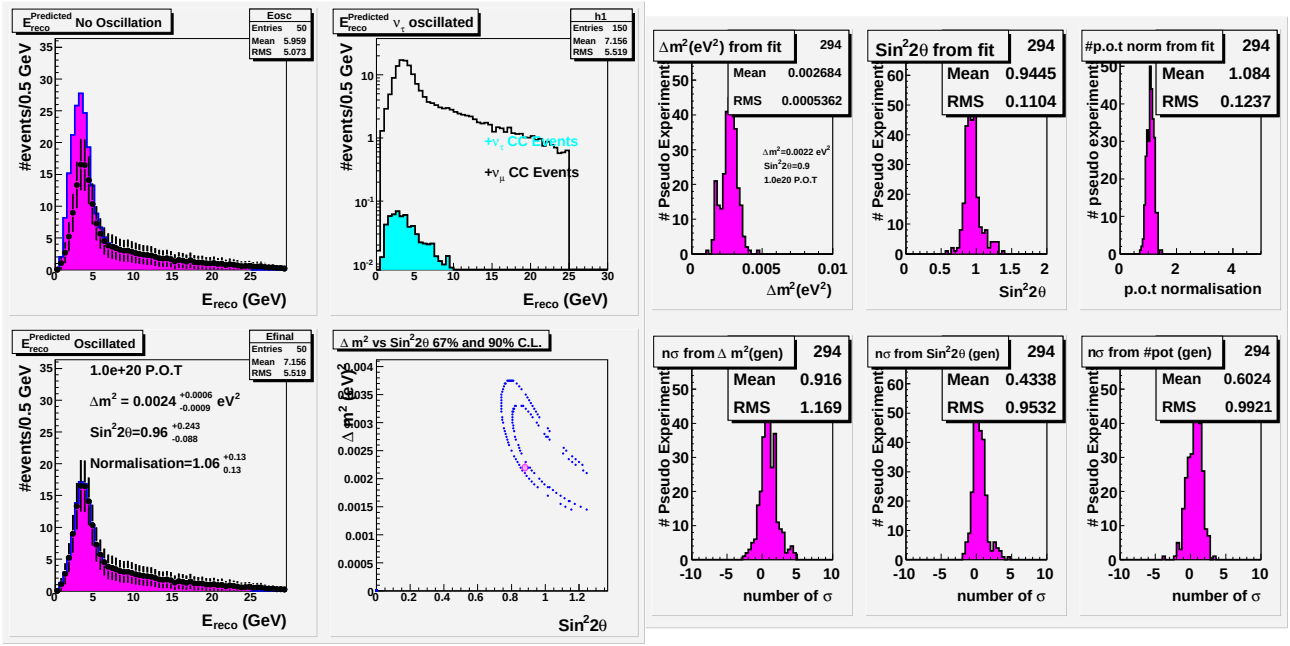


Figure 56: Sensitivity plot for a 10% increase in the first 7 bins in the ND only (left) and the results of 500 pseudo runs for this case (right)